

# The Optimal Shape of the Reflex Tube of a Bass Loudspeaker

Jevgenijs Jegorovs

Vom Fachbereich Mathematik  
der Universität Kaiserslautern  
zur Verleihung des akademischen Grades  
Doktor der Naturwissenschaften  
(Doctor rerum naturalium, Dr. rer. nat.)  
genehmigte Dissertation

April 2007



# The Optimal Shape of the Reflex Tube of a Bass Loudspeaker

Jevgenijs Jegorovs

Vom Fachbereich Mathematik  
der Universität Kaiserslautern  
zur Verleihung des akademischen Grades  
Doktor der Naturwissenschaften  
(Doctor rerum naturalium, Dr. rer. nat.)  
genehmigte Dissertation

1. Gutachter: Prof. Dr. Axel Klar
2. Gutachter: Prof. Dr. Wim Desmet

Tag der Disputation: 25.04.2007

D 386



## Abstract

In this thesis the author presents a mathematical model which describes the behaviour of the acoustical pressure (sound), produced by a bass loudspeaker. The underlying physical propagation of sound is described by the non-linear isentropic Euler system in a Lagrangian description. This system is expanded via asymptotical analysis up to third order in the displacement of the membrane of the loudspeaker. The differential equations which describe the behaviour of the key note and the first order harmonic are compared to classical results. The boundary conditions, which are derived up to third order, are based on the principle that the small control volume sticks to the boundary and is allowed to move only along it.

Using classical results of the theory of elliptic partial differential equations, the author shows that under appropriate conditions on the input data the appropriate mathematical problems admit, by the Fredholm alternative, unique solutions. Moreover, certain regularity results are shown.

Further, a novel Wave Based Method is applied to solve appropriate mathematical problems. However, the known theory of the Wave Based Method, which can be found in the literature, so far, allowed to apply WBM only in the cases of convex domains. The author finds the criterion which allows to apply the WBM in the cases of non-convex domains. In the case of 2D problems we represent this criterion as a small proposition. With the aid of this proposition one is able to subdivide arbitrary 2D domains such that the number of subdomains is minimal, WBM may be applied in each subdomain and the geometry is not altered, e.g. via polygonal approximation. Further, the same principles are used in the case of 3D problem. However, the formulation of a similar proposition in cases of 3D problems has still to be done.

Next, we show a simple procedure to solve an inhomogeneous Helmholtz equation using WBM. This procedure, however, is rather computationally expensive and can probably be improved. Several examples are also presented.

We present the possibility to apply the Wave Based Technique to solve steady-state acoustic problems in the case of an unbounded 3D domain. The main principle of the classical WBM is extended to the case of an external domain. Two numerical examples are also presented.

In order to apply the WBM to our problems we subdivide the computational domain into three subdomains. Therefore, on the interfaces certain coupling conditions are defined.

The description of the optimization procedure, based on the principles of the shape gradient method and level set method, and the results of the optimization finalize the thesis.

# Table of Contents

<b>Preface</b>	<b>3</b>
<b>1 Introduction</b>	<b>5</b>
<b>2 Mathematical Model</b>	<b>11</b>
2.1 Isentropic Euler Equations . . . . .	12
2.1.1 Lagrangian Form . . . . .	12
2.1.2 Non-dimensional Form . . . . .	14
2.1.3 Asymptotic Analysis of the Equation (2.17) . . . . .	15
2.1.4 Harmonically Oscillating Function . . . . .	16
2.2 Helmholtz Type Equations for the Pressure . . . . .	17
2.3 Comparison of the Models . . . . .	20
2.3.1 The Idea of Existence of a Displacement Potential . . . . .	21
2.3.2 Comparison with Kuznetsov's Model . . . . .	22
2.3.3 Bjorno-Beyer Model . . . . .	24
2.4 Computational Domain . . . . .	26
2.5 Boundary Conditions . . . . .	28
2.5.1 2D Domains . . . . .	28
2.5.2 3D Domains . . . . .	33
2.5.3 Radiative Boundary Conditions . . . . .	36
2.6 The Main Results of Chapter 2 . . . . .	38
<b>3 Existence, Uniqueness and Regularity of the Solution</b>	<b>41</b>
3.1 The Statement of the Problem and Definitions . . . . .	41
3.2 Fredholm Alternative . . . . .	43
3.3 $\sigma = \sigma(\mathbf{x}, \lambda)$ . . . . .	50
3.4 Second Fundamental Inequality . . . . .	51
3.5 Solvability of the Helmholtz Boundary Value Problem in $\mathcal{W}_2^2(\Omega)$	54
3.5.1 Solvability in $\mathcal{W}_2^2(\Omega)$ with $\partial\Omega \in \mathcal{C}^2$ . . . . .	54
3.5.2 Solvability in $\mathcal{W}_2^2(\Omega)$ for $\partial\Omega \in \mathcal{C}^2$ piecewise . . . . .	56

3.5.3	Solvability of the Helmholtz Boundary Value Problem in $\mathcal{W}_2^2(\Omega)$ Under Condition $\sigma \in \mathcal{L}_\infty(\partial\Omega)$ . . . . .	61
3.6	The Case of the Exterior Domain $\Omega^+$ . . . . .	63
3.7	The Main Results of Chapter 3 . . . . .	65
<b>4</b>	<b>Numerical Method and Simulations</b>	<b>67</b>
4.1	The Main Principles of the Wave Based Method . . . . .	69
4.2	On the Convergence of the Wave Based Method . . . . .	71
4.2.1	Classification of the Problems . . . . .	72
4.2.2	Convergence of the WBM Solution in a Non-Convex Domain . . . . .	73
4.2.3	Numerical Examples . . . . .	76
4.3	WBM in the Case of Inhomogeneous Helmholtz Equation . . . . .	78
4.4	WBM in an Unbounded 3D Domain . . . . .	80
4.5	Interface Continuity Conditions . . . . .	84
4.6	Numerical Simulations . . . . .	86
4.6.1	First Order Correction Function $p_1$ . . . . .	86
4.6.2	Second Order Correction Function $p_2$ . . . . .	89
4.7	The Main Results of Chapter 4 . . . . .	91
<b>5</b>	<b>Optimization</b>	<b>95</b>
5.1	Formulation of the Optimization Problem . . . . .	95
5.2	Optimization Procedure . . . . .	98
5.2.1	Shape Derivative . . . . .	98
5.2.2	Level Set Method . . . . .	103
5.2.3	Optimization Algorithm . . . . .	105
5.3	Optimal Shape . . . . .	106
5.4	The Main Results of the Chapter 5 . . . . .	106
<b>6</b>	<b>Conclusion</b>	<b>111</b>
	<b>Bibliography</b>	<b>113</b>

# Preface

Dear Reader,

The aim of this thesis is to find the optimal shape of the reflective tube of a bass loudspeaker. This, however, does not mean that the main topic of the thesis is certain optimization procedure. The work is structured in the way of classical mathematical modeling, i.e. I start up from an analysis of a real physical process and end up with certain virtual results, which are supposed to predict the reality. The thesis has been written in such a manner that each chapter can be considered as complete one. At the end of each chapter I include a section which shortly summarizes it.

Here, I would like to express my gratitude to Prof. Helmut Neunzert and Prof. Andris Buikis (University of Latvia) for giving me the opportunity of doing my PhD research in Kaiserslautern. I extend many thanks to Prof. Axel Klar who has given me a lot of freedom to choose the topics of my research. Also, I am very grateful to Prof. Wim Desmet (KU Leuven, Belgium) for being my co-referee.

I express my deepest gratitude to Dr. Jan Mohring for interesting discussions, carefully reading the manuscript and giving valuable hints and suggestions during my research. My special thanks I address to my colleagues of the groups "Transportvorgänge" and "Strömungen und komplexe Strukturen" at Fraunhofer ITWM for the pleasant working atmosphere and support, in particular to Dr. Sergiy Pereverzyev and Dr. Anna Naumovich, who always found the time to discuss certain scientific and everyday questions.

I also would like to thank my wife Natallia and my son Ilja, who brighten up and enliven all the time my private and scientific life. I am very grateful to my parents, my sister Jūlija and my parents-in-law for their help.

Many thanks go to M.Sc. Olga Arbidāne, Dr. Vita Rutka, Dr. Alexander Grm, Dr. Satyananda Panda, Dr. Christian Coclici, Dr. Thomas Götz, Dr. Bert Pluymers for their help.

This research project was financially supported by Fraunhofer ITWM, Department of Transport Processes.



This work is structured in the following way

- In the Chapter 1 I present the main steps of the mathematical modeling of certain physical process. Further chapters are supposed to represent these steps. Moreover, I define the main task of this thesis.
- The Chapter 2 deals with the model derivation, i.e. I define the differential equations of Helmholtz type, the computational domain and special boundary conditions which are supposed to describe the physical phenomenon, what I am interested in. This model has been compared to other models which can be found in the literature.
- After the mathematical model derivation I collect and adapt some theoretical results which particularly give an answer about the mathematical properties, i.e. existence, uniqueness and regularity of the solution, of the equation of Helmholtz type derived in the previous chapter.
- In the Chapter 4 I present a modern numerical method (Wave Based Method) which solves numerically the system of differential equations derived in the Chapter 2. I have to notice that this numerical method cannot be applied to our mathematical problem directly, therefore, I extended it. I showed that the WBM can be applied in the some cases of non-convex domains and the ideas of the WBM can be utilized in the cases of unbounded computational domains. In order to be sure that our numerical method gives adequate results, I compared it visually with the classical Finite Element Method.
- The Chapter 5 deals with the optimal shape design. This procedure is based on the principles of the shape derivative and the level set method, [4].
- The Chapter 6 summarizes and finalizes the work.

Enjoy the reading<sup>1</sup>.

---

<sup>1</sup>Please, read this work completely. Otherwise there will be no guarantee that phrases like "... and the main gear of the mechanism will be made from wood because nobody will read this thesis..." does not appear here.

# Chapter 1

## Introduction

The author very often has been asked by the young students about the main idea of applied mathematics. Namely, what kind of problems do the mathematicians solve? What do they actually do? Of course, the situation depends on the aim of a given problem. Mostly, the main idea of applied mathematics is to build up some model<sup>1</sup> which describes certain process, e.g. physical, biological, chemical, economical, social, etc. For example, one wants to investigate the acoustic properties of some bass loudspeaker.

First of all, we model a simplified process, for example, the air inside the loudspeaker is moving due to a piston motion. In the mathematical sense it means that we have to derive certain relations<sup>2</sup> between the unknown and known quantities in a certain computational domain. Before doing that we have to understand the physics of the air flow and to identify the unknown quantities and given data, i.e. known quantities. Also, the computational domain and certain conditions on the boundary of this domain have to be defined. We derived a mathematical model which is supposed to represent the reality. Next we would like to simplify those relations. In other words, we make adequate assumptions in order to simplify our mathematical model. One probably knows that the air is rather a non-viscous and compressible fluid. Thus, we are able to use these properties, in particular, we can neglect the viscosity of the air.

After the simplifications of all necessary equations and conditions (which can be either simple algebraic relations or the differential ones) and the definition of the computational domain, we have to investigate the solvability of the simplified problem<sup>3</sup>. Why should we do such an analysis? The matter of fact is that in mathematics many problems are not solvable, i.e. the solution does not exist, is not unique or does not depend smoothly on the data. In all cases one says that

---

<sup>1</sup>Or algorithm.

<sup>2</sup>I.e. equations.

<sup>3</sup>The set of equations, defined in the computational domain, together with the conditions, defined on the boundary of the computational domain, is called by the mathematical problem.

the mathematical problem is ill-posed. And it has to be regularized somehow in order to get the unique solution. Why we need exactly the unique solution? Obviously, we describe certain, always the same physical process, hence, the aim solution exists and stays always the same. If the aim solution changes then it means that something has been changed in the experiment. Unfortunately, the ill-posed mathematical problems can give something unpredictable. Thus, we have to show that our model is well-posed, i.e. the solution exists, it is unique and continuously depends on the input data, i.e. if we slightly change the input data, then the solution also changes slightly. This is so-called Hadamard definition of the well-posed problem.

We have to note that this analysis is rather difficult and, in some cases yet, even impossible to do. Hence, one can either try to analyze the properties of the model and, with certain probability, be lost in this analysis, or hope that the model is well-posed and try to find the solution. Of course, the right thing would be to take the first way, but usually applied mathematicians avoid this and choose the second way.

Next stage is the solving of the problem. Assume that the appropriate analysis mentioned above has been successfully done and we are sure that the problem is well-posed. Therefore, we are able to solve the problem and get the solution. Unfortunately, not always we can solve something analytically. This might be a consequence of the complexity of the model, in particular, the computational domain might be complicated enough to prevent an analytical solution. As a consequence, we solve the problem numerically, i.e. we find a numerical solution which approximates the analytical one. Therefore, we have to apply some numerical method. Note that the amount of numerical methods and, hence, the number of the numerical solutions is rather big. Hence, a numerical solution, depending on the accuracy, is never unique in this sense. We should not mix up the non-uniqueness of the analytical solution and the non-uniqueness of the numerical one. The most popular numerical methods nowadays, solving a system of partial differential equations<sup>4</sup>, are the finite element methods (FEM), the boundary element methods (BEM), the finite volume methods (FVM), the finite difference methods (FDM), etc. These methods are rather flexible and can be applied to solve a broad spectrum of problems.

If the mathematician wants to apply his own numerical method, then he has to investigate the properties of this method. Namely, one has to check the consistency, stability and the convergence ability of the method, i.e. the method has to properly approximate the equations, small changes in the input data have to lead to small changes in the numerical solution and the numerical solution has to converge to the analytical one if the numerical approximation of the problem

---

<sup>4</sup>We are interested to solve exactly such a system.

---

becomes more accurate. Also, very important thing is the computational speed (or time) of the method. Fast and accurate numerical methods are much more desirable than the slow and accurate ones.

There is an obvious risk that the numerical solution, which we have got, actually has nothing to do with the analytical one. However, if the numerical method is already approved by time, then no fear has to arise. Also, if one is able to apply another numerical method to solve the problem, and both numerical results look similar, then it is a good indication that our numerical method works.

Another way is to do the dimension reduction in the model up to 1D<sup>5</sup>. Often, it is possible to solve 1D problem analytically and we are able to compare the analytical and the numerical solutions in 1D (2D) case. This also gives clear picture how good our numerical method is.

Finally, we are also interested to compare our numerical solution to the measurements which, probably, can be collected in certain cases. The measurements of the experiment, however, are not always the perfect ones, i.e. in the measurements some noise is hidden. The comparison of the measurements and the solution<sup>6</sup> of the problem tells us about the correctness of the model. Unfortunately, it is not always possible to set up these experiments because they are expensive in most cases.

The procedure described above can be applied to simulate the behaviour of the sound in the simplified bass loudspeaker, i.e. instead of the curved membrane we consider some piston. Basically, we would like to simulate the behaviour of the sound for given geometry. Therefore, we change it and repeat the whole procedure again. Obviously, we do not derive the differential equations once more. They are already derived.

Everything, what we have done above, can be the complete task we have to do. But there is also one more stage which can be done. Namely, we can do an optimization of the geometry of the loudspeaker to get good sound properties. Before doing that one has to define an optimization problem. Next, one has to investigate the solvability of the optimization problem. This is also not always possible and, in some cases, is rather difficult to do. The optimal shape can also be not unique, i.e. not global one. Next, we have to apply certain optimization method which, finally, gives certain optimal shape. There also exist several optimization techniques which can be applied to our optimization problem.

The shape optimization, mostly, is the final stage what the mathematician does. Afterwards, the simulation and optimization results can be used by engineers. Hence, the theoretical work of the mathematician has been done.

The schematic representation of the whole procedure described above is pre-

---

<sup>5</sup>Or up to 2D in the cases, when the problem can be solved analytically.

<sup>6</sup>Analytical or numerical.

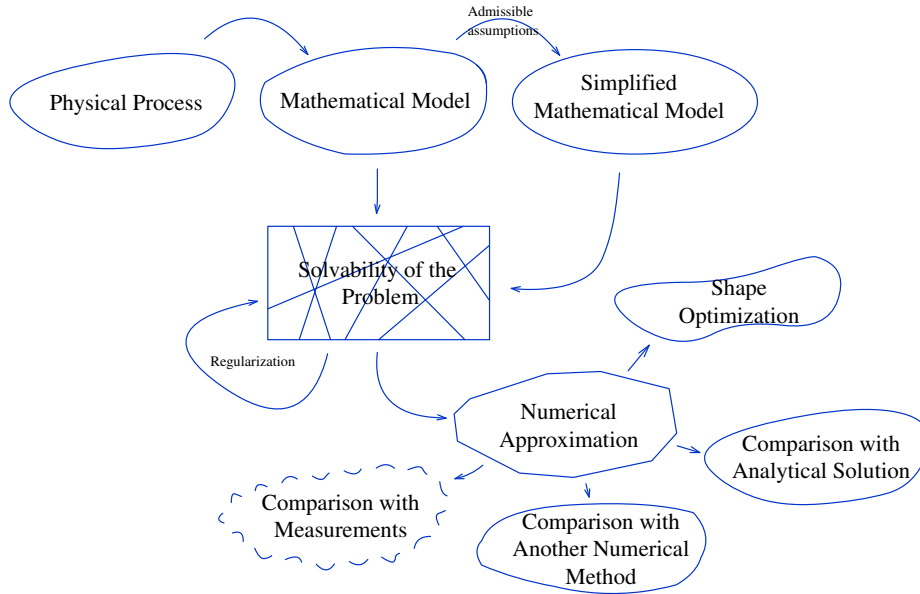


Figure 1.1: The modeling scheme.

sented in Fig. 1.1. In this thesis we will follow this scheme. The only deviation we would like to do is that we will not consider the case of a simplified geometry. It is not necessary in our case.

Let us define the task we have to deal with. The problem we consider comes from a small company, KS Beschallungstechnik GmbH, Hettenleidelheim, Germany, which produces powerful loudspeakers for big halls, for example. We consider a bass loudspeaker with the reflex tube. It has cylindrical geometry and all geometry parameters are given, cf. Fig. 2.1 and 2.5. Such a bass loudspeaker exists and has been used to do some tests and to compare the measurements and the results of the numerical simulations. The main task, which has to be resolved at the end, is to find the optimal shape of the reflex tube in such a way that the quality of the sound becomes better. Depending on the geometry of the loudspeaker the quality of the sound might be good or not. For example, the membrane oscillates with 65[Hz], but we hear also the sound of 130[Hz], 195[Hz], etc. And we would like to decrease the influence of high order harmonics on the key note by the reflex tube optimization.

One knows how the loudspeaker works. The membrane oscillates with certain frequency. The oscillations of the membrane are generated by an electromagnetic system and this process has to be carefully controlled. Otherwise, the electromagnetic system itself can affect the quality of the sound. The membrane vibrations are transferred to the surrounding medium (air) and travel as waves to the human ear. We assume that the electromagnetic system, which gives impulses to the membrane, works properly and does not create any error. Therefore, we

have to take care about the geometry of the loudspeaker, i.e. we have to find the optimal shape of the reflex tube. The details of the optimization will be presented in Chapter 5.

In this work we consider the sound propagation in the air. In this case the medium can be assumed to be homogeneous and inviscid. This fact allows to start our investigation from the Euler equations which have non-linear nature. The sound propagation in other mediums like liquids or solid matters forces us take into account all possible inhomogeneities of the medium, viscosity, etc. The governing mathematical models, therefore, become rather complicated.

In the next chapter we derive the mathematical model which describes the behaviour of the acoustic pressure. This quantity will play an important role in the optimization process.



## Chapter 2

# Mathematical Model

In the last decades mathematical modeling started to play an important role as a technology to solve the real world problems. The main idea is to describe real process by a certain mathematical model and to analyze features of physical phenomena using mathematical tools. Such an approach allows to decrease the experimental costs, to predict the behaviour of a solution for different input data, to increase nowadays the significance of mathematics, etc. In this chapter, we present a mathematical model which describes the propagation of the sound through a reflex tube of a bass loudspeaker, cf. Fig. 2.1.

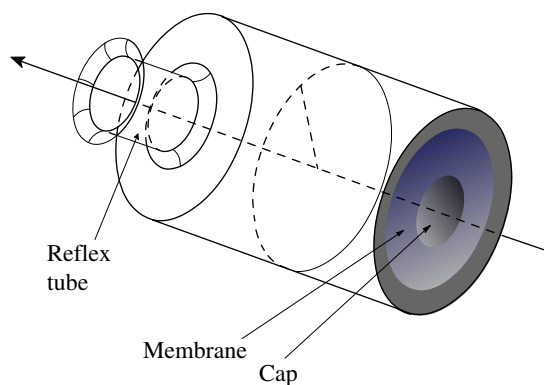


Figure 2.1: A bass loudspeaker.

It is well known that the sound is a pressure perturbation which propagates as a wave. Due to the vibrations of the membrane the air particles oscillate as well. These oscillations create small perturbations in the pressure. These perturbations we have to investigate. The motion of the air can be described by the Euler equations, cf. [21], [19], etc. We assume that the pressure depends only on the density, i.e.  $p = p(\rho)$ . It means that we have a so-called isentropic process. In this chapter, we derive Helmholtz type equations which describe the behaviour of the pressure perturbations. We ignore the heat exchange and the friction between the air particles and boundaries of a bass loudspeaker.



## 2.1 Isentropic Euler Equations

Consider an open, simply connected domain  $\tilde{\Omega} \subset \mathbb{R}^3$  and the isentropic Euler equations which hold in  $\tilde{\Omega}$

$$\frac{\partial \varrho}{\partial \tilde{t}} + \operatorname{div}_{\tilde{\mathbf{x}}}(\varrho \mathbf{u}) = 0, \quad (2.1)$$

$$\varrho \left[ \frac{\partial \mathbf{u}}{\partial \tilde{t}} + \langle \mathbf{u}, \nabla_{\tilde{\mathbf{x}}} \rangle \mathbf{u} \right] + \nabla_{\tilde{\mathbf{x}}} p = 0, \quad (2.2)$$

$$\frac{p}{p_0} - \left( \frac{\varrho}{\varrho_0} \right)^\gamma = 0. \quad (2.3)$$

Here, the density  $\varrho$ , the pressure  $p$  and the velocity  $\mathbf{u}$  are functions of time  $\tilde{t} > 0$  and space  $\tilde{\mathbf{x}} \in \tilde{\Omega} \subset \mathbb{R}^3$ . The gas specific heat constant  $\gamma \in \mathbb{R}_+$  is given.  $\varrho_0$  and  $p_0$  are the density and the pressure at rest, respectively. These quantities are also given. " $\sim$ " denotes Eulerian coordinates.

### 2.1.1 Lagrangian Form

In this subsection, we come from the Eulerian coordinate system to the Lagrangian one. This transformation has to be done since in the Lagrangian description moving boundaries of the domain are fixed. All the details presented below can be found in [49]. We just repeat them here. Let us choose some air particle at rest. We denote its position by  $\mathbf{x}$ . Assume that the particle moves some certain time  $t$  (here, the time  $t$  in the Lagrangian description equals to  $\tilde{t}$  in the Eulerian description). We find new position of our particle

$$\tilde{\mathbf{x}} = \mathbf{x} + \mathbf{h}(t, \mathbf{x}), \quad (2.4)$$

where  $\mathbf{h}$  is the displacement function. Obviously, the time derivative of  $\mathbf{h}$  is the velocity of the particle, i.e.

$$\mathbf{u} = \frac{\partial \mathbf{h}}{\partial t}. \quad (2.5)$$

The partial derivatives in the Lagrangian coordinate system look as follows

$$\frac{\partial}{\partial \tilde{t}} = \frac{\partial}{\partial t} + \left\langle \frac{\partial \mathbf{h}}{\partial t}, \nabla_{\tilde{\mathbf{x}}} \right\rangle, \quad \nabla_{\mathbf{x}} = F^T \nabla_{\tilde{\mathbf{x}}}, \quad (2.6)$$

where  $F$  is the deformation tensor.  $F$  depends on the position and has the form

$$F = \left[ \delta_{ij} + \frac{\partial h_i}{\partial x_j} \right]_{i,j=1}^3, \quad (2.7)$$

where  $\delta_{ij}$  is the Kronecker symbol.

Consider now some control volume  $D_0 \subset \tilde{\Omega}$  at rest. Assume that the particles of this control volume start to move. The particles, which initially belong to  $D_0$ ,

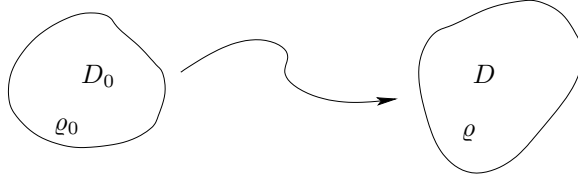


Figure 2.2: Transformation of a certain control volume.

after some time form the volume  $D = \{\tilde{\mathbf{x}}(t, \mathbf{x}) \mid \mathbf{x} \in D_0\}$ , cf. Fig. 2.2. The transformation theorem on volume integrals yields

$$\begin{aligned} \text{vol}(D) &= \int_D d\tilde{\mathbf{x}} \\ &= \int_{D_0} \det \left( \left[ \frac{\partial \tilde{x}_i}{\partial x_j} \right]_{i,j=1}^3 \right) d\mathbf{x} \\ &= \int_{D_0} \det F d\mathbf{x}. \end{aligned}$$

Obviously, the determinant of the deformation tensor  $F$  is equal to 1 for  $\mathbf{h} = \mathbf{0}$ . In a small neighbourhood of  $\mathbf{x}$  the determinant of  $F$  is continuous (the components of the Jacobi matrix are continuous, cf. [19]) and, consequently,  $\det F > 0$  in that small neighbourhood.

The masses of  $D_0$  and  $D$  should be the same. They are assumed to consist of the same particles. For any fixed  $t > 0$  we find

$$\frac{\varrho_0}{\varrho} = \lim_{\text{vol}(D_0) \rightarrow 0} \frac{\text{vol}(D)}{\text{vol}(D_0)} = \det F, \quad (2.8)$$

where  $\text{vol}(D_0) = \int_{D_0} d\mathbf{x}$ .

Since we have an isentropic process, we can express the density  $\varrho$  and the pressure  $p$  functions in terms of the displacement function  $\mathbf{h}$ . Equations (2.3) and (2.8) yield

$$\varrho = \varrho_0 (\det F)^{-1}, \quad (2.9)$$

$$p = \frac{\varrho_0 c_0^2}{\gamma} (\det F)^{-\gamma}, \quad (2.10)$$

where  $c_0 = \sqrt{\frac{\gamma p_0}{\varrho_0}}$  is the speed of sound at rest. Our aim is to rewrite the Euler equations in terms of the displacement  $\mathbf{h}$ . We substitute (2.5) and (2.6) in the

equation (2.2). The term  $\left[ \frac{\partial \mathbf{u}}{\partial t} + \langle \mathbf{u}, \nabla_{\tilde{\mathbf{x}}} \rangle \mathbf{u} \right]$  becomes

$$\begin{aligned} \frac{\partial \mathbf{u}}{\partial t} + \langle \mathbf{u}, \nabla_{\tilde{\mathbf{x}}} \rangle \mathbf{u} &= \frac{\partial \mathbf{u}}{\partial t} - \left\langle \frac{\partial \mathbf{h}}{\partial t}, F^{-T} \nabla_{\mathbf{x}} \right\rangle \frac{\partial \mathbf{h}}{\partial t} + \left\langle \frac{\partial \mathbf{h}}{\partial t}, F^{-T} \nabla_{\mathbf{x}} \right\rangle \frac{\partial \mathbf{h}}{\partial t} \\ &= \frac{\partial^2 \mathbf{h}}{\partial t^2}, \end{aligned}$$

where  $F^{-T} := (F^T)^{-1}$ . Inserting (2.9) and (2.10) into (2.2) we get on the right hand side

$$\begin{aligned} -\frac{\nabla_{\tilde{\mathbf{x}}} p}{\varrho} &= -\frac{\frac{\varrho_0 c_0^2}{\gamma} F^{-T} \nabla_{\mathbf{x}} ((\det F)^{-\gamma})}{\varrho_0 (\det F)^{-1}} \\ &= c_0^2 F^{-T} \nabla_{\mathbf{x}} (\det F) (\det F)^{-\gamma}. \end{aligned}$$

Hence, we end up with the isentropic Euler equations in terms of the displacement  $\mathbf{h}$ .

$$(\det F)^\gamma F^T \frac{\partial^2 \mathbf{h}}{\partial t^2} = c_0^2 \nabla_{\mathbf{x}} (\det F), \quad F^T = I + \nabla_{\mathbf{x}} \mathbf{h}^T. \quad (2.11)$$

The mass is conserved because of (2.8).

### 2.1.2 Non-dimensional Form

As we already mentioned above, we consider the air movement inside a bass loudspeaker. The membrane inside the loudspeaker typically oscillates at high power. In the case of low frequencies it means that the amplitude of the membrane has to be rather big. Therefore, it can exceed a centimeter. Let us denote a typical amplitude by  $\ell$  and a typical angular frequency by  $\omega$ . By definition, the angular frequency  $\omega$  might be expressed by the relation between the so-called wave number  $\kappa$  and the sound of speed  $c_0$  at rest, i.e.

$$\omega = \kappa c_0. \quad (2.12)$$

On the other hand, the wave length  $\lambda$  can be expressed as

$$\lambda = c_0 / f, \quad (2.13)$$

where

$$f = \omega / 2\pi \quad (2.14)$$

is the usual frequency. Further, we write  $\lambda = 2\pi / \kappa$ . Hence, for low frequencies  $f$  the wave length  $\lambda$  is rather large and, consequently,  $\kappa$  is rather small. Multiplying the wave number  $\kappa$  by  $\ell$ , which is assumed to be much smaller than a typical wave length, we get a small non-dimensional parameter

$$\varepsilon = \ell \kappa. \quad (2.15)$$

In order to linearize the non-linear equation (2.11) we have to transform it first into non-dimensional form. Therefore, we introduce non-dimensional variables defined below

$$\tau = \omega t, \quad \boldsymbol{\xi} = \kappa \mathbf{x}, \quad \boldsymbol{\eta} = \ell^{-1} \mathbf{h}. \quad (2.16)$$

Inserting them into (2.11) we get the non-dimensional form of the equation (2.11), i.e.

$$\varepsilon (\det F)^\gamma F^T \frac{\partial^2 \boldsymbol{\eta}}{\partial \tau^2} = \nabla_{\boldsymbol{\xi}} (\det F), \quad F^T = I + \varepsilon \nabla_{\boldsymbol{\xi}} \boldsymbol{\eta}^T. \quad (2.17)$$

This equation is the starting point for the further asymptotic analysis.

### 2.1.3 Asymptotic Analysis of the Equation (2.17)

To linearize the non-linear equation (2.17) we have to assume that the function  $\boldsymbol{\eta}$  has some appropriate properties. These properties have to correspond to a physical behaviour of the function. Following the idea of [50] or [49] we assume that the scaled displacement  $\boldsymbol{\eta}$  has an expansion of the form

$$\boldsymbol{\eta}(\tau, \boldsymbol{\xi}) = \boldsymbol{\eta}_1(\tau, \boldsymbol{\xi}) + \varepsilon \boldsymbol{\eta}_2(\tau, \boldsymbol{\xi}) + \varepsilon^2 \boldsymbol{\eta}_3(\tau, \boldsymbol{\xi}) + \mathcal{O}(\varepsilon^3). \quad (2.18)$$

Here, we assume the convergence of (2.18). We have to note that the third order term play a special role in some acoustical applications.

In the following, we will use Einstein's summation convention, i.e. products containing repeated indices have to be summed up from 1 to 3. For example,  $a_{ij} b_i^j c_k^2$  means  $\sum_{i,j,k=1}^3 a_{ij} b_i^j c_k^2$ . Let us expand the determinant of the deformation tensor  $F$  up to fourth order using (2.18)

$$\begin{aligned} \det F &= \sum_{\sigma \in \pi(3)} \text{sign}(\sigma) \prod_{i=1}^3 \left( \delta_{i\sigma(i)} + \varepsilon \frac{\partial \eta_{1i}}{\partial \xi_{\sigma(i)}} + \varepsilon^2 \frac{\partial \eta_{2i}}{\partial \xi_{\sigma(i)}} + \varepsilon^3 \frac{\partial \eta_{3i}}{\partial \xi_{\sigma(i)}} + \dots \right) \\ &= 1 + \varepsilon \frac{\partial \eta_{1i}}{\partial \xi_i} + \varepsilon^2 \left\{ \frac{\partial \eta_{2i}}{\partial \xi_i} + \frac{1}{2} \left( \frac{\partial \eta_{1i}}{\partial \xi_i} \frac{\partial \eta_{1j}}{\partial \xi_j} - \frac{\partial \eta_{1i}}{\partial \xi_j} \frac{\partial \eta_{1j}}{\partial \xi_i} \right) \right\} \\ &+ \varepsilon^3 \left\{ \frac{\partial \eta_{3i}}{\partial \xi_i} + \left( \frac{\partial \eta_{1i}}{\partial \xi_i} \frac{\partial \eta_{2j}}{\partial \xi_j} - \frac{\partial \eta_{1i}}{\partial \xi_j} \frac{\partial \eta_{2j}}{\partial \xi_i} \right) \right. \\ &+ \left. \frac{1}{6} \left( 2 \frac{\partial \eta_{1i}}{\partial \xi_j} \frac{\partial \eta_{1j}}{\partial \xi_k} \frac{\partial \eta_{1k}}{\partial \xi_i} + \frac{\partial \eta_{1i}}{\partial \xi_i} \frac{\partial \eta_{1j}}{\partial \xi_j} \frac{\partial \eta_{1k}}{\partial \xi_k} - 3 \frac{\partial \eta_{1i}}{\partial \xi_j} \frac{\partial \eta_{1j}}{\partial \xi_i} \frac{\partial \eta_{1k}}{\partial \xi_k} \right) \right\} \\ &+ \mathcal{O}(\varepsilon^4), \end{aligned} \quad (2.19)$$

where  $\pi(3)$  is the set of all possible permutations and  $i, j, k \in \{1, 2, 3\}$ . In order to find an asymptotic expansion of the term  $(\det F)^\gamma$  we apply Taylor series

about 1, i.e.

$$\begin{aligned}
(\det F)^\gamma &= 1 + \varepsilon \binom{\gamma}{1} \frac{\partial \eta_{1i}}{\partial \xi_i} \\
&+ \varepsilon^2 \left\{ \binom{\gamma}{1} \left( \frac{\partial \eta_{2i}}{\partial \xi_i} + \frac{1}{2} \left( \frac{\partial \eta_{1i}}{\partial \xi_i} \frac{\partial \eta_{1j}}{\partial \xi_j} - \frac{\partial \eta_{1i}}{\partial \xi_j} \frac{\partial \eta_{1j}}{\partial \xi_i} \right) \right) \right. \\
&\left. + \binom{\gamma}{2} \left[ \frac{\partial \eta_{1i}}{\partial \xi_i} \right]^2 \right\} + \mathcal{O}(\varepsilon^3), \tag{2.20}
\end{aligned}$$

where  $\binom{\gamma}{n} := \frac{\gamma(\gamma-1)\cdots(\gamma-n+1)}{n!}$ ,  $n \in \mathbb{Z}_+$  and  $i, j \in \{1, 2, 3\}$ .

Inserting expressions (2.19) and (2.20) into (2.17) and collecting coefficients of equal  $\varepsilon$  powers, we get nine differential equations for the components of the functions  $\boldsymbol{\eta}_1$ ,  $\boldsymbol{\eta}_2$  and  $\boldsymbol{\eta}_3$

$$\frac{\partial^2 \eta_{1j}}{\partial \xi_i \partial \xi_j} - \frac{\partial^2 \eta_{1i}}{\partial \tau^2} = 0, \tag{2.21}$$

$$\frac{\partial^2 \eta_{2j}}{\partial \xi_i \partial \xi_j} - \frac{\partial^2 \eta_{2i}}{\partial \tau^2} = \frac{\partial \eta_{1j}}{\partial \xi_i} \frac{\partial^2 \eta_{1j}}{\partial \tau^2} + \frac{1}{2} \frac{\partial}{\partial \xi_i} \left( (\gamma-1) \left( \frac{\partial \eta_{1j}}{\partial \xi_j} \right)^2 + \frac{\partial \eta_{1j}}{\partial \xi_m} \frac{\partial \eta_{1m}}{\partial \xi_j} \right), \tag{2.22}$$

$$\begin{aligned}
\frac{\partial^2 \eta_{3j}}{\partial \xi_i \partial \xi_j} - \frac{\partial^2 \eta_{3i}}{\partial \tau^2} &= \gamma \frac{\partial^2 \eta_{1i}}{\partial \tau^2} \left( \frac{\gamma-1}{2} \left[ \frac{\partial \eta_{1j}}{\partial \xi_j} \right]^2 + \frac{\partial \eta_{2j}}{\partial \xi_j} \right. \\
&+ \left. \frac{1}{2} \left( \frac{\partial \eta_{1j}}{\partial \xi_j} \frac{\partial \eta_{1k}}{\partial \xi_k} - \frac{\partial \eta_{1j}}{\partial \xi_k} \frac{\partial \eta_{1k}}{\partial \xi_j} \right) \right) \\
&+ \gamma \frac{\partial \eta_{1j}}{\partial \xi_j} \left( \frac{\partial^2 \eta_{2i}}{\partial \tau^2} + \frac{\partial \eta_{1k}}{\partial \xi_i} \frac{\partial^2 \eta_{1k}}{\partial \tau^2} \right) + \left( \frac{\partial \eta_{1j}}{\partial \xi_i} \frac{\partial^2 \eta_{2j}}{\partial \tau^2} + \frac{\partial \eta_{2j}}{\partial \xi_i} \frac{\partial^2 \eta_{1j}}{\partial \tau^2} \right) \\
&- \frac{\partial}{\partial \xi_i} \left( \left( \frac{\partial \eta_{1j}}{\partial \xi_j} \frac{\partial \eta_{2k}}{\partial \xi_k} - \frac{\partial \eta_{1j}}{\partial \xi_k} \frac{\partial \eta_{2k}}{\partial \xi_j} \right) \right) \\
&+ \frac{1}{3} \frac{\partial \eta_{1j}}{\partial \xi_k} \frac{\partial \eta_{1k}}{\partial \xi_n} \frac{\partial \eta_{1n}}{\partial \xi_j} + \frac{1}{6} \frac{\partial \eta_{1j}}{\partial \xi_j} \frac{\partial \eta_{1k}}{\partial \xi_k} \frac{\partial \eta_{1n}}{\partial \xi_n} - \frac{1}{2} \frac{\partial \eta_{1j}}{\partial \xi_k} \frac{\partial \eta_{1k}}{\partial \xi_j} \frac{\partial \eta_{1n}}{\partial \xi_n}. \tag{2.23}
\end{aligned}$$

Here,  $i, j, k, n \in \{1, 2, 3\}$ .

#### 2.1.4 Harmonically Oscillating Function

In the previous subsection we derived nine differential equations for the components of the functions  $\boldsymbol{\eta}_1(\tau, \boldsymbol{\xi})$ ,  $\boldsymbol{\eta}_2(\tau, \boldsymbol{\xi})$  and  $\boldsymbol{\eta}_3(\tau, \boldsymbol{\xi})$  which approximate the unknown function  $\boldsymbol{\eta}(\tau, \boldsymbol{\xi})$ . These equations, however, have to be simplified, yet. Therefore, we have to assume that the function  $\boldsymbol{\eta}(\tau, \boldsymbol{\xi})$  oscillates harmonically

in time<sup>1</sup>, i.e. it can be written in the following way

$$\begin{aligned} \boldsymbol{\eta}(\tau, \boldsymbol{\xi}) &= \Re(\boldsymbol{\eta}_1(\boldsymbol{\xi})e^{i\tau}) + \varepsilon \Re(\boldsymbol{\eta}_2(\boldsymbol{\xi})e^{2i\tau} + \boldsymbol{\theta}_2(\boldsymbol{\xi})) \\ &+ \varepsilon^2 \Re(\boldsymbol{\eta}_3(\boldsymbol{\xi})e^{3i\tau} + \boldsymbol{\theta}_3(\boldsymbol{\xi})e^{i\tau}) + \mathcal{O}(\varepsilon^3), \end{aligned} \quad (2.24)$$

where the functions  $\boldsymbol{\eta}_1(\boldsymbol{\xi})$ ,  $\boldsymbol{\eta}_2(\boldsymbol{\xi})$ ,  $\boldsymbol{\eta}_3(\boldsymbol{\xi})$ ,  $\boldsymbol{\theta}_2(\boldsymbol{\xi})$  and  $\boldsymbol{\theta}_3(\boldsymbol{\xi})$  are sufficiently smooth complex valued functions. Such a structure does not contradict the expansion (2.18)<sup>2</sup>, hence, the structure of the equations (2.21)–(2.23) remains unchanged. We have to mention that we do not investigate the question of covering all possible solutions by (2.24).

Taking into account the harmonic dependence on temporal variable, cf. (2.24), we are able to rewrite the equations (2.21)–(2.23) into simpler vector form, i.e.

$$\nabla_{\boldsymbol{\xi}} \langle \nabla_{\boldsymbol{\xi}}, \boldsymbol{\eta}_1 \rangle + \boldsymbol{\eta}_1 = 0, \quad (2.25)$$

$$\nabla_{\boldsymbol{\xi}} \langle \nabla_{\boldsymbol{\xi}}, \boldsymbol{\eta}_2 \rangle + 4\boldsymbol{\eta}_2 = \frac{\nabla_{\boldsymbol{\xi}}}{4} \left[ (\gamma - 1) \langle \nabla_{\boldsymbol{\xi}}, \boldsymbol{\eta}_1 \rangle^2 - \langle \boldsymbol{\eta}_1, \boldsymbol{\eta}_1 \rangle + \frac{\partial \eta_{1j}}{\partial \xi_k} \frac{\partial \eta_{1k}}{\partial \xi_j} \right], \quad (2.26)$$

$$\begin{aligned} \nabla_{\boldsymbol{\xi}} \langle \nabla_{\boldsymbol{\xi}}, \boldsymbol{\eta}_3 \rangle + 9\boldsymbol{\eta}_3 &= \frac{\nabla_{\boldsymbol{\xi}}}{2} \left[ -\frac{(\gamma - 1)^2}{12} \langle \nabla_{\boldsymbol{\xi}}, \boldsymbol{\eta}_1 \rangle^3 - \langle \boldsymbol{\eta}_1, \boldsymbol{\eta}_2 \rangle \right. \\ &- \frac{\gamma - 1}{4} \langle \nabla_{\boldsymbol{\xi}}, \boldsymbol{\eta}_1 \rangle \frac{\partial \eta_{1j}}{\partial \xi_k} \frac{\partial \eta_{1k}}{\partial \xi_j} - \frac{1}{6} \frac{\partial \eta_{1j}}{\partial \xi_k} \frac{\partial \eta_{1k}}{\partial \xi_n} \frac{\partial \eta_{1n}}{\partial \xi_j} + \frac{\partial \eta_{1j}}{\partial \xi_k} \frac{\partial \eta_{2k}}{\partial \xi_j} \\ &\left. + (\gamma - 1) \langle \nabla_{\boldsymbol{\xi}}, \boldsymbol{\eta}_1 \rangle \langle \nabla_{\boldsymbol{\xi}}, \boldsymbol{\eta}_2 \rangle \right] - \frac{3}{2} \left( \frac{\partial \eta_{1j}}{\partial \xi_i} \eta_{2j} \right)_{i=1}^3, \end{aligned} \quad (2.27)$$

where the term  $\left( \frac{\partial \eta_{1j}}{\partial \xi_i} \eta_{2j} \right)_{i=1}^3$  denotes the vector  $\left( \frac{\partial \eta_{1j}}{\partial \xi_1} \eta_{2j}, \frac{\partial \eta_{1j}}{\partial \xi_2} \eta_{2j}, \frac{\partial \eta_{1j}}{\partial \xi_3} \eta_{2j} \right)^T$ . The equations for the functions  $\boldsymbol{\theta}_2$  and  $\boldsymbol{\theta}_3$  can be derived in a straightforward manner.

## 2.2 Helmholtz Type Equations for the Pressure

It seems to be inconvenient to solve all nine differential equations (2.25)–(2.27) instead of solving the complete Euler system (2.1)–(2.3). Moreover, the type of the equations (2.25)–(2.27) cannot be determined at the first glance. We do not really know either these equations do have solutions in some suitable space or they do not have (we also have to define boundary conditions). Moreover, we

<sup>1</sup>In practice, such an assumption may not hold. This is the problem of the right control of the electromagnetic system but not the modeling problem.

<sup>2</sup>For the sake of simplicity we do not introduce new variables here to denote  $\boldsymbol{\eta}_1(\boldsymbol{\xi})$ ,  $\boldsymbol{\eta}_2(\boldsymbol{\xi})$  and  $\boldsymbol{\eta}_3(\boldsymbol{\xi})$ , but we have to distinguish them from the functions defined in (2.18).

have to find an appropriate numerical scheme to solve these equations if there exists at most one solution. Therefore, it seems to be worth to simplify the equations (2.25)–(2.27) further in order to get, hopefully, beautiful equations of certain type.

Let us assume the existence of the expansion for the pressure function  $p(\tau, \boldsymbol{\xi})$ , i.e.

$$\begin{aligned} p(\tau, \boldsymbol{\xi}) = & \varrho_0 c_0^2 \Re \left[ \frac{1}{\gamma} + \varepsilon p_1(\boldsymbol{\xi}) e^{i\tau} + \varepsilon^2 (p_2(\boldsymbol{\xi}) e^{2i\tau} + q_2(\boldsymbol{\xi})) \right. \\ & \left. + \varepsilon^3 (p_3(\boldsymbol{\xi}) e^{3i\tau} + q_3(\boldsymbol{\xi}) e^{i\tau}) \right] + \mathcal{O}(\varepsilon^4). \end{aligned} \quad (2.28)$$

This expansion will be frequently used in the following analysis. Hopefully, this expansion does not contradict the physical behaviour of the sound. It arises due to harmonic oscillations of the membrane and propagates through non-linear medium.

On the other hand, let us consider the isentropic state equation (2.3) (written in Eulerian coordinates) and its equivalent expression (2.10) (written in Lagrangian form). We expand this later expression in terms of the displacement function  $\boldsymbol{\eta}$ , collect the terms of equal  $\varepsilon$  powers and time factors and compare with appropriate terms in (2.28). As a result we get

$$p_1 = -\langle \nabla_{\boldsymbol{\xi}}, \boldsymbol{\eta}_1 \rangle, \quad (2.29)$$

$$p_2 = -\langle \nabla_{\boldsymbol{\xi}}, \boldsymbol{\eta}_2 \rangle + \frac{\gamma}{4} \langle \nabla_{\boldsymbol{\xi}}, \boldsymbol{\eta}_1 \rangle^2 + \frac{1}{4} \frac{\partial \eta_{1j}}{\partial \xi_k} \frac{\partial \eta_{1k}}{\partial \xi_j}, \quad (2.30)$$

$$\begin{aligned} p_3 = & -\langle \nabla_{\boldsymbol{\xi}}, \boldsymbol{\eta}_3 \rangle + \frac{\gamma}{2} \langle \nabla_{\boldsymbol{\xi}}, \boldsymbol{\eta}_1 \rangle \langle \nabla_{\boldsymbol{\xi}}, \boldsymbol{\eta}_2 \rangle + \frac{1}{2} \frac{\partial \eta_{1j}}{\partial \xi_k} \frac{\partial \eta_{2k}}{\partial \xi_j} - \frac{\gamma^2}{24} \langle \nabla_{\boldsymbol{\xi}}, \boldsymbol{\eta}_1 \rangle^3 \\ & - \frac{\gamma}{8} \frac{\partial \eta_{1j}}{\partial \xi_k} \frac{\partial \eta_{1k}}{\partial \xi_j} \langle \nabla_{\boldsymbol{\xi}}, \boldsymbol{\eta}_1 \rangle - \frac{1}{12} \frac{\partial \eta_{1j}}{\partial \xi_k} \frac{\partial \eta_{1k}}{\partial \xi_n} \frac{\partial \eta_{1n}}{\partial \xi_j}. \end{aligned} \quad (2.31)$$

Applying the gradient operator to both sides of the relations (2.29), (2.30) and (2.31), taking into account the equations (2.25), (2.26) and (2.27) we get the expressions for the functions  $\boldsymbol{\eta}_1$ ,  $\boldsymbol{\eta}_2$  and  $\boldsymbol{\eta}_3$  written in terms of  $p_1$ ,  $p_2$  and  $p_3$ . Inserting these relations into the equations (2.25), (2.26) and (2.27) and integrating the results with respect to  $\xi_i$ ,  $i \in \{1, 2, 3\}$  (we assume that the integration constants are zeros), we end up with the equations for the functions

$p_1$ ,  $p_2$  and  $p_3$ , i.e.

$$\Delta_{\xi} p_1 + p_1 = 0, \quad (2.32)$$

$$\Delta_{\xi} p_2 + 4p_2 = \left( \gamma - \frac{1}{2} \right) p_1^2 + \frac{3}{2} \left( \frac{\partial^2 p_1}{\partial \xi_j \partial \xi_k} \right)^2, \quad (2.33)$$

$$\begin{aligned} \Delta_{\xi} p_3 + 9p_3 &= -\frac{3 \left( \gamma - \frac{1}{2} \right) \left( \gamma - \frac{1}{3} \right)}{4} p_1^3 + \frac{9\gamma - 5}{2} p_1 p_2 - \frac{1}{8} p_1 \left( \frac{\partial^2 p_1}{\partial \xi_j \partial \xi_k} \right)^2 \\ &+ \frac{7}{4} \frac{\partial^2 p_1}{\partial \xi_j \partial \xi_k} \frac{\partial^2 p_2}{\partial \xi_j \partial \xi_k} - \frac{5}{8} \frac{\partial p_1}{\partial \xi_j} \frac{\partial^2 p_1}{\partial \xi_k \partial \xi_n} \frac{\partial^3 p_1}{\partial \xi_j \partial \xi_k \partial \xi_n} \\ &- \frac{13}{8} \frac{\partial^2 p_1}{\partial \xi_j \partial \xi_k} \frac{\partial^2 p_1}{\partial \xi_k \partial \xi_n} \frac{\partial^2 p_1}{\partial \xi_n \partial \xi_j} - \frac{5}{8} \frac{\partial p_1}{\partial \xi_j} \frac{\partial p_1}{\partial \xi_k} \frac{\partial^2 p_1}{\partial \xi_j \partial \xi_k}. \end{aligned} \quad (2.34)$$

In dimensional variables these equations look as follows

$$\Delta_{\mathbf{x}} p_1 + \kappa^2 p_1 = 0, \quad (2.35)$$

$$\Delta_{\mathbf{x}} p_2 + 4\kappa^2 p_2 = \left( \gamma - \frac{1}{2} \right) \kappa^2 p_1^2 + \frac{3}{2\kappa^2} \left( \frac{\partial^2 p_1}{\partial x_j \partial x_k} \right)^2, \quad (2.36)$$

$$\begin{aligned} \Delta_{\mathbf{x}} p_3 + 9\kappa^2 p_3 &= \kappa^2 p_1 \left[ -\frac{3 \left( \gamma - \frac{1}{2} \right) \left( \gamma - \frac{1}{3} \right)}{4} p_1^2 + \frac{9\gamma - 5}{2} p_2 \right. \\ &- \left. \frac{1}{8\kappa^4} p_1 \left( \frac{\partial^2 p_1}{\partial x_j \partial x_k} \right)^2 \right] + \frac{7}{4\kappa^2} \frac{\partial^2 p_1}{\partial x_j \partial x_k} \frac{\partial^2 p_2}{\partial x_j \partial x_k} \\ &- \frac{5}{8\kappa^4} \frac{\partial p_1}{\partial x_j} \frac{\partial^2 p_1}{\partial x_k \partial x_n} \frac{\partial^3 p_1}{\partial x_j \partial x_k \partial x_n} \\ &- \frac{13}{8\kappa^4} \frac{\partial^2 p_1}{\partial x_j \partial x_k} \frac{\partial^2 p_1}{\partial x_k \partial x_n} \frac{\partial^2 p_1}{\partial x_n \partial x_j} - \frac{5}{8\kappa^2} \frac{\partial p_1}{\partial x_j} \frac{\partial p_1}{\partial x_k} \frac{\partial^2 p_1}{\partial x_j \partial x_k}. \end{aligned} \quad (2.37)$$

We have got three decoupled scalar equations of Helmholtz type for the unknowns  $p_1$ ,  $p_2$  and  $p_3$ . Very important to note that the function  $q_3$  affects the behaviour of the linear component of the pressure, cf. (2.28). The equations for the functions  $q_2$  and  $q_3$  can be derived in the same manner. In the non-dimensional variables the equations are the following

$$q_2 = \frac{1}{4} |p_1|^2 + \frac{1}{4} \left| \frac{\partial p_1}{\partial \xi_j} \right|^2, \quad (2.38)$$



$$\begin{aligned}
\Delta_{\xi} q_3 + q_3 &= \frac{-2\gamma^2 + 9\gamma - 5}{8} p_1 |p_1|^2 + \frac{\gamma - 5}{2} p_2 \bar{p}_1 + \frac{3}{4} \bar{p}_1 \left( \frac{\partial^2 p_1}{\partial \xi_j \partial \xi_k} \right)^2 \\
&+ \frac{\gamma - 1}{4} p_1 \left| \frac{\partial p_1}{\partial \xi_j} \right|^2 + \frac{3}{4} \frac{\partial^2 p_2}{\partial \xi_j \partial \xi_k} \frac{\partial^2 \bar{p}_1}{\partial \xi_j \partial \xi_k} + \frac{1}{2} \frac{\partial p_1}{\partial \xi_j} \frac{\partial \bar{p}_1}{\partial \xi_k} \frac{\partial^2 p_1}{\partial \xi_j \partial \xi_k} \\
&- \frac{1}{8} \frac{\partial p_1}{\partial \xi_j} \frac{\partial p_1}{\partial \xi_k} \frac{\partial^2 \bar{p}_1}{\partial \xi_j \partial \xi_k} + \frac{1}{8} p_1 \left| \frac{\partial^2 p_1}{\partial \xi_j \partial \xi_k} \right|^2 + 2 \frac{\partial^2 p_1}{\partial \xi_j \partial \xi_k} \frac{\partial^2 s_2}{\partial \xi_j \partial \xi_k} \\
&- \frac{5}{8} \frac{\partial^2 p_1}{\partial \xi_j \partial \xi_k} \frac{\partial^2 p_1}{\partial \xi_k \partial \xi_m} \frac{\partial^2 \bar{p}_1}{\partial \xi_m \partial \xi_j} + \frac{1}{4} \frac{\partial \bar{p}_1}{\partial \xi_j} \frac{\partial^2 p_1}{\partial \xi_k \partial \xi_m} \frac{\partial^3 p_1}{\partial \xi_j \partial \xi_k \partial \xi_m} \\
&- \frac{1}{8} \frac{\partial p_1}{\partial \xi_j} \frac{\partial^2 \bar{p}_1}{\partial \xi_k \partial \xi_m} \frac{\partial^3 p_1}{\partial \xi_j \partial \xi_k \partial \xi_m} + \frac{1}{4} \frac{\partial p_1}{\partial \xi_j} \frac{\partial^2 p_1}{\partial \xi_k \partial \xi_m} \frac{\partial^3 \bar{p}_1}{\partial \xi_j \partial \xi_k \partial \xi_m}. \quad (2.39)
\end{aligned}$$

Here, the function  $s_2$  is a potential of the function  $\theta_2$ , cf. (2.24). This assumption we made in order to simplify our derivation.  $s_2$  is auxiliary quantity and it is the solution of the Poisson's equation, where the right hand side depends on the function  $p_1$  and its derivatives

$$\Delta_{\xi} s_2 = \frac{\gamma - 1}{4} |p_1|^2 - \frac{1}{4} \left| \frac{\partial p_1}{\partial \xi_j} \right|^2 + \frac{1}{4} \left| \frac{\partial^2 p_1}{\partial \xi_j \partial \xi_k} \right|^2. \quad (2.40)$$

In dimensional variables the above mentioned equations are

$$q_2 = \frac{1}{4} |p_1|^2 + \frac{1}{4\kappa^2} \left| \frac{\partial p_1}{\partial x_j} \right|^2, \quad (2.41)$$

$$\begin{aligned}
\Delta_{\mathbf{x}} q_3 + \kappa^2 q_3 &= \frac{-2\gamma^2 + 9\gamma - 5}{8} \kappa^2 p_1 |p_1|^2 + \frac{\gamma - 5}{2} \kappa^2 p_2 \bar{p}_1 + \frac{3}{4\kappa^2} \bar{p}_1 \left( \frac{\partial^2 p_1}{\partial x_j \partial x_k} \right)^2 \\
&+ \frac{\gamma - 1}{4} p_1 \left| \frac{\partial p_1}{\partial x_j} \right|^2 + \frac{3}{4\kappa^2} \frac{\partial^2 p_2}{\partial x_j \partial x_k} \frac{\partial^2 \bar{p}_1}{\partial x_j \partial x_k} + \frac{1}{2\kappa^2} \frac{\partial p_1}{\partial x_j} \frac{\partial \bar{p}_1}{\partial x_k} \frac{\partial^2 p_1}{\partial x_j \partial x_k} \\
&- \frac{1}{8\kappa^2} \frac{\partial p_1}{\partial x_j} \frac{\partial p_1}{\partial x_k} \frac{\partial^2 \bar{p}_1}{\partial x_j \partial x_k} + \frac{1}{8\kappa^2} p_1 \left| \frac{\partial^2 p_1}{\partial x_j \partial x_k} \right|^2 \\
&- \frac{5}{8\kappa^4} \frac{\partial^2 p_1}{\partial x_j \partial x_k} \frac{\partial^2 p_1}{\partial x_k \partial x_m} \frac{\partial^2 \bar{p}_1}{\partial x_m \partial x_j} + \frac{1}{4\kappa^4} \frac{\partial \bar{p}_1}{\partial x_j} \frac{\partial^2 p_1}{\partial x_k \partial x_m} \frac{\partial^3 p_1}{\partial x_j \partial x_k \partial x_m} \\
&- \frac{1}{8\kappa^4} \frac{\partial p_1}{\partial x_j} \frac{\partial^2 \bar{p}_1}{\partial x_k \partial x_m} \frac{\partial^3 p_1}{\partial x_j \partial x_k \partial x_m} + \frac{1}{4\kappa^4} \frac{\partial p_1}{\partial x_j} \frac{\partial^2 p_1}{\partial x_k \partial x_m} \frac{\partial^3 \bar{p}_1}{\partial x_j \partial x_k \partial x_m} \\
&+ \frac{2}{\kappa^2} \frac{\partial^2 p_1}{\partial x_j \partial x_k} \frac{\partial^2 s_2}{\partial x_j \partial x_k} \quad (2.42)
\end{aligned}$$

and

$$\Delta_{\mathbf{x}} s_2 = \frac{\gamma - 1}{4} \kappa^2 |p_1|^2 - \frac{1}{4} \left| \frac{\partial p_1}{\partial x_j} \right|^2 + \frac{1}{4\kappa^2} \left| \frac{\partial^2 p_1}{\partial x_j \partial x_k} \right|^2. \quad (2.43)$$

### 2.3 Comparison of the Models

Obviously, there are many other ways to linearize given Euler system (2.1)–(2.3). Mostly, in the literature a second order approximation is considered. In

this section, we compare the equations for the pressure derived above with other models.

### 2.3.1 The Idea of Existence of a Displacement Potential

Several years ago Dr. Jan Mohring derived the equations (2.35) and (2.36) using a bit different approach, cf. [49], [50]. The starting point in this case was the equation (2.11) and, hence, its non-dimensional form (2.17). Also, the asymptotic expansion (2.18) has been assumed. Using (2.18) one was able to expand the equation (2.17) with respect to  $\varepsilon$  and to get two<sup>3</sup> equations (2.21)–(2.22), cf. [49], [50]. The equation (2.23) was derived later in [40]. Until now all the transformations are identical. Starting from this point several assumptions about the air flow inside the loudspeaker have been made:

1. The initial air flow is irrotational;
2. The gradient of the velocity remains uniformly bounded;
3. The moving surface oscillates harmonically at angular frequency  $\omega$ .

The claim was the following: if the first two conditions are satisfied then the flow will always be irrotational, cf. [49], [21]. Third condition allows to simplify the derivations of the equations and boundary conditions<sup>4</sup>. Further, one assumes the following ansatz for the components of the displacement  $\boldsymbol{\eta}$

$$\boldsymbol{\eta}_1 = \nabla_{\boldsymbol{\xi}}\varphi_1 = \nabla_{\boldsymbol{\xi}}\Re(\phi_1(\boldsymbol{\xi})e^{i\tau}), \quad (2.44)$$

$$\boldsymbol{\eta}_2 = \nabla_{\boldsymbol{\xi}}\varphi_2 = \nabla_{\boldsymbol{\xi}}\Re(\phi_2(\boldsymbol{\xi})e^{2i\tau} + \psi_2(\boldsymbol{\xi})). \quad (2.45)$$

For the further analysis we present also the ansatz for the function  $\boldsymbol{\eta}_3$

$$\boldsymbol{\eta}_3 = \nabla_{\boldsymbol{\xi}}\varphi_3 = \nabla_{\boldsymbol{\xi}}\Re(\phi_3(\boldsymbol{\xi})e^{3i\tau} + \psi_3(\boldsymbol{\xi})e^{i\tau}). \quad (2.46)$$

Here, the functions  $\phi_1, \phi_2, \phi_3, \psi_2$  and  $\psi_3$  are sufficiently smooth complex valued potentials.

The idea was to derive the differential equations for the potentials of the displacement functions. These equations are of Helmholtz type. Inserting (2.44) and (2.45) into (2.21) and (2.22), respectively, collecting for the time factors  $e^{\pm i\tau}$  and  $e^{\pm 2i\tau}$ , and integrating once with respect to  $\boldsymbol{\xi}$  we got

$$\Delta_{\boldsymbol{\xi}}\phi_1 + \phi_1 = 0, \quad (2.47)$$

$$\Delta_{\boldsymbol{\xi}}\phi_2 + 4\phi_2 = \frac{1}{4} \left[ (\gamma - 1)\phi_1^2 - (\nabla_{\boldsymbol{\xi}}\phi_1)^2 + \left( \frac{\partial^2 \phi_1}{\partial \xi_j \partial \xi_k} \right)^2 \right]. \quad (2.48)$$

<sup>3</sup>The author was interested only in the second order correction.

<sup>4</sup>We also made such an assumption in the section 2.1.4.

The integration constants, obviously, were chosen equal to zero. This does not influence the result because the potentials are unique only up to a constant.

Further, the relations (2.10) and (2.28) have been used in order to find the relations between the pressure and potential functions. These relations are the following

$$\phi_1 = p_1, \quad (2.49)$$

$$\phi_2 = \frac{1}{4}p_2 - \frac{1}{16}p_1^2 - \frac{1}{16}(\nabla_{\boldsymbol{\xi}}p_1)^2. \quad (2.50)$$

Inserting these relations into (2.47) and (2.48) we end up with the equations (2.32) and (2.33), and, hence, with the equations (2.35) and (2.36).

Here, we have to mention that this idea of the displacement potentials does not help to derive the equation for  $p_3$  function. Precisely speaking, no potential for the function  $\boldsymbol{\eta}_3$  exists. There are at least two rather simple ways to prove non-existence of the displacement potential  $\varphi_3$ . One of them can be found in [40] and [43] another one we present here. The idea is very simple: we apply the operator  $\nabla_{\boldsymbol{\xi}} \times$  (or simply rotor) to the equation (2.27). There is well known property

$$\nabla_{\boldsymbol{\xi}} \times \nabla_{\boldsymbol{\xi}} \varphi = 0 \text{ (for all } \varphi \text{ smooth enough)}$$

which we would like to use in our analysis. Obviously, if the potential of the  $\boldsymbol{\eta}_3$  function would exist, then the rotor of the right hand side of (2.27) has to be equal identically to zero. But, unfortunately, it is not the case. The expression

$$\nabla_{\boldsymbol{\xi}} \times \left( \frac{\partial \eta_{1j}}{\partial \xi_1} \eta_{2j}, \frac{\partial \eta_{1j}}{\partial \xi_2} \eta_{2j}, \frac{\partial \eta_{1j}}{\partial \xi_3} \eta_{2j} \right)^T,$$

in general, is not equal to zero. Hence, if the displacement function  $\boldsymbol{\eta}_3$  would have certain potential  $\varphi_3$ , we would get nonsense. Therefore, the function  $\phi_3$  does not exist and we cannot apply the idea of displacement potential in order to derive the equation (2.37).

As a consequence, we have to mention that the derivations of the equations (2.35) and (2.36) using our approach and using the idea of displacement potential do not differ too much. These two approaches have the same kernel, namely, the equations (2.21) and (2.22). However, in our derivation we do not utilize any assumption about the fluid flow. This is rather nice advantage, because we are not restricted to consider only some special fluid flows. Also, as a consequence, we are able to derive third order correction, i.e. differential equation (2.37) for the function  $p_3$ .

### 2.3.2 Comparison with Kuznetsov's Model

In order to check legality of the equations (2.35)–(2.37) we can compare them to some really classical result. One of the most famous equation is so-called

Kuznetsov's equation. It has been derived in 1969 by the Russian mathematician V.P.Kuznetsov. Kuznetsov's equation has been obtained from the set of equations (Navier–Stokes system) for the dynamics of a 3D viscous heat-conducting fluid under assumption of a potential character motion, cf. [45]. This set of equations reduces to a single nonlinear wave equation<sup>5</sup> for the scalar potential  $W$  (here,  $\mathbf{u} = -\nabla_{\tilde{\mathbf{x}}}W$ ), i.e.

$$\frac{\partial^2 W}{\partial \tilde{t}^2} - c_0^2 \Delta_{\tilde{\mathbf{x}}} W = \frac{\partial}{\partial \tilde{t}} \left[ b \Delta_{\tilde{\mathbf{x}}} W + (\nabla_{\tilde{\mathbf{x}}} W)^2 + a \left( \frac{\partial W}{\partial \tilde{t}} \right)^2 \right], \quad (2.51)$$

where " $\sim$ " denotes the Euler coordinates,  $a = \frac{\gamma-1}{2c_0^2}$ .  $b$  depends on the shear and bulk viscosities, on the thermal conductivity and on the heat capacities at constant pressure and constant volume. The parameter  $b$  is equal to zero if we neglect the viscosity of the fluid and heat exchange in the system. Further, to compare our model to Kuznetsov's model, we have to non-dimensionalize the equation (2.51)<sup>6</sup>, i.e. we introduce non-dimensional velocity potential  $U := \frac{\kappa}{\ell\omega}W$  and rewrite

$$\frac{\partial^2 U}{\partial \tilde{\tau}^2} - \Delta_{\tilde{\boldsymbol{\xi}}} U = \varepsilon \frac{\partial}{\partial \tilde{\tau}} \left[ (\nabla_{\tilde{\boldsymbol{\xi}}} U)^2 + \frac{\gamma-1}{2} \left( \frac{\partial U}{\partial \tilde{\tau}} \right)^2 \right]. \quad (2.52)$$

Here, as above, we introduced non-dimensional time  $\tilde{\tau} = \omega \tilde{t}$  and non-dimensional space coordinate  $\tilde{\boldsymbol{\xi}} = \kappa \tilde{\mathbf{x}}$ . In order to compare the equations (2.35) and (2.36) to the equation (2.52) we have to rewrite the latter equation in Lagrangian coordinates. Omitting the details, which can be easily obtained by straightforward calculations, we end up with Kuznetsov's equation written in Lagrangian coordinates

$$\begin{aligned} \frac{\partial^2 U}{\partial \tau^2} - \Delta_{\boldsymbol{\xi}} U &= \varepsilon \left[ \frac{\partial}{\partial \tau} \left( \frac{\partial \eta_j}{\partial \tau} \frac{\partial U}{\partial \xi_j} \right) + \frac{\partial \eta_j}{\partial \tau} \frac{\partial^2 U}{\partial \xi_j \partial \tau} - \frac{\partial}{\partial \xi_i} \left( \frac{\partial \eta_j}{\partial \xi_i} \frac{\partial U}{\partial \xi_j} \right) \right. \\ &\quad \left. - \frac{\partial \eta_j}{\partial \xi_i} \frac{\partial^2 U}{\partial \xi_j \partial \xi_i} + \frac{\partial}{\partial \tau} \left( (\nabla_{\boldsymbol{\xi}} U)^2 + \frac{\gamma-1}{2} \left( \frac{\partial U}{\partial \tau} \right)^2 \right) \right]. \end{aligned} \quad (2.53)$$

We expand the function  $U$  into series<sup>7</sup> with respect to  $\varepsilon$  in the same manner as we expanded the function  $\boldsymbol{\eta}$ , cf. (2.18). Moreover, because of the harmonic movement of the membrane inside the loudspeaker<sup>8</sup>, we define

$$U(\boldsymbol{\xi}, \tau) = \Re (U_1(\boldsymbol{\xi})e^{i\tau} + \varepsilon (U_2(\boldsymbol{\xi})e^{2i\tau} + V_2(\boldsymbol{\xi})) + \mathcal{O}(\varepsilon^2)). \quad (2.54)$$

Now, we have to find the relations between the functions  $p_1$ ,  $p_2$  and  $U_1$ ,  $U_2$ . Remember, the velocity can be expressed in terms of displacement function  $\mathbf{h}$ .

<sup>5</sup>Which is written in Eulerian coordinates.

<sup>6</sup>Taking into account that  $b = 0$ .

<sup>7</sup>The convergence of the series is assumed.

<sup>8</sup>We made this assumption earlier.

Hence, the non-dimensional velocity expresses as

$$\frac{1}{\ell\omega}\mathbf{u} = \frac{1}{\ell\omega}\frac{\partial\mathbf{h}}{\partial t} = \frac{\partial\boldsymbol{\eta}}{\partial\tau}. \quad (2.55)$$

On the other hand, we know that  $\mathbf{u} = -\nabla_{\bar{\mathbf{x}}}W$  or  $\frac{1}{\ell\omega}\mathbf{u} = -\nabla_{\xi}U$ . Transforming the latter expression into Lagrangian coordinates and taking into account the relation (2.55) we obtain

$$\frac{\partial\eta_i}{\partial\tau} + \varepsilon\frac{\partial\eta_j}{\partial\tau}\frac{\partial\eta_j}{\partial\xi_i} = -\frac{\partial U}{\partial\xi_i}, \quad i, j \in \{1, 2, 3\}. \quad (2.56)$$

From the expression (2.56) we get the relations between the functions  $p_1$ ,  $p_2$  and  $U_1$ ,  $U_2$ , i.e.

$$U_1 = -ip_1, \quad (2.57)$$

$$U_2 = -\frac{i}{2}p_2 + \frac{i}{8}\langle\nabla_{\xi}, \nabla_{\xi}p_1\rangle^2 - \frac{i}{8}(\nabla_{\xi}p_1)^2. \quad (2.58)$$

Using these relations and the equation (2.53) we get exactly the equations (2.32) and (2.33), cf. Sections 2.1.3–2.2. Consequently, we can asseverate that our model (up to second correction order) is of the same accuracy as Kuznetsov's model. From our point of view our model is much more convenient. The acoustic pressure is the unknown quantity, and experimentally easier to measure exactly the pressure perturbations rather than the potential of the velocity.

### 2.3.3 Bjorno–Beyer Model

Another rather popular model was given in [16], [11] and [9]. Unfortunately, it differs from our model by few terms. Let us consider the mass conservation law written in Lagrangian coordinates, i.e.

$$\frac{\partial\varrho}{\partial t} + \varrho F^{-T}\nabla_{\mathbf{x}}\frac{\partial\mathbf{h}}{\partial t} = 0. \quad (2.59)$$

Assume that the density function  $\varrho$  can be represented as a series

$$\varrho = \varrho_0 + \varrho_1 + \varrho_2 + \dots, \quad (2.60)$$

where  $\varrho_0$  is a constant (density of a fluid at rest) and each term  $\varrho_j$  satisfies the condition  $\varrho_j = o(\varrho_k)$ , where  $k < j \in \mathbb{N}_0$ . In other words, the series given above represents an asymptotic expansion with respect to some "small" quantity. Similar expansion we assume for the displacement  $\mathbf{h}$ , i.e.

$$\mathbf{h} = \mathbf{h}_1 + \mathbf{h}_2 + \dots \quad (2.61)$$

Next, we insert both expansions of  $\varrho$  and  $\mathbf{h}$  functions into the equation (2.59) and after the collection of similar terms we end up with first and second order

differential equations for unknown functions  $\varrho_1$ ,  $\varrho_2$ ,  $\mathbf{h}_1$  and  $\mathbf{h}_2$ , i.e.

$$\frac{\partial \varrho_1}{\partial t} = -\varrho_0 \left\langle \nabla_{\mathbf{x}}, \frac{\partial \mathbf{h}_1}{\partial t} \right\rangle, \quad (2.62)$$

$$\frac{\partial \varrho_2}{\partial t} = -\varrho_0 \left\langle \nabla_{\mathbf{x}}, \frac{\partial \mathbf{h}_2}{\partial t} \right\rangle + \varrho_0 \left\langle \nabla_{\mathbf{x}} \mathbf{h}_1^T \nabla_{\mathbf{x}}, \frac{\partial \mathbf{h}_1}{\partial t} \right\rangle - \varrho_1 \left\langle \nabla_{\mathbf{x}}, \frac{\partial \mathbf{h}_1}{\partial t} \right\rangle. \quad (2.63)$$

Now, we consider the mass conservation equation which was considered in [16], i.e.

$$\frac{\varrho_0 - \varrho}{\varrho} = \langle \nabla_{\mathbf{x}}, \mathbf{h} \rangle. \quad (2.64)$$

Plugging the expansions (2.60) and (2.61) into (2.64) we get first and second order differential equations

$$\varrho_1 = -\varrho_0 \langle \nabla_{\mathbf{x}}, \mathbf{h}_1 \rangle, \quad (2.65)$$

$$\varrho_2 = -\varrho_0 \langle \nabla_{\mathbf{x}}, \mathbf{h}_2 \rangle + \frac{\varrho_1^2}{\varrho_0}. \quad (2.66)$$

The equations (2.62)<sup>9</sup> and (2.65) coincide. Obviously, if the terms  $\frac{\partial h_{1j}}{\partial x_k}$  in (2.63) would vanish for  $j \neq k$ , then the second order differential equations (2.63)<sup>10</sup> and (2.66) would completely coincide. But we do not see any reason why the above mentioned terms have to vanish. Moreover, we present a rather simple example which shows exactly the opposite. Namely, we consider a sphere which oscillates with certain frequency. Obviously, the magnitude of the wave speed decreases with the distance to the sphere. The same is also valid for the displacement function  $\mathbf{h}$ . As it is shown in Fig. 2.3 the components of the displacement vector  $\mathbf{h}_1$  vanish at infinity. Hence, there exist  $k \neq j$  such that  $\frac{\partial h_{1j}}{\partial x_k} \neq 0$ , cf. Fig. 2.3. Therefore, the model given in [16] seems to be doubtful.

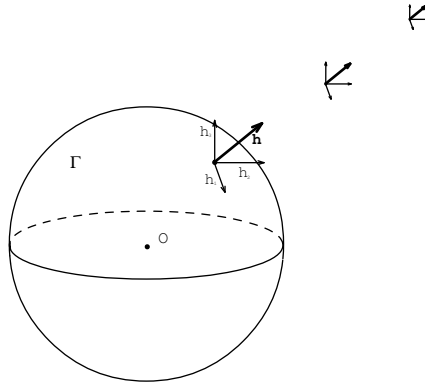


Figure 2.3: Counter-example

<sup>9</sup>After the integration with respect to time.

<sup>10</sup>After certain simplifications.

**Remark 2.3.1** We have to mention that in 1D case the above mentioned equations (2.62) and (2.63) completely coincide with (2.65) and (2.66), respectively.

There are also other models which can be compared to our model, cf. [26], [17]. But all of them have been considered under certain specific conditions and we will not consider them here.

## 2.4 Computational Domain

In this section, we define the computational domain denoted in the sequel by  $\Omega \subset \mathbb{R}^3$  or by  $\Omega^+ \subset \mathbb{R}^3$ . Apparently,  $\Omega$  does not consist only of the bass loudspeaker itself. The reason is simple: we are not only interested in the behaviour of the sound inside the loudspeaker or exactly in the aperture of the reflex tube, cf. Fig. 2.1. We are interested in the prediction of the sound behaviour in some surrounding area. Therefore, the computational domain has to consist of two parts: the loudspeaker itself and certain surrounding area. It is also clear that the computational domain in some cases has to be bounded. For example, in the cases when one uses finite element methods<sup>11</sup> to simulate the pressure field. Because of this boundedness one has to define an artificial boundary, say,  $\Gamma_r$ . On the other hand, one is able to define an exterior domain  $\Omega^+$ . To simulate the sound behaviour in such a domain some special methods are needed. Let us also note that the computational domain in Eulerian description changes its shape. To keep it fixed we introduced and use the Lagrangian coordinates only.

Let us define two possible kinds of domains which we will use in parallel in this thesis. First of all we define bounded computational domain  $\Omega \subset \mathbb{R}^3$ , cf. Fig. 2.4.

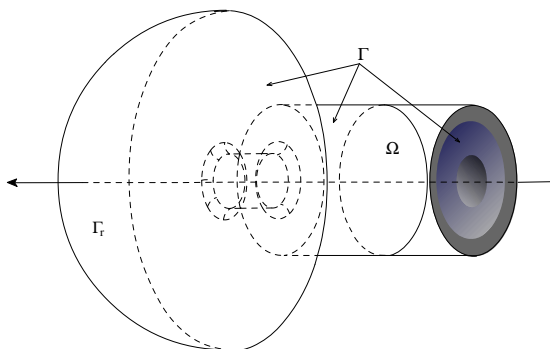


Figure 2.4: Bounded computational domain  $\Omega$

Here, all the parameters of  $\Omega$  are given and are presented in Fig. 2.5. Almost the

<sup>11</sup>We assume that the reader knows what FEM is, if not, then we refer to [8] and [13] to fill the gap.

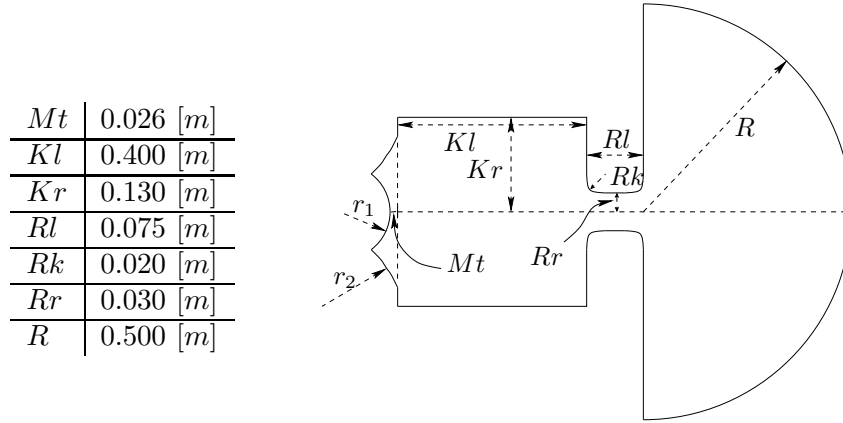


Figure 2.5: The parameters of the bass loudspeaker and surrounding area (on the left) and scheme of the bounded computational domain  $\Omega$  (2D cut) (on the right)

same parameters are used to define the exterior domain  $\Omega^+ \subset \mathbb{R}^3$ , cf. Fig. 2.6. It consists of two parts: interior and exterior part. To define the interior subdomain we used  $R = Rk + Rr$ . The only difference is that the radius  $R = Rk + Rr$ .

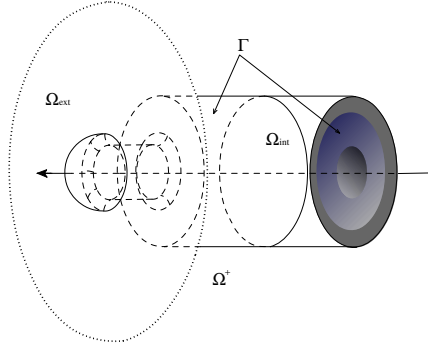


Figure 2.6: Unbounded exterior domain  $\Omega^+$ , which consists of two main parts, i.e.  $\bar{\Omega}^+ = \bar{\Omega}_{\text{ext}} \cup \bar{\Omega}_{\text{int}}$

In both cases we are able to use obvious symmetry of the domain to reduce the dimension of the problem<sup>12</sup>. But we will not reduce it because of two reasons: first of all, bass loudspeakers, in general, may have different shapes, e.g. cuboid, hexagonal or octagonal prism, etc., cf. Fig. 2.7. Therefore, there is no way to reduce the dimension of the problem<sup>13</sup> and we would have to consider exactly 3D problem. Second, the boundary conditions may be inappropriate for dimension reduction. Therefore, we would like to present certain methodology to get the

<sup>12</sup>Of course, one needs appropriate ("nice") boundary conditions.

<sup>13</sup>Even if we are lucky with the boundary conditions.



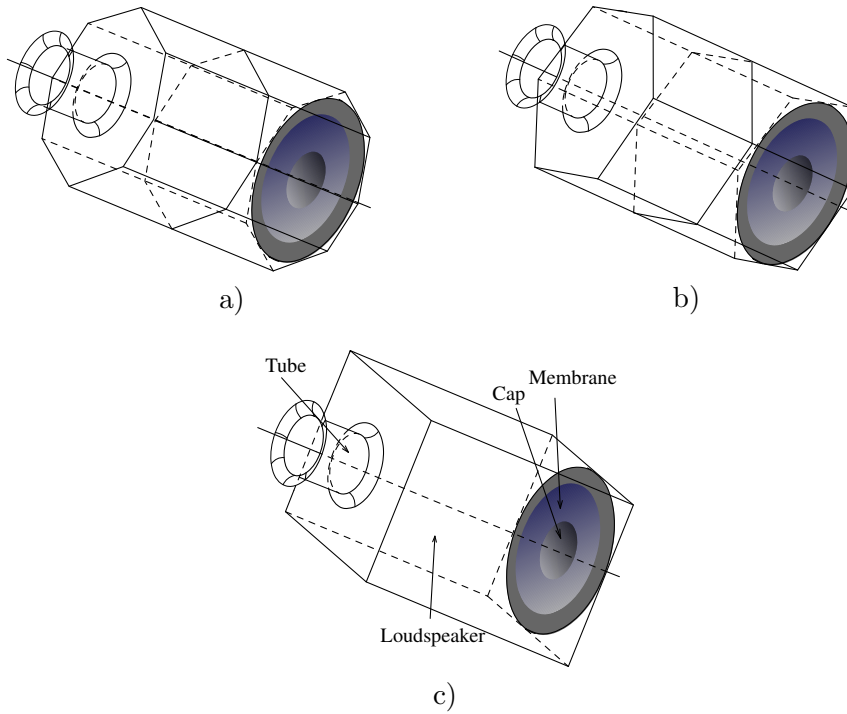


Figure 2.7: Different possible loudspeakers

solution of the problem discussed in Chapter 1, but not to solve just "some" problem.

## 2.5 Boundary Conditions

Boundary conditions are conditions which (in some cases) help to pick out an appropriate solution of a system of differential equations. Without them the system is unclosed. In order to illustrate the main idea we first consider the case of 2D domain and then come to 3D domains.

### 2.5.1 2D Domains

#### Circular Boundaries

Let us consider some part of a circle<sup>14</sup> of fixed radius  $r$  and denote it by  $\Gamma$ , cf. Fig. 2.8a. We denote the position of the center of this circle by  $\mathbf{x}_0$ . Now, we choose at a certain point  $\mathbf{x}$  on  $\Gamma$  a small control volume  $D_0$ . Next, we start to move  $\Gamma$  harmonically with angular frequency  $\omega$  along a given direction  $\boldsymbol{\nu}$ , cf. Fig. 2.8b. During the oscillations the position of the center expresses by coordinates  $\mathbf{x}_0 + \mathbf{h}_0(t)$ , where  $\mathbf{h}_0(t)$  is given and assumed to be equal to

<sup>14</sup>Note that straight lines are circles of infinite radius and from now on we will not make any difference between them.

$\ell \nu \Re(e^{i\omega t})$ . The control volume  $D_0$ , due to oscillations of  $\Gamma$  and due to very small viscosity of the air, is moving along  $\Gamma$  (we assume that the control volume sticks to  $\Gamma$ ). We do not know the position of  $D_0$ , but we know that the distance between the center of the circle and the control volume is constant, cf. Fig. 2.8b. Let us denote the position of  $D_0$  at rest by  $\mathbf{x}$  and the position after some time  $t$

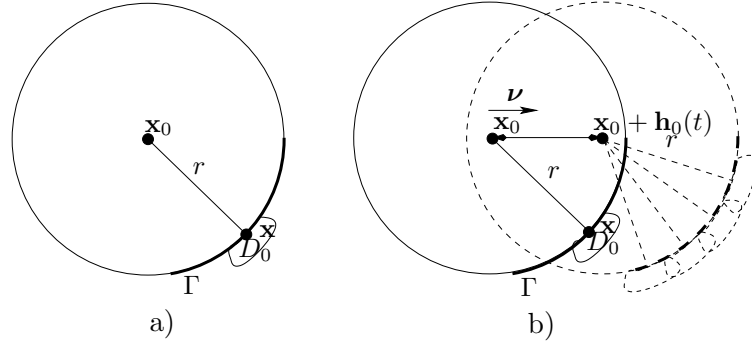


Figure 2.8: The behaviour of the circular boundary

by  $\mathbf{x} + \mathbf{h}(t, \mathbf{x})$ . In this case the following relation is fulfilled

$$|\mathbf{x} + \mathbf{h}(t, \mathbf{x}) - \mathbf{x}_0 - \mathbf{h}_0(t)|^2 = r^2. \quad (2.67)$$

This relation is written in dimensional form. For the further analysis we rewrite it in non-dimensional form

$$|-\rho \mathbf{n} + \varepsilon \boldsymbol{\eta} - \varepsilon \boldsymbol{\eta}_0|^2 = \rho^2, \quad (2.68)$$

where  $\boldsymbol{\eta}_0 = \boldsymbol{\nu} \Re(e^{i\tau})$  is given,  $\mathbf{x} - \mathbf{x}_0 = -r \mathbf{n}$ ,  $\rho = \kappa r$  is non-dimensional radius and  $\mathbf{n}$  is an outer normal (to  $\Gamma$ ) vector. From the relation (2.68) we get

$$\langle \mathbf{n}, \boldsymbol{\eta} - \boldsymbol{\eta}_0 \rangle = \varepsilon \frac{|\boldsymbol{\eta} - \boldsymbol{\eta}_0|^2}{2\rho}, \quad (2.69)$$

Inserting the relation (2.24) into (2.69) and collecting appropriate terms we end up with the boundary conditions in the case of circular boundary  $\Gamma$

$$\langle \mathbf{n}, \boldsymbol{\eta}_1 \rangle = \langle \mathbf{n}, \boldsymbol{\nu} \rangle, \quad (2.70)$$

$$\langle \mathbf{n}, \boldsymbol{\eta}_2 \rangle = \frac{1}{4\rho} (\boldsymbol{\eta}_1 - \boldsymbol{\nu})^2, \quad (2.71)$$

$$\langle \mathbf{n}, \boldsymbol{\eta}_3 \rangle = \frac{1}{2\rho} \langle \boldsymbol{\eta}_1 - \boldsymbol{\nu}, \boldsymbol{\eta}_2 \rangle. \quad (2.72)$$

These relations one can derive using straightforward asymptotic analysis. Remember, the functions  $\boldsymbol{\eta}_1$ ,  $\boldsymbol{\eta}_2$  and  $\boldsymbol{\eta}_3$  can be substituted by the pressure compo-

nents  $p_1$ ,  $p_2$  and  $p_3$ , i.e. the boundary conditions become

$$\frac{\partial p_1}{\partial \mathbf{n}} = \langle \mathbf{n}, \boldsymbol{\nu} \rangle, \quad (2.73)$$

$$\frac{\partial p_2}{\partial \mathbf{n}} = \frac{1}{\rho} (\nabla_{\boldsymbol{\xi}} p_1 - \boldsymbol{\nu})^2 + \frac{1}{4} \left\langle \mathbf{n}, \nabla_{\boldsymbol{\xi}} (p_1^2) + \nabla_{\boldsymbol{\xi}} \left( (\nabla_{\boldsymbol{\xi}} p_1)^2 \right) \right\rangle, \quad (2.74)$$

$$\begin{aligned} \frac{\partial p_3}{\partial \mathbf{n}} &= \left\langle \mathbf{n}, \frac{1}{2} \nabla_{\boldsymbol{\xi}} (p_1 p_2) - \frac{\gamma+1}{24} \nabla_{\boldsymbol{\xi}} (p_1^3) \right\rangle + \frac{n_i}{16} \left[ 8 \frac{\partial^2 p_1}{\partial \xi_i \partial \xi_j} \frac{\partial p_2}{\partial \xi_j} \right. \\ &+ 2 \frac{\partial^2 p_2}{\partial \xi_i \partial \xi_j} \frac{\partial p_1}{\partial \xi_j} - \frac{\partial p_1}{\partial \xi_i} (\nabla_{\boldsymbol{\xi}} p_1)^2 - 5 \frac{\partial p_1}{\partial \xi_j} \frac{\partial^2 p_1}{\partial \xi_j \partial \xi_i} p_1 \\ &- \left. 5 \frac{\partial^2 p_1}{\partial \xi_j \partial \xi_i} \frac{\partial p_1}{\partial \xi_k} \frac{\partial^2 p_1}{\partial \xi_j \partial \xi_k} - \frac{\partial p_1}{\partial \xi_j} \frac{\partial p_1}{\partial \xi_k} \frac{\partial^3 p_1}{\partial \xi_j \partial \xi_k \partial \xi_i} \right] \\ &+ \frac{9}{8\rho} \left\langle \nabla_{\boldsymbol{\xi}} p_1 - \boldsymbol{\nu}, \nabla_{\boldsymbol{\xi}} p_2 - \frac{1}{4} \nabla_{\boldsymbol{\xi}} (p_1^2) - \frac{1}{4} \nabla_{\boldsymbol{\xi}} \left( (\nabla_{\boldsymbol{\xi}} p_1)^2 \right) \right\rangle. \quad (2.75) \end{aligned}$$

In dimensional form these relations look as follows

$$\frac{\partial p_1}{\partial \mathbf{n}} = \langle \mathbf{n}, \kappa \boldsymbol{\nu} \rangle, \quad (2.76)$$

$$\frac{\partial p_2}{\partial \mathbf{n}} = \frac{1}{\kappa^2 r} (\nabla_{\mathbf{x}} p_1 - \kappa \boldsymbol{\nu})^2 + \frac{1}{4} \left\langle \mathbf{n}, \nabla_{\mathbf{x}} (p_1^2) + \frac{1}{\kappa^2} \nabla_{\mathbf{x}} \left( (\nabla_{\mathbf{x}} p_1)^2 \right) \right\rangle, \quad (2.77)$$

$$\begin{aligned} \frac{\partial p_3}{\partial \mathbf{n}} &= \left\langle \mathbf{n}, \frac{1}{2} \nabla_{\mathbf{x}} (p_1 p_2) - \frac{\gamma+1}{24} \nabla_{\mathbf{x}} (p_1^3) \right\rangle + \frac{n_i}{16\kappa^2} \left[ 8 \frac{\partial^2 p_1}{\partial x_i \partial x_j} \frac{\partial p_2}{\partial x_j} \right. \\ &+ 2 \frac{\partial^2 p_2}{\partial x_i \partial x_j} \frac{\partial p_1}{\partial x_j} - \frac{\partial p_1}{\partial x_i} (\nabla_{\mathbf{x}} p_1)^2 - 5 \frac{\partial p_1}{\partial x_j} \frac{\partial^2 p_1}{\partial x_j \partial x_i} p_1 \\ &- \left. \frac{5}{\kappa^2} \frac{\partial^2 p_1}{\partial x_j \partial x_i} \frac{\partial p_1}{\partial x_k} \frac{\partial^2 p_1}{\partial x_j \partial x_k} - \frac{1}{\kappa^2} \frac{\partial p_1}{\partial x_j} \frac{\partial p_1}{\partial x_k} \frac{\partial^3 p_1}{\partial x_j \partial x_k \partial x_i} \right] \\ &+ \frac{9}{8\kappa^2 r} \left\langle \nabla_{\mathbf{x}} p_1 - \kappa \boldsymbol{\nu}, \nabla_{\mathbf{x}} p_2 - \frac{1}{4} \nabla_{\mathbf{x}} (p_1^2) - \frac{1}{4\kappa^2} \nabla_{\mathbf{x}} \left( (\nabla_{\mathbf{x}} p_1)^2 \right) \right\rangle. \quad (2.78) \end{aligned}$$

Here, we used Einstein's summation convention. We emphasize once more that these are the boundary conditions for the functions  $p_1$ ,  $p_2$  and  $p_3$  in the case of arbitrary circular boundary  $\Gamma$ .

### General Non-circular Boundaries

Fortunately<sup>15</sup>, not only circular boundaries can be found in the real world and, hence, any general shaped curve may be chosen as a boundary  $\Gamma$ . Therefore, we have to find another way to define the boundary conditions for  $p_1$ ,  $p_2$  and  $p_3$  functions.

Let us consider some general non-circular curve  $\Gamma$ , cf. Fig. 2.9. The main idea is to approximate given boundary  $\Gamma$  at certain point  $\mathbf{P}$ <sup>16</sup> by a third order

<sup>15</sup>Or unfortunately.

<sup>16</sup>We assume for the further analysis that the boundary  $\Gamma$  is smooth enough at the point  $\mathbf{P}$  and in its neighbourhood.

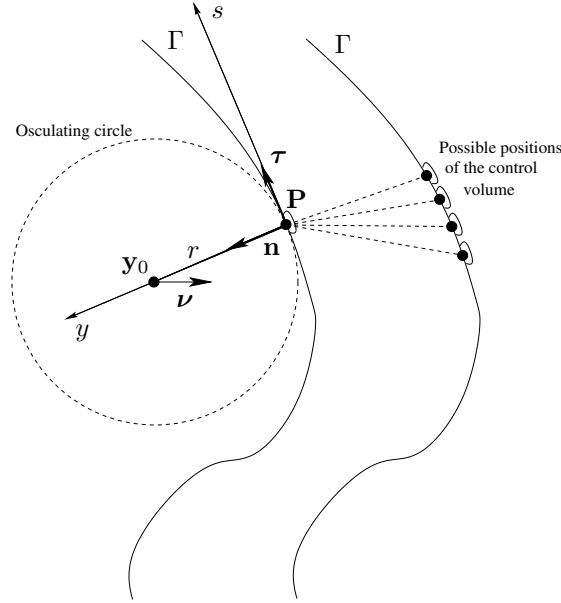


Figure 2.9: The behaviour of general 2D non-circular boundary

polynomial. Moreover, we introduce new coordinate system  $(s, y)$  with the origin at  $\mathbf{P}$ , where  $y$ -axis and the outer normal  $\mathbf{n}$  directions coincide and  $s$ -axis is tangent to  $\Gamma$  at  $\mathbf{P}$ , cf. Fig. 2.9. In the neighbourhood of the origin the boundary<sup>17</sup>  $\Gamma$  might be expressed as a function of  $s$ , say  $y(s)$ . Hence, the Taylor expansion of  $y(s)$  in the neighbourhood of the origin looks as

$$y(s) = y(0) + y'(0)s + \frac{y''(0)}{2}s^2 + \frac{y'''(0)}{6}s^3 + \mathcal{O}(s^4). \quad (2.79)$$

Simplifying the expression (2.79) and omitting the remainder  $\mathcal{O}(s^4)$  we get an approximation of the function  $y(s)$  at the point  $\mathbf{P}$

$$y(s) = \frac{\zeta}{2}s^2 + \frac{\zeta'}{6}s^3, \quad (2.80)$$

where  $\zeta = \frac{1}{r}$  represents the curvature of  $y(s)$  at the point  $s = 0$  and  $r$  is the radius of so-called osculating to  $y(s)$  circle at  $s = 0$ , cf. [32].

Let us again choose a small control volume  $D_0$  with the position at  $\mathbf{P}$  as before. Now, we move the boundary  $\Gamma$  harmonically with the angular frequency  $\omega$  along  $\boldsymbol{\nu}$ . Again, we assume the control volume  $D_0$  is moving along the boundary  $\Gamma$  only. The position of  $D_0$  at time  $t = 0$  is assumed to be equal to  $\mathbf{P} = (P_1, P_2)$ . At time  $t > 0$  new position of  $D_0$  can be expressed by

$$(P_1 + h_1(t, \mathbf{P}), P_2 + h_2(t, \mathbf{P}))^T = \mathbf{P} + \mathbf{h}(t, \mathbf{P}). \quad (2.81)$$

<sup>17</sup>Without loss of generality, we assume that the boundary  $\Gamma$  is convex at  $\mathbf{P}$  with respect to chosen coordinate system  $(s, y)$ . The concave case can be considered similarly.

From the latter relation and the expression (2.80) we obtain the boundary condition

$$\begin{aligned} \langle \mathbf{n}, \mathbf{h}(t, \mathbf{P}) - \mathbf{h}_0(t) \rangle &= \frac{\varsigma(\mathbf{P})}{2} \langle \boldsymbol{\tau}, \mathbf{h}(t, \mathbf{P}) - \mathbf{h}_0(t) \rangle^2 \\ &+ \frac{\varsigma'(\mathbf{P})}{6} \langle \boldsymbol{\tau}, \mathbf{h}(t, \mathbf{P}) - \mathbf{h}_0(t) \rangle^3 \end{aligned} \quad (2.82)$$

which again is written in dimensional form. Non-dimensional variant looks as

$$\begin{aligned} \langle \mathbf{n}, \boldsymbol{\eta}(\tau, \mathbf{P}) - \boldsymbol{\eta}_0(\tau) \rangle &= \frac{\varepsilon}{2\rho} \langle \boldsymbol{\tau}, \boldsymbol{\eta}(\tau, \mathbf{P}) - \boldsymbol{\eta}_0(\tau) \rangle^2 \\ &- \frac{\varepsilon^2 \rho'}{6\rho^2} \langle \boldsymbol{\tau}, \boldsymbol{\eta}(\tau, \mathbf{P}) - \boldsymbol{\eta}_0(\tau) \rangle^3. \end{aligned} \quad (2.83)$$

Here,  $-\frac{\rho'}{\rho^2}$  denotes non-dimensional derivative of the curvature  $\varsigma$  at the point  $\mathbf{P}$ . Clearly, the relation (2.83) is valid for any arbitrary  $\mathbf{P} \in \Gamma$ . Inserting the relation (2.24) into (2.83) and collecting appropriate terms we end up with the following boundary conditions for the functions  $\boldsymbol{\eta}_1$ ,  $\boldsymbol{\eta}_2$  and  $\boldsymbol{\eta}_3$  in the case of general, non-circular boundary  $\Gamma$

$$\langle \mathbf{n}, \boldsymbol{\eta}_1 \rangle = \langle \mathbf{n}, \boldsymbol{\nu} \rangle, \quad (2.84)$$

$$\langle \mathbf{n}, \boldsymbol{\eta}_2 \rangle = \frac{1}{4\rho} \langle \boldsymbol{\tau}, \boldsymbol{\eta}_1 - \boldsymbol{\nu} \rangle^2, \quad (2.85)$$

$$\langle \mathbf{n}, \boldsymbol{\eta}_3 \rangle = \frac{1}{2\rho} \langle \boldsymbol{\tau}, \boldsymbol{\eta}_1 - \boldsymbol{\nu} \rangle \langle \boldsymbol{\tau}, \boldsymbol{\eta}_2 \rangle - \frac{\rho'}{24\rho^2} \langle \boldsymbol{\tau}, \boldsymbol{\eta}_1 - \boldsymbol{\nu} \rangle^3. \quad (2.86)$$

Actually, the last two conditions can be simplified, i.e. from the condition (2.84) one notices orthogonality of two vectors  $\mathbf{n}$  and  $\boldsymbol{\eta}_1 - \boldsymbol{\nu}$ . Consequently, vectors  $\boldsymbol{\tau}$  and  $\boldsymbol{\eta}_1 - \boldsymbol{\nu}$  are collinear and the scalar product  $\langle \boldsymbol{\tau}, \boldsymbol{\eta}_1 - \boldsymbol{\nu} \rangle$  is equal to  $\pm |\boldsymbol{\eta}_1 - \boldsymbol{\nu}|$ . Further, owing to collinearity of vectors  $\boldsymbol{\tau}$  and  $\boldsymbol{\eta}_1 - \boldsymbol{\nu}$ , we simplify

$$\langle \boldsymbol{\tau}, \boldsymbol{\eta}_1 - \boldsymbol{\nu} \rangle \langle \boldsymbol{\tau}, \boldsymbol{\eta}_2 \rangle = \pm |\boldsymbol{\eta}_1 - \boldsymbol{\nu}| \left\langle \frac{\boldsymbol{\eta}_1 - \boldsymbol{\nu}}{\pm |\boldsymbol{\eta}_1 - \boldsymbol{\nu}|}, \boldsymbol{\eta}_2 \right\rangle = \langle \boldsymbol{\eta}_1 - \boldsymbol{\nu}, \boldsymbol{\eta}_2 \rangle.$$

Finally, the boundary conditions for the functions  $\boldsymbol{\eta}_2$  and  $\boldsymbol{\eta}_3$  are following

$$\langle \mathbf{n}, \boldsymbol{\eta}_2 \rangle = \frac{1}{4\rho} |\boldsymbol{\eta}_1 - \boldsymbol{\nu}|^2, \quad (2.87)$$

$$\langle \mathbf{n}, \boldsymbol{\eta}_3 \rangle = \frac{1}{2\rho} \langle \boldsymbol{\eta}_1 - \boldsymbol{\nu}, \boldsymbol{\eta}_2 \rangle \mp \frac{\rho'}{24\rho^2} |\boldsymbol{\eta}_1 - \boldsymbol{\nu}|^3. \quad (2.88)$$

The relations (2.84), (2.87) and (2.88) are the desired boundary conditions in the case of general boundary  $\Gamma$ . Please note, if the boundary  $\Gamma$  is a circle, then the last term in (2.88) is equal to zero (the curvature is constant for all  $\mathbf{P} \in \Gamma$ ) and, hence, we get exactly (2.69).

We do not derive here the boundary conditions for  $p_1$ ,  $p_2$  and  $p_3$  functions because of similarities of the relations, i.e. (2.70) and (2.84) are the same; (2.71)

and (2.87) are almost the same, i.e. the curvature in the case of (2.71) is constant, but in the case of (2.87) it is a function of  $\boldsymbol{\xi}$ ; (2.88) has also additional term which appears due to third order approximation of the boundary  $\Gamma$ .

Finalizing the analysis of the case of 2D domain we emphasize that the boundary conditions were derived under the following assumption: *the control volume  $D_0$  during the harmonic oscillations of  $\Gamma$  moves along  $\Gamma$* . In the case of 3D domain we also make this crucial assumption.

### 2.5.2 3D Domains

In order to derive the boundary conditions for the functions  $p_1$ ,  $p_2$  and  $p_3$  in dimensional form in 3D case we apply the same principles as in the cases of 2D domains. It is clear that both the circular and spherical boundaries are only special cases. Therefore, we start to consider a general boundary of 3D domain which we denote by  $\Gamma$ , as usual.

Let us derive the boundary conditions for the functions  $\boldsymbol{\eta}_1$ ,  $\boldsymbol{\eta}_2$  and  $\boldsymbol{\eta}_3$ <sup>18</sup>. We choose an arbitrary point  $\mathbf{P}$  on the surface  $\Gamma$ . Similarly, as we did in 2D case, we construct the local coordinate system  $(s_1, s_2, y)^T = C(\mathbf{x} - \mathbf{P})$  in the neighbourhood of  $\mathbf{P}$ <sup>19</sup>, cf. Fig. 2.10, such that  $y$  is directed along outer normal  $\mathbf{n}$ , the  $s_1$ - and  $s_2$ -axes belong to tangential plane to  $\Gamma$  at  $\mathbf{P}$  and the matrix  $C$  is orthogonal. Next, we approximate the surface  $\Gamma$  at the point  $\mathbf{P}$  by a third order polynomial

$$\begin{aligned} y(s_1, s_2) &= y(0, 0) + y'_{s_1}(0, 0)s_1 + y'_{s_2}(0, 0)s_2 \\ &+ \frac{1}{2} [y''_{s_1 s_1}(0, 0)s_1^2 + y''_{s_2 s_2}(0, 0)s_2^2] \\ &+ \frac{1}{6} [y'''_{s_1 s_1 s_1}(0, 0)s_1^3 + 3y'''_{s_1 s_1 s_2}(0, 0)s_1^2 s_2 \\ &+ 3y'''_{s_1 s_2 s_2}(0, 0)s_1 s_2^2 + y'''_{s_2 s_2 s_2}(0, 0)s_2^3], \end{aligned} \quad (2.89)$$

where mixed derivative  $y''_{s_1 s_2}(0, 0)$  is assumed to be equal to zero (this can always be done by an orthogonal transformation of  $s_1$  and  $s_2$ ), cf. [46]. Also, the first three summands have to be equal to zero by definition of the coordinate system  $(s_1, s_2, y)$ , i.e. we simplify the expression (2.89)

$$\begin{aligned} y(s_1, s_2) &= \frac{1}{2} [y''_{s_1 s_1}(0, 0)s_1^2 + y''_{s_2 s_2}(0, 0)s_2^2] \\ &+ \frac{1}{6} [y'''_{s_1 s_1 s_1}(0, 0)s_1^3 + 3y'''_{s_1 s_1 s_2}(0, 0)s_1^2 s_2 \\ &+ 3y'''_{s_1 s_2 s_2}(0, 0)s_1 s_2^2 + y'''_{s_2 s_2 s_2}(0, 0)s_2^3], \end{aligned} \quad (2.90)$$

<sup>18</sup>The boundary conditions for  $p_1$ ,  $p_2$  and  $p_3$  functions one can derive immediately.

<sup>19</sup>We assume that the surface  $\Gamma$  is smooth enough at this point

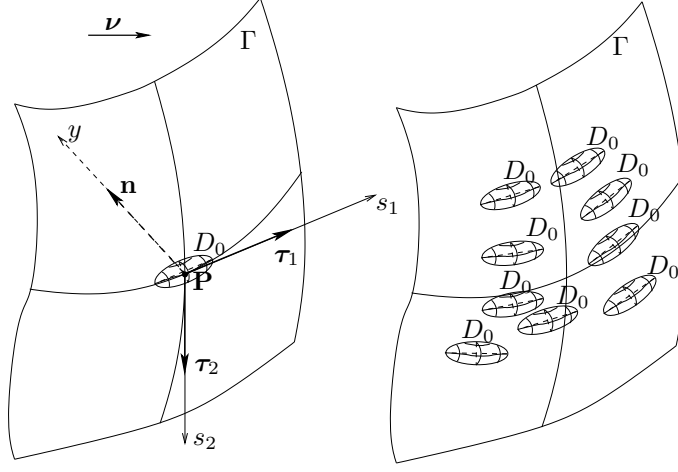


Figure 2.10: The behaviour of general boundary (3D case) and possible positions of a small control volume after certain time.

We associate the point  $\mathbf{P}$  with the position of a small control volume  $D_0$ , cf. Fig. 2.10. Again, as in 2D case, the surface  $\Gamma$  starts to oscillate and small control volume starts to slip along  $\Gamma$ . New position of  $D_0$  after some time  $t$  is  $\mathbf{P} + \mathbf{h}(t, \mathbf{P})$ . Using the relation (2.89) we derive the condition

$$\begin{aligned} \langle \mathbf{n}, \mathbf{h} - \mathbf{h}_0 \rangle &= \frac{\zeta_1}{2} \langle \boldsymbol{\tau}_1, \mathbf{h} - \mathbf{h}_0 \rangle^2 + \frac{\zeta_2}{2} \langle \boldsymbol{\tau}_2, \mathbf{h} - \mathbf{h}_0 \rangle^2 \\ &+ \frac{\zeta'_{1s_1}}{6} \left( \langle \boldsymbol{\tau}_1, \mathbf{h} - \mathbf{h}_0 \rangle^3 + 3 \langle \boldsymbol{\tau}_1, \mathbf{h} - \mathbf{h}_0 \rangle \langle \boldsymbol{\tau}_2, \mathbf{h} - \mathbf{h}_0 \rangle^2 \right) \\ &+ \frac{\zeta'_{2s_2}}{6} \left( \langle \boldsymbol{\tau}_2, \mathbf{h} - \mathbf{h}_0 \rangle^3 + 3 \langle \boldsymbol{\tau}_1, \mathbf{h} - \mathbf{h}_0 \rangle^2 \langle \boldsymbol{\tau}_2, \mathbf{h} - \mathbf{h}_0 \rangle \right), \end{aligned} \quad (2.91)$$

where  $\zeta_j$  denotes so-called normal curvature in  $\boldsymbol{\tau}_j$  direction at the point  $\mathbf{P}$ , cf. [32], and  $\zeta'_{js_j}$  denotes the derivative of  $\zeta_j$  with respect to  $s_j$  at the point  $\mathbf{P}$ ,  $j \in \{1, 2\}$ . Again, we non-dimensionalize the relation (2.91) and derive the boundary conditions for the functions  $\boldsymbol{\eta}_1$ ,  $\boldsymbol{\eta}_2$  and  $\boldsymbol{\eta}_3$

$$\langle \mathbf{n}, \boldsymbol{\eta}_1 \rangle = \langle \mathbf{n}, \boldsymbol{\nu} \rangle, \quad (2.92)$$

$$\langle \mathbf{n}, \boldsymbol{\eta}_2 \rangle = \frac{1}{4\rho_1} \langle \boldsymbol{\tau}_1, \boldsymbol{\eta}_1 - \boldsymbol{\nu} \rangle^2 + \frac{1}{4\rho_2} \langle \boldsymbol{\tau}_2, \boldsymbol{\eta}_1 - \boldsymbol{\nu} \rangle^2, \quad (2.93)$$

$$\begin{aligned} \langle \mathbf{n}, \boldsymbol{\eta}_3 \rangle &= \frac{1}{2\rho_1} \langle \boldsymbol{\tau}_1, \boldsymbol{\eta}_1 - \boldsymbol{\nu} \rangle \langle \boldsymbol{\tau}_1, \boldsymbol{\eta}_2 \rangle + \frac{1}{2\rho_2} \langle \boldsymbol{\tau}_2, \boldsymbol{\eta}_1 - \boldsymbol{\nu} \rangle \langle \boldsymbol{\tau}_2, \boldsymbol{\eta}_2 \rangle \\ &- \frac{\rho'_{1s_1}}{24\rho_1^2} \left( \langle \boldsymbol{\tau}_1, \boldsymbol{\eta}_1 - \boldsymbol{\nu} \rangle^3 + 3 \langle \boldsymbol{\tau}_1, \boldsymbol{\eta}_1 - \boldsymbol{\nu} \rangle \langle \boldsymbol{\tau}_2, \boldsymbol{\eta}_1 - \boldsymbol{\nu} \rangle^2 \right) \\ &- \frac{\rho'_{2s_2}}{24\rho_2^2} \left( \langle \boldsymbol{\tau}_2, \boldsymbol{\eta}_1 - \boldsymbol{\nu} \rangle^3 + 3 \langle \boldsymbol{\tau}_1, \boldsymbol{\eta}_1 - \boldsymbol{\nu} \rangle^2 \langle \boldsymbol{\tau}_2, \boldsymbol{\eta}_1 - \boldsymbol{\nu} \rangle \right), \end{aligned} \quad (2.94)$$

where  $\frac{1}{\rho_j}$  is non-dimensional analogue of the dimensional curvature  $\zeta_j$ ,  $j \in \{1, 2\}$  and  $\rho_j$  is non-dimensional radius of normal curvature  $\zeta_j$ ,  $j \in \{1, 2\}$ , cf. [32].

Finally, we are able to conclude that, in general, the boundary conditions in 2D and 3D cases look similar, cf. (2.84), (2.87), (2.88) and (2.92), (2.93), (2.94). In some cases the conditions (2.93) and (2.94) can be simplified. To show this, we consider two examples.

### Spherical Boundaries

In the cases, when the boundary  $\Gamma$  is a sphere or some part of it, the boundary condition (2.93), due to obvious equality  $\rho_1 = \rho_2 =: \rho$  and the orthogonality condition (2.92), can be written as

$$\begin{aligned} \langle \mathbf{n}, \boldsymbol{\eta}_2 \rangle &= \frac{1}{4\rho_1} \langle \boldsymbol{\tau}_1, \boldsymbol{\eta}_1 - \boldsymbol{\nu} \rangle^2 + \frac{1}{4\rho_2} \langle \boldsymbol{\tau}_2, \boldsymbol{\eta}_1 - \boldsymbol{\nu} \rangle^2 \\ &= \frac{1}{4\rho} \left[ |\boldsymbol{\tau}_1|^2 |\boldsymbol{\eta}_1 - \boldsymbol{\nu}|^2 \cos^2 \alpha + |\boldsymbol{\tau}_2|^2 |\boldsymbol{\eta}_1 - \boldsymbol{\nu}|^2 \sin^2 \alpha \right] \\ &= \frac{1}{4\rho} |\boldsymbol{\eta}_1 - \boldsymbol{\nu}|^2, \end{aligned} \quad (2.95)$$

where  $\alpha$  is the angle between two vectors  $\boldsymbol{\tau}_1$  and  $\boldsymbol{\eta}_1 - \boldsymbol{\nu}$ . One can notice that (2.95) coincides exactly with (2.71) and (2.87). The boundary condition (2.94) also reduces, i.e.

$$\begin{aligned} \langle \mathbf{n}, \boldsymbol{\eta}_3 \rangle &= \frac{1}{2\rho} [\langle \boldsymbol{\tau}_1, \boldsymbol{\eta}_1 - \boldsymbol{\nu} \rangle \langle \boldsymbol{\tau}_1, \boldsymbol{\eta}_2 \rangle + \langle \boldsymbol{\tau}_2, \boldsymbol{\eta}_1 - \boldsymbol{\nu} \rangle \langle \boldsymbol{\tau}_2, \boldsymbol{\eta}_2 \rangle] \\ &= \frac{1}{2\rho} \left[ |\boldsymbol{\tau}_1|^2 |\boldsymbol{\eta}_1 - \boldsymbol{\nu}| |\boldsymbol{\eta}_2| \cos \alpha \cos \beta + |\boldsymbol{\tau}_2|^2 |\boldsymbol{\eta}_1 - \boldsymbol{\nu}| |\boldsymbol{\eta}_2| \sin \alpha \sin \beta \right] \\ &= \frac{1}{2\rho} |\boldsymbol{\eta}_1 - \boldsymbol{\nu}| |\boldsymbol{\eta}_2| [\cos \alpha \cos \beta + \sin \alpha \sin \beta] \\ &= \frac{1}{2\rho} |\boldsymbol{\eta}_1 - \boldsymbol{\nu}| |\boldsymbol{\eta}_2| \cos(\alpha - \beta) \\ &= \frac{1}{2\rho} \langle \boldsymbol{\eta}_1 - \boldsymbol{\nu}, \boldsymbol{\eta}_2 \rangle, \end{aligned} \quad (2.96)$$

where the angle  $\alpha - \beta$  is exactly the angle between two vectors  $\boldsymbol{\eta}_1 - \boldsymbol{\nu}$  and  $\boldsymbol{\eta}_2$ , and the terms  $\frac{\rho'_{1s1}}{\rho_1^2} = \frac{\rho'_{2s2}}{\rho_2^2} = 0$ . Again, (2.96) coincides with (2.72) and (2.88).

### Surfaces of Revolution

A surface of revolution is a surface generated by rotating a two-dimensional curve about an axis. The resulting surface therefore always has azimuthal symmetry. Examples of surfaces of revolution include the apple, cylinder (excluding the ends), hyperboloid, lemon, oblate spheroid, paraboloid, prolate spheroid, pseudosphere, sphere, spheroid, etc. In our case, cf. Fig. 2.4 and Fig. 2.6, the most of the boundaries are exactly of this kind of surfaces (the loudspeaker itself, the membrane, the tube). Therefore, it is important to try to simplify the boundary conditions exactly in such cases.



Let us note that the membrane and the cap oscillate along the rotation axis of the loudspeaker, i.e.  $\boldsymbol{\nu}$  and the rotation axis are collinear. By some coincidence  $\boldsymbol{\tau}_1$  and  $\boldsymbol{\tau}_2$  may be chosen in such a way that  $\boldsymbol{\tau}_1 \parallel \boldsymbol{\nu}$  and  $\boldsymbol{\tau}_2 \perp \boldsymbol{\nu}$ . Moreover, some small control volume on the wall of the loudspeaker (which does not move) during the membrane and cap oscillations will slip along  $\boldsymbol{\nu}$ . Having all this we conclude that  $\langle \boldsymbol{\tau}_2, \boldsymbol{\eta}_1 \rangle = 0$  and the values of normal curvature  $\varsigma_2$  are not important any more. Finally, we simplify the boundary conditions (2.93) and (2.94) in the case of surfaces of revolution

$$\langle \mathbf{n}, \boldsymbol{\eta}_2 \rangle = \frac{1}{4\rho_1} |\boldsymbol{\eta}_1|^2, \quad (2.97)$$

$$\langle \mathbf{n}, \boldsymbol{\eta}_3 \rangle = \frac{1}{2\rho_1} \langle \boldsymbol{\eta}_1, \boldsymbol{\eta}_2 \rangle \mp \frac{\rho'_{1s_1}}{24\rho_1^2} |\boldsymbol{\eta}_1|^3. \quad (2.98)$$

And we again see that the conditions (2.97) and (2.98) are similar to the 2D case, cf. (2.87) and (2.88).

### 2.5.3 Radiative Boundary Conditions

So far we derived the boundary conditions for the functions  $\boldsymbol{\eta}_1$ ,  $\boldsymbol{\eta}_2$  and  $\boldsymbol{\eta}_3$  on moving and fixed 3D parts of the loudspeaker. From these conditions one is able to derive (straightforwardly) the boundary conditions for  $p_1$ ,  $p_2$  and  $p_3$ . Now we have to impose certain conditions on the unknown functions on artificial boundary  $\Gamma_r$  in the case of bounded computational domain  $\Omega$ , cf. Fig. 2.4, and to impose certain conditions on the unknown functions at infinity in the case of the exterior domain  $\Omega^+$ , cf. Fig. 2.6.

#### The Case of a Bounded Computational Domain $\Omega$

To define the boundary conditions on the artificial boundary  $\Gamma_r$  we consider first the following problem

$$\Delta_{\mathbf{x}} u + \kappa^2 u = \delta_0 \text{ in } \mathbb{R}^3,$$

where  $\delta_0(\mathbf{x})$  is Dirac Delta function.  $\delta_0(\mathbf{x})$  defines the point source at the point  $\mathbf{0}$ . The solution of this problem looks as follows, cf. [35] and [19],

$$u(\mathbf{r}) = -\frac{1}{4\pi} \frac{e^{-i\kappa r}}{r}. \quad (2.99)$$

Here  $\mathbf{r}$  denotes the distance from  $\mathbf{0}$  to  $\mathbf{x}$ . Let us define a sphere  $\Gamma_R$  of certain radius  $R$ <sup>20</sup> with the center at  $\mathbf{0}$ . This is so-called artificial boundary which we can choose arbitrarily. Next, we find the normal derivative on the sphere  $\Gamma_R$

$$\left. \frac{\partial u}{\partial \mathbf{n}} \right|_R = -\left( i\kappa + \frac{1}{R} \right) u(R). \quad (2.100)$$

<sup>20</sup>We assume that  $R$  is large enough.

The relation (2.100) is exactly the boundary condition we are interested in. Let us explain why we really can use this boundary condition in our case. Obviously, the aperture of the reflex tube can be considered as a kind of sound source. If we are rather far away from this sound source it can be assumed that we deal with the point source. Hence, the boundary condition (2.100) on  $\Gamma_R$  has to be valid. Therefore, the boundary conditions for the functions  $p_1$ ,  $p_2$  and  $p_3$  on the artificial boundary  $\Gamma_R$  are the following<sup>21</sup>

$$\frac{\partial p_1}{\partial \mathbf{n}} = -\left(\kappa i + \frac{1}{R}\right) p_1, \quad (2.101)$$

$$\frac{\partial p_2}{\partial \mathbf{n}} = -\left(2\kappa i + \frac{1}{R}\right) p_2, \quad (2.102)$$

$$\frac{\partial p_3}{\partial \mathbf{n}} = -\left(3\kappa i + \frac{1}{R}\right) p_3, \quad (2.103)$$

where  $R$  is the radius of  $\Gamma_R$ , cf. Fig. 2.4.

### The Case of the Exterior Domain $\Omega^+$

In the previous case of the bounded computational domain the artificial boundary  $\Gamma_R$  and, hence, the computational domain  $\Omega$  itself depend on the choice of the radius  $R$ . We used there, let say, point source principle to define the boundary conditions on  $\Gamma_R$ . It would be ideal to use so-called Sommerfeld radiation boundary condition at infinity

$$\lim_{\mathbf{r} \rightarrow \infty} \mathbf{r} \left( \frac{\partial u}{\partial \mathbf{r}} + i\kappa u \right) = 0,$$

In practice, we consider only bounded computational domains and, hence, on  $\Gamma_R$  we use certain approximations of the Sommerfeld radiation condition. Such an approximation has been used above. The main disadvantage is that the condition on  $\Gamma_R$  is “a source” of generation of so-called spurious reflections back into domain. Physically such modeling phenomenon is incorrect.

In the case of the exterior domain  $\Omega^+$  we impose on the functions  $p_1$ ,  $p_2$  and  $p_3$  at infinity the Sommerfeld radiation conditions, i.e.

$$\lim_{\mathbf{r} \rightarrow \infty} \mathbf{r} \left( \frac{\partial p_1}{\partial \mathbf{r}} + i\kappa p_1 \right) = 0, \quad (2.104)$$

$$\lim_{\mathbf{r} \rightarrow \infty} \mathbf{r} \left( \frac{\partial p_2}{\partial \mathbf{r}} + 2i\kappa p_2 \right) = 0, \quad (2.105)$$

$$\lim_{\mathbf{r} \rightarrow \infty} \mathbf{r} \left( \frac{\partial p_3}{\partial \mathbf{r}} + 3i\kappa p_3 \right) = 0. \quad (2.106)$$

---

<sup>21</sup>This approach is commonly used in linear acoustics, but has to be justified more thoroughly for  $p_2$  and  $p_3$ .

Obviously, we are not able to represent an unbounded computational domain in the computer. But in Chapter 4 we will present a numerical approach which uses the Sommerfeld principle. We do not show the details of this approach here. All the details will be shown in Chapter 4. We only mention that the wave, which comes out from the aperture of the loudspeaker, will propagate from the loudspeaker away, but it never should come back towards the loudspeaker. This approach, as we will see later on, gives more accurate<sup>22</sup> behaviour of the functions  $p_1$ ,  $p_2$  and  $p_3$  at any point outside<sup>23</sup> the loudspeaker than in the previous case.

## 2.6 The Main Results of Chapter 2

In this section, we summarize all the results we have got in this chapter. First of all we have to mention that the starting equations are the so-called Euler equations. These non-linear equations describe the behaviour of an inviscid compressible fluid flow, and in our case this fluid is the air. Basically, the Euler equations are written in the Eulerian or actual coordinate system. For our convenience we rewrote the Euler equations in the Lagrangian or material coordinate system, cf. (2.11). Parallel, we introduced new unknown quantity  $\mathbf{h}$  which represents the displacement. To linearize the equation (2.11) we transformed it into non-dimensional form and introduced a small quantity  $\varepsilon$ , cf. (2.17). Further, the existence of the series (2.18) has been assumed. This allowed us to apply the regular asymptotic analysis to the equation (2.17). As a consequence, we derived linear differential equations (2.21)–(2.23) for the unknown  $\boldsymbol{\eta}_1$ ,  $\boldsymbol{\eta}_2$  and  $\boldsymbol{\eta}_3$  functions. However, these equations has been also simplified using the assumption about the harmonic dependence of  $\boldsymbol{\eta}_1$ ,  $\boldsymbol{\eta}_2$  and  $\boldsymbol{\eta}_3$  on the non-dimensional temporal variable  $\tau$ , cf. (2.25)–(2.27).

To make life easier we applied several tricks to the equations (2.25)–(2.27) and, finally, derived the equations of Helmholtz type for the pressure functions  $p_1$ ,  $p_2$  and  $p_3$ , cf. (2.35)–(2.37). By this we “killed” several “rabbits” at once, i.e. we have got the equations of certain type (here, of Helmholtz type), and this will help to analyze the properties of the solution, cf. Chapter 3; we reduced the number of the equations from 9 till 3 (or, basically, from 5 till 3); if one wants to compare the results of simulation to the measurements, then the pressure field is exactly the field what can easily be measured; etc.

Further, we compared our approach of derivation of the equations (2.35) and (2.36) to other approaches, i.e. to the idea of the existence of a displacement potential function and to the idea of the existence of a velocity potential function. As a consequence we concluded that our approach is not worse than these two,

---

<sup>22</sup>At least theoretically.

<sup>23</sup>We claim also that the behaviour of  $p_1$ ,  $p_2$  and  $p_3$  inside the loudspeaker is better as well.

but in some sense it is even better.

In the next section we defined two domains  $\Omega$  and  $\Omega^+$ , respectively, which we would like to consider (and compare the results) in Chapter 4. First of them is bounded and the second one is unbounded. The reason is to apply two different numerical methods, cf. Chapter 4, to solve partial differential equations which we derived above, and to show the main differences of these approaches.

The boundary conditions finalize the chapter. We considered 2D and 3D cases to show the main principles of the derivation of the boundary conditions. It has been shown that the boundary conditions are similar in both 2D and 3D cases. And in some cases they completely coincide. It, in some sense, emphasizes the correctness of all derivations.

**Remark 2.6.1** We have to mention that in the sequel we will consider the behaviour of the functions  $p_1$  and  $p_2$  only. The reason is simple: all the equations can be solved numerically, hence, an approximation of third order derivatives of  $p_1$ <sup>24</sup>, for example, might give certain instabilities of the solution  $p_3$ . To solve the complete problem, cf. Chapter 1, using only  $p_1$  and  $p_2$  functions, is already nontrivial task.

---

<sup>24</sup>Cf. (2.37) and (2.78).



## Chapter 3

# Existence, Uniqueness and Regularity of the Solution

In the previous chapter we derived three differential equations of Helmholtz type, which are defined inside the computational domain  $\Omega$ , cf. Fig. 2.4 or 2.6, with appropriate boundary conditions on the boundary  $\partial\Omega$ . All this forms three boundary value problems which can be solved sequentially. It makes sense to solve these problems only in case when they are well-posed. Therefore, we have to investigate the existence, the uniqueness and the regularity of the solutions  $p_1$  and  $p_2$ <sup>1</sup>. Also, we have to note that all results of this chapter can be applied to the problem (2.35), (2.76) and (2.101) only.

In this chapter, we would like to collect and adapt some well-known theory to prove the uniqueness and existence of the solution of a general Helmholtz boundary value problem. Some regularity results will be also presented.

### 3.1 The Statement of the Problem and Definitions

We consider the case of a non-homogeneous Helmholtz type equation in a given domain  $\Omega \subset \mathbb{R}^3$  with Robin type boundary conditions on a piecewise smooth boundary  $\partial\Omega = \Gamma \cup \Gamma_r$ . Let us note that the computational domain  $\Omega$  is assumed to be bounded here. The case of exterior domain will be considered separately and the domain will be denoted by  $\Omega^+$ .

The Helmholtz equation reads as

$$-\Delta_{\mathbf{x}}u = \lambda u - f \quad \text{in } \Omega, \quad (3.1)$$

where  $\lambda$  is any complex non-zero number. The boundary condition, as mentioned above, is of Robin type and reads as follows

$$\frac{\partial u}{\partial \mathbf{n}} + \sigma u = g \quad \text{on } \partial\Omega, \quad (3.2)$$

---

<sup>1</sup>Remember, we do not consider  $p_3$  any more, cf. remark 2.6.1

$\Gamma$	$g(\mathbf{x})$	$\sigma(\mathbf{x})$
$\Gamma$	$g(\mathbf{x})$	0
$\Gamma_r$	0	$\tilde{\sigma}(\mathbf{x})$

Table 3.1: Definition of the functions  $g$  and  $\sigma$  on the boundary  $\partial\Omega$ .

where the functions  $g$  and  $\sigma$  depend on the type of the boundary, cf. Table 3.1 and Fig. 2.4. Here, the functions  $g$  and  $\tilde{\sigma}$  are known and  $\tilde{\sigma}$  does not depend on  $\lambda$ .

Next, we give several important definitions which can be found in [33], [46] or [2].

**Definition 3.1.1** *A bounded simply connected open domain  $\Omega \subset \mathbb{R}^N$  is called a Lipschitz domain, if  $\forall P \in \partial\Omega$  there exist a rectangular coordinate system  $(x, s)$  ( $x \in \mathbb{R}^{N-1}, s \in \mathbb{R}$ ), a neighbourhood  $\mathcal{V}(P) = \prod_{i=1}^N (\alpha_i, \beta_i) = \mathcal{V}' \times (\alpha, \beta) \subset \mathbb{R}^N$  of  $P$  in these coordinates, and a Lipschitz continuous function  $\varphi_P : \mathcal{V}' \rightarrow (\alpha, \beta)$  such that*

- (a)  $\mathcal{V}(P) \cap \Omega = \{(x, s) \in \mathcal{V}(P) | s > \varphi_P(x)\} \cap \mathcal{V}(P)$ ;
- (b)  $\mathcal{V}(P) \cap \partial\Omega = \{(x, \varphi_P(x)), x \in \mathcal{V}'\}$ .

The boundary  $\partial\Omega$  of Lipschitz domain  $\Omega$  is then called Lipschitz continuous.

In the sequel we will consider only Lipschitz continuous domains  $\Omega$ . The function  $u$  is complex valued, in general. Because of this we will search for the solution of the problem (3.1), (3.2) in the complex Sobolev space  $\mathcal{W}_2^1(\Omega)$ .

**Definition 3.1.2** *Let  $d \geq 1$ ,  $\Omega$  is an open subset of  $\mathbb{R}^d$ ,  $p \in [1, \infty]$  and  $m \in \mathbb{N}$ , then the Sobolev space  $\mathcal{W}_p^m(\Omega)$  is defined by*

$$\mathcal{W}_p^m(\Omega) = \{u \in \mathcal{L}_p(\Omega) | \forall |\alpha| \leq m, \partial_{\mathbf{x}}^{\alpha} u \in \mathcal{L}_p(\Omega)\},$$

where  $\mathcal{L}_p(\Omega)$  denotes the space of  $p$ -integrable functions,  $\alpha = (\alpha_1, \dots, \alpha_d)$ ,  $|\alpha| = \alpha_1 + \dots + \alpha_d$  and the derivatives  $\partial_{\mathbf{x}}^{\alpha} u = \partial_{x_1}^{\alpha_1} \dots \partial_{x_d}^{\alpha_d} u$  are taken in a weak sense. The norm is defined by

$$\|u\|_{\mathcal{W}_p^m(\Omega)} = \sum_{|\alpha| \leq m} \|\partial_{\mathbf{x}}^{\alpha} u\|_{\mathcal{L}_p(\Omega)}.$$

$\mathcal{W}_p^m(\Omega)$  is a Banach space. In the special case  $p = 2$ ,  $\mathcal{W}_2^m(\Omega)$  is a Hilbert space with the inner product

$$(u, v)_m = \sum_{|\alpha| \leq m} \int_{\Omega} \partial_{\mathbf{x}}^{\alpha} u \overline{\partial_{\mathbf{x}}^{\alpha} v} \, d\mathbf{x}.$$

Therefore,

$$\|u\|_{\mathcal{W}_2^m(\Omega)} := \sqrt{(u, u)_m}.$$

For the inner product in the space  $\mathcal{W}_2^1(\Omega)$  we will use the notation  $(\cdot, \cdot) := (\cdot, \cdot)_1$ .

### 3.2 Existence and Uniqueness of the Solution in $\mathcal{W}_2^1(\Omega)$ Space: Fredholm Alternative

The main tool to prove the existence and uniqueness of the solution of the Helmholtz boundary value problem is the so-called Fredholm alternative.

**Theorem 3.2.1 (Fredholm Alternative)** *Let  $H$  be a complex Hilbert space,  $A$  a compact operator,  $f \in H$ . Then we have:*

(a) *Outside of any neighbourhood of 0 the spectrum of the operator  $A$  has no more than a finite number of elements of a finite multiplicity.*

(b) *The equation*

$$(I + A)u = f$$

*has a solution for every  $f$  if and only if the homogeneous equation*

$$(I + A)u = 0$$

*has only the trivial solution. If the homogeneous equation has non-trivial solutions, then for the existence of the solution necessary and sufficient condition is:*

$$(f, v) = 0$$

*for every  $v$  such that*

$$(I + A^*)v = 0.$$

Here  $A^*$  is the adjoint of  $A$ . For the details we refer to [33] or [22].

We are interested to find certain conditions for the existence and the uniqueness of the solution. For an arbitrary function from  $\mathcal{W}_2^1(\Omega)$  it makes no sense to say that it satisfies the boundary condition (3.2) because its gradient is defined only almost everywhere in  $\Omega$  and may fail to be defined on the boundary  $\partial\Omega$ . Therefore, we need to put the condition (3.2) and the equation (3.1) in an integral form such that it will be suitable for an arbitrary function  $\mathcal{W}_2^1(\Omega)$ . We rewrite the equation (3.1) as follows: we multiply both sides by the complex conjugate of an arbitrarily chosen function  $\eta \in \mathcal{W}_2^1(\Omega)$  and integrate the resulting expression over the domain  $\Omega$

$$-\int_{\Omega} \Delta_{\mathbf{x}} u \bar{\eta} \, d\mathbf{x} = \int_{\Omega} \lambda u \bar{\eta} \, d\mathbf{x} - \int_{\Omega} f \bar{\eta} \, d\mathbf{x}. \quad (3.3)$$

Because the boundary  $\partial\Omega$  of the domain  $\Omega$  is Lipschitz continuous, we may apply Green's formula, cf. [30], and rewrite the equation (3.3) in the form

$$\int_{\Omega} \langle \nabla_{\mathbf{x}} u, \nabla_{\mathbf{x}} \bar{\eta} \rangle - \operatorname{div}(\bar{\eta} \nabla_{\mathbf{x}} u) \, d\mathbf{x} = \lambda \int_{\Omega} u \bar{\eta} \, d\mathbf{x} - \int_{\Omega} f \bar{\eta} \, d\mathbf{x}. \quad (3.4)$$



Using Gauss–Ostrogradsky theorem, cf. [30], we rewrite (3.4) as follows

$$\int_{\Omega} \langle \nabla_{\mathbf{x}} u, \nabla_{\mathbf{x}} \bar{\eta} \rangle \, d\mathbf{x} - \int_{\partial\Omega} \frac{\partial u}{\partial n} \bar{\eta} \, dS = \lambda \int_{\Omega} u \bar{\eta} \, d\mathbf{x} - \int_{\Omega} f \bar{\eta} \, d\mathbf{x}, \quad (3.5)$$

or substituting (3.2) into the latter expression we formally get the expression

$$\int_{\Omega} \langle \nabla_{\mathbf{x}} u, \nabla_{\mathbf{x}} \bar{\eta} \rangle \, d\mathbf{x} + \int_{\partial\Omega} \sigma u \bar{\eta} \, dS = \lambda \int_{\Omega} u \bar{\eta} \, d\mathbf{x} + \int_{\partial\Omega} g \bar{\eta} \, dS - \int_{\Omega} f \bar{\eta} \, d\mathbf{x}. \quad (3.6)$$

In order to show that this equation is well–defined we have to make some assumptions. We assume that the function  $f$  belongs to  $\mathcal{L}_2(\Omega)$ , the function  $g$  belongs to  $\mathcal{L}_2(\partial\Omega)$  and  $\sigma$  is bounded almost everywhere, i.e.  $\sigma \in \mathcal{L}_{\infty}(\Omega)$ . Under these assumptions all of the integrals in the equation (3.6) are finite. Let us consider the volume integrals first. Using the Cauchy–Schwartz inequality, cf. [30], we find the following estimates

$$\begin{aligned} \left| \int_{\Omega} \langle \nabla_{\mathbf{x}} u, \nabla_{\mathbf{x}} \bar{\eta} \rangle \, d\mathbf{x} \right| &\leq \left( \int_{\Omega} |\nabla_{\mathbf{x}} u|^2 \, d\mathbf{x} \right)^{\frac{1}{2}} \left( \int_{\Omega} |\nabla_{\mathbf{x}} \bar{\eta}|^2 \, d\mathbf{x} \right)^{\frac{1}{2}} \\ &\leq \|u\|_{\mathcal{W}_2^1(\Omega)} \|\eta\|_{\mathcal{W}_2^1(\Omega)}, \end{aligned} \quad (3.7)$$

$$\begin{aligned} \left| \lambda \int_{\Omega} u \bar{\eta} \, d\mathbf{x} \right| &\leq |\lambda| \left( \int_{\Omega} |u|^2 \, d\mathbf{x} \right)^{\frac{1}{2}} \left( \int_{\Omega} |\bar{\eta}|^2 \, d\mathbf{x} \right)^{\frac{1}{2}} \\ &\leq |\lambda| \|u\|_{\mathcal{W}_2^1(\Omega)} \|\eta\|_{\mathcal{W}_2^1(\Omega)}, \end{aligned} \quad (3.8)$$

$$\left| \int_{\Omega} f \bar{\eta} \, d\mathbf{x} \right| \leq \left( \int_{\Omega} |f|^2 \, d\mathbf{x} \right)^{\frac{1}{2}} \left( \int_{\Omega} |\bar{\eta}|^2 \, d\mathbf{x} \right)^{\frac{1}{2}} \leq \|f\|_{\mathcal{L}_2(\Omega)} \|\eta\|_{\mathcal{W}_2^1(\Omega)}. \quad (3.9)$$

To estimate the boundary integrals in the equation (3.6) we need

**Theorem 3.2.2 (Trace Theorem)** *Let  $\Omega \subset \mathbb{R}^3$  be open, bounded domain with Lipschitz continuous boundary, then there exists a unique, continuous and linear map  $B : \mathcal{W}_2^1(\Omega) \rightarrow \mathcal{L}_2(\partial\Omega)$  such that  $Bu = u|_{\partial\Omega} \forall u \in \mathcal{W}_2^1(\Omega)$ , i.e. there exists a constant  $C_t > 0$  such that*

$$\|u\|_{\mathcal{L}_2(\partial\Omega)} \leq C_t \|u\|_{\mathcal{W}_2^1(\Omega)} \quad \forall u \in \mathcal{W}_2^1(\Omega). \quad (3.10)$$

The formulation of this theorem one can find in [36], the proof in [2]. As we mentioned earlier the boundary  $\partial\Omega$  is assumed to be Lipschitz continuous and we may apply the trace theorem. Thus

$$\left| \int_{\partial\Omega} g \bar{\eta} \, d\mathbf{x} \right| \leq \left( \int_{\partial\Omega} |g|^2 \, d\mathbf{x} \right)^{\frac{1}{2}} \left( \int_{\partial\Omega} |\bar{\eta}|^2 \, d\mathbf{x} \right)^{\frac{1}{2}} \leq C_t \|g\|_{\mathcal{L}_2(\partial\Omega)} \|\eta\|_{\mathcal{W}_2^1(\Omega)}, \quad (3.11)$$

$$\begin{aligned}
\left| \int_{\partial\Omega} \sigma u \bar{\eta} \, d\mathbf{x} \right| &\leq \operatorname{ess\,max}_{\partial\Omega} |\sigma| \left( \int_{\partial\Omega} |u|^2 \, d\mathbf{x} \right)^{\frac{1}{2}} \left( \int_{\partial\Omega} |\bar{\eta}|^2 \, d\mathbf{x} \right)^{\frac{1}{2}} \\
&\leq C_t^2 \operatorname{ess\,max}_{\partial\Omega} |\sigma| \|u\|_{\mathcal{W}_2^1(\Omega)} \|\eta\|_{\mathcal{W}_2^1(\Omega)}. \tag{3.12}
\end{aligned}$$

Consequently, every integral in the equation (3.6) is finite.

We call a function  $u \in \mathcal{W}_2^1(\Omega)$  a generalized solution in  $\mathcal{W}_2^1(\Omega)$  of the equation (3.1) if it satisfies the integral identity (3.6) for all  $\eta \in \mathcal{W}_2^1(\Omega)$ . If the restriction  $u|_{\Omega'}$  of the function  $u$  belongs to  $\mathcal{W}_2^1(\Omega') \cap \mathcal{W}_2^2(\Omega')$  for all  $\bar{\Omega}' \subset \Omega$  and satisfies (3.1) almost everywhere in  $\Omega$ , then (3.6) follows from (3.1). Under these conditions  $u(\mathbf{x})$  is then the generalized solution in  $\mathcal{W}_2^1(\Omega)$  of the equation (3.1). The converse is also true: any generalized solution of (3.6) in  $\mathcal{W}_2^1(\Omega)$  whose restriction belongs to  $\mathcal{W}_2^2(\Omega')$  for all  $\bar{\Omega}' \subset \Omega$ , satisfies (3.1) almost everywhere in  $\Omega$ . The equation (3.1) follows from (3.6) almost everywhere in  $\Omega$ , since  $\Delta_{\mathbf{x}}u + \lambda u - f \in \mathcal{L}_2(\Omega')$  and for all  $\eta \in \mathcal{W}_2^1(\Omega)$ . Thus, the definition that we have given for a generalized solution is indeed an extension of the classical concept of a solution of the problem (3.1), (3.2), cf. [46] or [47] for the details.

Let us now rewrite the equation (3.6) in the ‘‘operator’’ form. By the representation theorem of F.Riesz, cf. [63], [30], we can find a bounded linear operator  $L : \mathcal{W}_2^1(\Omega) \rightarrow \mathcal{W}_2^1(\Omega)$  such that a bounded sesquilinear form  $l(u, v)$  can be written in the form  $l(u, v) = (Lu, v)$ , for any  $v \in \mathcal{W}_2^1(\Omega)$ . Applying this result the equation (3.6) reads as follows

$$(u, \eta) + (Au, \eta) + (Cu, \eta) = \lambda(Bu, \eta) + (G, \eta) + (F, \eta), \quad \forall \eta \in \mathcal{W}_2^1(\Omega), \tag{3.13}$$

where

$$(Au, \eta) = -(Bu, \eta) = - \int_{\Omega} u \bar{\eta} \, d\mathbf{x}, \tag{3.14}$$

$$(Cu, \eta) = \int_{\partial\Omega} \sigma u \bar{\eta} \, dS, \tag{3.15}$$

$$(F, \eta) = - \int_{\Omega} f \bar{\eta} \, d\mathbf{x}, \tag{3.16}$$

$$(G, \eta) = \int_{\partial\Omega} g \bar{\eta} \, dS, \tag{3.17}$$

and  $A, B$  and  $C$  are bounded linear operators, and  $F$  and  $G$  are elements of  $\mathcal{W}_2^1(\Omega)$ . The equation (3.13) holds for any  $\eta$  and, hence, it is equivalent to

$$u + Au + Cu = \lambda Bu + G + F \tag{3.18}$$

or more compactly

$$u + \tilde{A}u = \lambda Bu + \tilde{F}, \quad (3.19)$$

where  $\tilde{A} := A+C$ ,  $\tilde{F} := G+F$ . It is obvious that the equation (3.19) is equivalent to the problem (3.1), (3.2).

In order to apply further theory we have to show that the operators  $A$ ,  $B$ ,  $C$  and, hence,  $\tilde{A}$  are completely continuous<sup>2</sup>. But first, to clarify certain terminology, we give several useful definitions and theorems.

**Definition 3.2.3** *The operator  $A$  is completely continuous, if it is continuous and compact.*

**Theorem 3.2.4** *Every bounded linear operator is continuous.*

**Definition 3.2.5** *Let  $X$  and  $Y$  be normed spaces and  $A$  an operator from  $X$  into  $Y$ . The operator  $A$  is called compact if  $A(U)$  is precompact in  $Y$  whenever  $U$  is bounded in  $X$ , i.e. every sequence in  $\overline{A(U)}^{\|\cdot\|_Y}$  has a subsequence convergent in  $Y$  to an element of  $A(U)$ .*

We mention another two useful theorems which we apply in the proof of complete continuity of the operators mentioned above.

**Theorem 3.2.6** *An operator  $A$  is compact if and only if  $A$  transforms every weakly convergent sequence into a strongly convergent sequence.*

**Theorem 3.2.7 (Rellich's theorem)** *Let  $m \geq 0$  and  $\Omega \subset \mathbb{R}^n$  a Lipschitz domain. Then the embedding from  $\mathcal{W}_2^{m+1}(\Omega)$  into  $\mathcal{W}_2^m(\Omega)$  is compact.*

Cf. [2], [10], [13] and [46] for the details and definitions.

**Lemma 3.2.8**  *$A$ ,  $B$ ,  $C$  and  $\tilde{A}$  are completely continuous.*

**Proof** We consider the operator  $A$  first. Choose an arbitrary sequence  $\{u_n\}_{n \in \mathbb{N}}$  weakly convergent in  $\mathcal{W}_2^1(\Omega)$ . Because the operator  $A$  is bounded, the sequence  $\{Au_n\}_{n \in \mathbb{N}}$  converges weakly to  $Au$ , where  $u$  is the weak limit of  $\{u_n\}_{n \in \mathbb{N}}$ . Moreover, because of the compactness of the embedding operator of  $\mathcal{W}_2^1(\Omega)$  into  $\mathcal{L}_2(\Omega)$ , cf. Theorem 3.2.7, the sequences  $\{u_n\}_{n \in \mathbb{N}}$  and  $\{Au_n\}_{n \in \mathbb{N}}$  converge strongly in  $\mathcal{L}_2(\Omega)$  to  $u$  and  $Au$ , respectively. If we use the definition of the operator  $A$  we

---

<sup>2</sup>And, hence, compact

obtain the bounds

$$\begin{aligned}
\|A(u_n - u_m)\|_{\mathcal{W}_2^1(\Omega)}^2 &= (A(u_n - u_m), A(u_n - u_m)) \\
&= \int_{\Omega} (u_n - u_m) \overline{A(u_n - u_m)} \, d\mathbf{x} \\
&\leq \int_{\Omega} |u_n - u_m| |A(u_n - u_m)| \, d\mathbf{x} \\
&\leq \left( \int_{\Omega} (u_n - u_m)^2 \, d\mathbf{x} \right)^{\frac{1}{2}} \left( \int_{\Omega} (Au_n - Au_m)^2 \, d\mathbf{x} \right)^{\frac{1}{2}} \\
&= \|u_n - u_m\|_{\mathcal{L}_2(\Omega)} \|Au_n - Au_m\|_{\mathcal{L}_2(\Omega)}. \tag{3.20}
\end{aligned}$$

It means that the sequence  $\{Au_n\}_{n \in \mathbb{N}}$  converges strongly in  $\mathcal{W}_2^1(\Omega)$ . The same holds for the operator  $B$ , because  $B = -A$ , cf. formula (3.14). For the operator  $C$  we have to do the same steps, i.e.

$$\begin{aligned}
\|C(u_n - u_m)\|_{\mathcal{W}_2^1(\Omega)}^2 &= (C(u_n - u_m), C(u_n - u_m)) \\
&= \int_{\partial\Omega} \sigma(u_n - u_m) \overline{C(u_n - u_m)} \, dS \\
&\leq \operatorname{ess\,max}_{\partial\Omega} |\sigma| \int_{\partial\Omega} |u_n - u_m| |C(u_n - u_m)| \, dS \\
&\leq \operatorname{ess\,max}_{\partial\Omega} |\sigma| \left( \int_{\partial\Omega} (u_n - u_m)^2 \, dS \right)^{\frac{1}{2}} \left( \int_{\partial\Omega} (Cu_n - Cu_m)^2 \, dS \right)^{\frac{1}{2}} \\
&= \operatorname{ess\,max}_{\partial\Omega} |\sigma| \|u_n - u_m\|_{\mathcal{L}_2(\partial\Omega)} \|Cu_n - Cu_m\|_{\mathcal{L}_2(\partial\Omega)}. \tag{3.21}
\end{aligned}$$

Because the embedding of  $\mathcal{W}_2^1(\Omega)$  into  $\mathcal{L}_2(\partial\Omega)$  is compact (for piecewise-smooth domains with cone property at the non-smoothness points), the right hand side tends to zero when  $n, m \rightarrow \infty$ . Hence, the operator  $C$  is completely continuous. The sum of two completely continuous operators  $A$  and  $C$ , i.e.  $\tilde{A} = A + C$ , is completely continuous. ■

Let us consider the equation (3.19) and denote  $D \equiv (I + \tilde{A} + \lambda_0 B)$ . Using this operator the equation (3.19) reads as

$$Du = (\lambda + \lambda_0) Bu + \tilde{F}. \tag{3.22}$$

The operator  $D$  has a bounded inverse for suitable (large) real  $\lambda_0 > 0$ . Let us denote  $Du \equiv v$ . Consider the following estimate

$$\begin{aligned}
\Re(v, u) &= \Re\left(\left(I + \tilde{A} + \lambda_0 B\right)u, u\right) \\
&= \Re\left(\int_{\Omega} \langle \nabla_{\mathbf{x}} u, \nabla_{\mathbf{x}} \bar{u} \rangle \, d\mathbf{x} + \int_{\partial\Omega} \sigma u \bar{u} \, dS\right) + \lambda_0 \|u\|_{\mathcal{L}_2(\Omega)}^2 \\
&= \int_{\Omega} |\nabla_{\mathbf{x}} u|^2 \, d\mathbf{x} + \int_{\partial\Omega} \sigma |u|^2 \, dS + \lambda_0 \|u\|_{\mathcal{L}_2(\Omega)}^2 \\
&\geq \|\nabla_{\mathbf{x}} u\|_{\mathcal{L}_2(\Omega)}^2 + \operatorname{ess\,min}_{\partial\Omega} |\sigma| \|u\|_{\mathcal{L}_2(\partial\Omega)}^2 + \lambda_0 \|u\|_{\mathcal{L}_2(\Omega)}^2,
\end{aligned}$$

here  $\|u\|_{\mathcal{L}_2(\partial\Omega)}^2$  is bounded, cf. Theorem 3.2.2, and  $\min_{\partial\Omega} |\sigma| \equiv 0$ , cf. Table 3.1. Using this we simplify

$$\begin{aligned}
\Re(v, u) &\geq \|\nabla_{\mathbf{x}} u\|_{\mathcal{L}_2(\Omega)}^2 + \lambda_0 \|u\|_{\mathcal{L}_2(\Omega)}^2 \\
&\geq \min(1, \lambda_0) \|u\|_{\mathcal{W}_2^1(\Omega)}^2.
\end{aligned}$$

Applying the triangle rule, i.e.  $|(u, v)_X| \leq \|u\|_X \|v\|_X$  we get

$$\|u\|_{\mathcal{W}_2^1(\Omega)}^2 \leq C_1 \|Du\|_{\mathcal{W}_2^1(\Omega)} \|u\|_{\mathcal{W}_2^1(\Omega)} \quad (3.23)$$

or

$$\|u\|_{\mathcal{W}_2^1(\Omega)} \leq C_1 \|Du\|_{\mathcal{W}_2^1(\Omega)}, \quad (3.24)$$

where  $C_1 = \frac{1}{\min(1, \lambda_0)}$ . It means that  $D^{-1}$ , in fact, is bounded on all  $\mathcal{W}_2^1(\Omega)$  for such  $\lambda_0$ . Let us rewrite (3.22) in the form

$$u = (\lambda + \lambda_0) D^{-1} B u + D^{-1} \tilde{F}. \quad (3.25)$$

In order to apply the Theorem 3.2.1 directly to the equation (3.25) we have to rewrite it

$$\tilde{A}_1 u = \lambda D^{-1} B u + D^{-1} \tilde{F}, \quad (3.26)$$

where  $\tilde{A}_1 := (I - \lambda_0 D^{-1} B)$ . We are allowed to choose  $\lambda_0$  such that it is rather large and  $\tilde{A}_1$  has bounded inverse (it could be done because the operator  $D^{-1} B$  is compact and, hence, it has discrete spectrum, cf. [22] or [62]). Then  $\tilde{A}_1^{-1}$  is bounded. We may write

$$u = \lambda \tilde{A}_1^{-1} D^{-1} B u + \tilde{A}_1^{-1} D^{-1} \tilde{F}, \quad (3.27)$$

where the operator  $\tilde{A}_1^{-1}D^{-1}B$  is completely continuous and, hence, compact. Applying Fredholm alternative to the equation (3.27) we prove the existence and uniqueness of the solution  $u$  of the problem (3.1), (3.2) in  $\mathcal{W}_2^1(\Omega)$ . The only thing we have to show is that the homogeneous equation  $u = \lambda\tilde{A}_1^{-1}D^{-1}Bu$  has only trivial solution if  $\lambda$  does not belong to the spectrum of the problem (3.1), (3.2).

If  $\lambda$  does not belong to the spectrum of the problem (3.1), (3.2), then the operator  $I - \lambda\tilde{A}_1^{-1}D^{-1}B$  has a bounded inverse in  $\mathcal{W}_2^1(\Omega)$ , according to the theory of linear equations of this form. Consequently,

$$\|u\|_{\mathcal{W}_2^1(\Omega)} = \left\| \left( I - \lambda\tilde{A}_1^{-1}D^{-1}B \right)^{-1} \tilde{A}_1^{-1}D^{-1}\tilde{F} \right\|_{\mathcal{W}_2^1(\Omega)} \leq C_\lambda \left\| \tilde{A}_1^{-1}D^{-1}\tilde{F} \right\|_{\mathcal{W}_2^1(\Omega)}, \quad (3.28)$$

where  $C_\lambda$  is the majorant of  $\left( I - \lambda\tilde{A}_1^{-1}D^{-1}B \right)^{-1}$  as an operator in  $\mathcal{W}_2^1(\Omega)$ . Further estimation will be the following

$$\|u\|_{\mathcal{W}_2^1(\Omega)} \leq C_\lambda C_{\tilde{A}_1^{-1}} C_{D^{-1}} \|\tilde{F}\|_{\mathcal{W}_2^1(\Omega)}, \quad (3.29)$$

where  $C_{\tilde{A}_1^{-1}}$  is the majorant of the operator  $\tilde{A}_1^{-1}$ . If we now recall the connection of  $\tilde{F}$  and  $f$  and  $g$ , we can bound  $\|\tilde{F}\|_{\mathcal{W}_2^1(\Omega)}$  in terms of  $\|f\|_{\mathcal{L}_2(\Omega)}$  and  $\|g\|_{\mathcal{L}_2(\partial\Omega)}$

$$\begin{aligned} \|\tilde{F}\|_{\mathcal{W}_2^1(\Omega)} &= \sup_{\|\eta\|_{\mathcal{W}_2^1(\Omega)} \leq 1} \left| (\tilde{F}, \eta) \right| \\ &= \sup_{\|\eta\|_{\mathcal{W}_2^1(\Omega)} \leq 1} |(G - F, \eta)| \\ &= \sup_{\|\eta\|_{\mathcal{W}_2^1(\Omega)} \leq 1} \left| \int_{\partial\Omega} g\bar{\eta} \, dS - \int_{\Omega} f\bar{\eta} \, dx \right| \\ &\leq \sup_{\|\eta\|_{\mathcal{W}_2^1(\Omega)} \leq 1} [\|g\|_{\mathcal{L}_2(\partial\Omega)} \|\eta\|_{\mathcal{L}_2(\partial\Omega)} + \|f\|_{\mathcal{L}_2(\Omega)} \|\eta\|_{\mathcal{L}_2(\Omega)}] \\ &\stackrel{\text{trace thm}}{\leq} \sup_{\|\eta\|_{\mathcal{W}_2^1(\Omega)} \leq 1} \left[ C_t \|g\|_{\mathcal{L}_2(\partial\Omega)} \|\eta\|_{\mathcal{W}_2^1(\Omega)} + \|f\|_{\mathcal{L}_2(\Omega)} \|\eta\|_{\mathcal{W}_2^1(\Omega)} \right] \\ &\leq \max(C_t, 1) (\|g\|_{\mathcal{L}_2(\partial\Omega)} + \|f\|_{\mathcal{L}_2(\Omega)}). \end{aligned} \quad (3.30)$$

Inserting this expression into the estimation (3.29) one gets

$$\|u\|_{\mathcal{W}_2^1(\Omega)} \leq \max(C_t, 1) C_\lambda C_{\tilde{A}_1^{-1}} C_{D^{-1}} (\|g\|_{\mathcal{L}_2(\partial\Omega)} + \|f\|_{\mathcal{L}_2(\Omega)}). \quad (3.31)$$

If the free term  $f$  and the function  $g$  would be zeros, then, according to the expression (3.31), we would get zero as the solution of the problem (3.1), (3.2)

(if  $\lambda$  does not belong to the spectrum of this problem). It means that the generalized solution  $u$  is unique in  $\mathcal{W}_2^1(\Omega)$ . The solvability of the problem (3.1), (3.2) is guaranteed by the Fredholm alternative.

### 3.3 $\sigma = \sigma(\mathbf{x}, \lambda)$

In our model the coefficient  $\sigma$  in the boundary condition (3.2) depends on  $\lambda$ , i.e. via the radiation boundary condition, cf. (2.101). This fact complicates everything. Let us consider some special case when the function  $\sigma$  has some special form, i.e.:  $\sigma(\mathbf{x}, \lambda) = \sigma_\lambda(\mathbf{x}) = \sigma_1(\mathbf{x}) + \gamma(\lambda)\sigma_2(\mathbf{x})$ , where  $\lambda$  is some fixed parameter and  $\mathbf{x} \in \partial\Omega$ .

Consider the problem (3.1), (3.2) in the integral form, i.e. the equation (3.6) and substitute the expression for the function  $\sigma$

$$\begin{aligned} \int_{\Omega} \langle \nabla_{\mathbf{x}} u, \nabla_{\mathbf{x}} \bar{\eta} \rangle d\mathbf{x} + \int_{\partial\Omega} \sigma_1 u \bar{\eta} dS + \gamma(\lambda) \int_{\partial\Omega} \sigma_2 u \bar{\eta} dS &= \lambda \int_{\Omega} u \bar{\eta} d\mathbf{x} + \int_{\partial\Omega} g \bar{\eta} dS \\ &- \int_{\Omega} f \bar{\eta} d\mathbf{x}. \end{aligned} \quad (3.32)$$

Obviously, all the integrals are finite in the latter expression. As we did before, we apply F.Riesz theorem. In addition to the operators  $A$  and  $B$  we define two new operators:  $C_\sigma$  and  $C_\gamma$  which are defined as follows

$$(C_\sigma u, \eta) = - \int_{\partial\Omega} \sigma_1 u \bar{\eta} dS, \quad (3.33)$$

$$(C_\gamma u, \eta) = - \int_{\partial\Omega} \sigma_2 u \bar{\eta} dS. \quad (3.34)$$

Using these relations we rewrite the equation (3.32) in the ‘‘operator’’ form, i.e.

$$u + Au - C_\sigma u = \lambda Bu + \gamma(\lambda)C_\gamma u + G + F \quad (3.35)$$

or

$$u + \tilde{A}u = \lambda Bu + \gamma(\lambda)C_\gamma u + \tilde{F}, \quad (3.36)$$

where  $\tilde{A} = A - C_\sigma$ ,  $\tilde{F} = G + F$ . As we did before, we add to the left and to the right hand sides of the equation (3.36) the term  $\lambda_0 Bu$ , where  $\lambda_0$  is sufficiently large positive number. The operator  $D \equiv I + \tilde{A} + \lambda_0 B$  has bounded inverse (the reason is similar to the previous one, cf. Section 3.2), and the equation (3.36) transforms to

$$u = D^{-1} ((\lambda + \lambda_0) B + \gamma(\lambda)C_\gamma) u + D^{-1} \tilde{F}. \quad (3.37)$$

Next, we may choose the parameter  $\lambda_0$  in such a way that the term  $I - \lambda_0 D^{-1}B$  has a bounded inverse. So, the equation (3.37) can be written in the form

$$u = (I - \lambda_0 D^{-1}B)^{-1} (\lambda B + \gamma(\lambda)C_\gamma) u + (I - \lambda_0 D^{-1}B)^{-1} D^{-1} \tilde{F}. \quad (3.38)$$

Let us note that the operator  $M := (I - \lambda_0 D^{-1}B)^{-1} (\lambda B + \gamma(\lambda)C_\gamma)$  is completely continuous because  $B$  and  $C_\gamma$  are completely continuous, and  $D^{-1}$  and  $(I - \lambda_0 D^{-1}B)^{-1}$  are bounded. Hence, we may apply Fredholm alternative in order to show the solvability and (in some cases) uniqueness of the equation

$$u - Mu = \tilde{F}_1, \quad (3.39)$$

where  $\tilde{F}_1 := (I - \lambda_0 D^{-1}B)^{-1} D^{-1} \tilde{F}$ .

### 3.4 Second Fundamental Inequality

In this section, we derive so-called second fundamental inequality. We show that under certain conditions on  $\partial\Omega$ ,  $g$  and  $\sigma$  the norm  $\|u\|_{\mathcal{W}_2^2(\Omega)}$  is bounded in terms of  $\|\Delta_{\mathbf{x}}u + \lambda u\|_{\mathcal{L}_2(\Omega)}$  and  $\|g\|_{\mathcal{W}_2^1(\partial\Omega)}$ , where  $u$  is the solution of the problem (3.1), (3.2).

**Remark 3.4.1** In order to be completely correct with further derivations we have to specify which functions we use, i.e. either  $u \in \mathcal{W}_2^2(\Omega \subset \mathbb{R}^3, \mathbb{R})$  or  $u \in \mathcal{W}_2^2(\Omega \subset \mathbb{R}^3, \mathbb{C})$ . Obviously, everything what is done below holds for the first case ( $u$  is real function). For a complex valued function all further estimates have to be done in a bit different way, i.e. we consider each part (real and imaginary) of  $u$  separately and get the same form of inequalities for each component of  $u$ . Without loss of generality, all estimates below will be done for a real valued function  $u$ . The case of complex valued function is completely analogous.

In order to get second fundamental inequality we apply the following theorem, cf. [34], for our further proof

**Theorem 3.4.2** *Let  $\Omega$  be a bounded open subset of  $\mathbb{R}^n$  with  $\mathcal{C}^2$  boundary  $\partial\Omega$ , and let  $\mathbf{v} \in \mathcal{W}_2^1(\Omega)^n$ . Then we have*

$$\begin{aligned} \int_{\Omega} |\operatorname{div}_{\mathbf{x}} \mathbf{v}|^2 d\mathbf{x} - \int_{\Omega} \frac{\partial v_i}{\partial x_j} \frac{\partial v_j}{\partial x_i} d\mathbf{x} &= -2 \int_{\partial\Omega} \langle \mathbf{v}_T, \nabla_T \langle \mathbf{v}, \mathbf{n} \rangle \rangle dS \\ &\quad - \int_{\partial\Omega} \mathcal{B}(\mathbf{v}_T, \mathbf{v}_T) + \operatorname{tr}(\mathcal{B}) \langle \mathbf{v}, \mathbf{n} \rangle^2 dS. \end{aligned} \quad (3.40)$$

Here  $\mathbf{n}$  is the unit normal vector,  $\mathcal{B}(\boldsymbol{\xi}, \boldsymbol{\eta})$  is the so-called second fundamental bilinear form,  $\operatorname{tr}(\mathcal{B})$  is the trace of the bilinear form and  $\mathbf{v}_T$  and  $\nabla_T$  denote a projection of the vectors  $\mathbf{v}$  and  $\nabla_{\mathbf{x}}$  on the tangential hyperplane to  $\partial\Omega$ .



In fact, one can apply this theorem in the case of  $\mathcal{C}^{1,1}$  boundary, cf. [34].

Let us consider the problem (3.1), (3.2) for the function  $u \in \mathcal{W}_2^2(\Omega)$  in some convex domain  $\Omega \subset \mathbb{R}^3$  with a  $\mathcal{C}^2$  boundary  $\partial\Omega$ , cf. Fig.3.1a. The corresponding

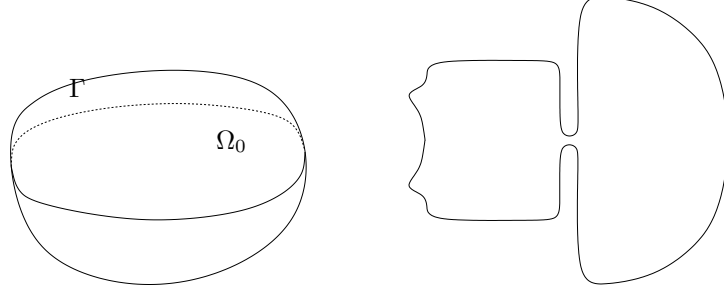


Figure 3.1: Convex (left) and 2D concave (right) domains

estimate is the following

**Theorem 3.4.3** *Let  $\Omega$  be a convex, bounded open subset of  $\mathbb{R}^3$  with a  $\mathcal{C}^2$  boundary  $\partial\Omega$ . Then we have*

$$\|u\|_{\mathcal{W}_2^2(\Omega)} \leq \hat{C}_1 \|\Delta_{\mathbf{x}}u + \lambda u\|_{\mathcal{L}^2(\Omega)} + \hat{C}_2 \|g\|_{\mathcal{W}_2^1(\partial\Omega)}, \quad (3.41)$$

for all  $u \in \mathcal{W}_2^2(\Omega)$  such that  $\frac{\partial u}{\partial \mathbf{n}} + \sigma u = g$  on  $\partial\Omega$ , for all  $g \in \mathcal{W}_2^1(\partial\Omega)$  and  $\sigma \in \mathcal{W}_\infty^1(\partial\Omega)$ . Here  $\hat{C}_1$  and  $\hat{C}_2$  do not depend on the curvature of the concave parts of the boundary  $\partial\Omega$ .

**Proof** Apply the theorem 3.4.2 to the vector function  $\mathbf{v} = \nabla_{\mathbf{x}}u$ . The boundary condition now means that  $\langle \mathbf{v}, \mathbf{n} \rangle = -\sigma u + g$  on  $\partial\Omega$ . Thus we get

$$\begin{aligned} \int_{\Omega} (\Delta_{\mathbf{x}}u)^2 \, d\mathbf{x} &= \int_{\Omega} |u_{x_i x_j}|^2 \, d\mathbf{x} \\ &= -2 \int_{\partial\Omega} \langle \nabla_{\mathbf{T}}u, \nabla_{\mathbf{T}}(-\sigma u + g) \rangle \, dS \\ &= \int_{\partial\Omega} \mathcal{B}(\nabla_{\mathbf{T}}u|_{\partial\Omega}, \nabla_{\mathbf{T}}u|_{\partial\Omega}) + \text{tr}(\mathcal{B})(-\sigma u + g)^2 \, dS. \end{aligned} \quad (3.42)$$

Here,  $u_{x_i x_j}$  denotes the Einstein's summation ( $i, j \in \{1, 2, 3\}$ ). Due to the convexity of  $\Omega$ ,  $\mathcal{B}$  is non-positive, cf. [34], hence,

$$\int_{\Omega} (\Delta_{\mathbf{x}}u)^2 \, d\mathbf{x} - \int_{\Omega} |u_{x_i x_j}|^2 \, d\mathbf{x} \geq -2 \int_{\partial\Omega} \langle \nabla_{\mathbf{T}}u, \nabla_{\mathbf{T}}(-\sigma u + g) \rangle \, dS \quad (3.43)$$

or

$$\int_{\Omega} |u_{x_i x_j}|^2 \, d\mathbf{x} \leq \int_{\Omega} (\Delta_{\mathbf{x}}u)^2 \, d\mathbf{x} + 2 \int_{\partial\Omega} \langle \nabla_{\mathbf{T}}u, \nabla_{\mathbf{T}}(-\sigma u + g) \rangle \, dS. \quad (3.44)$$

Using the so-called "Cauchy's inequality with  $\varepsilon > 0$ ", i.e.  $|ab| \leq \frac{\varepsilon}{2}|a|^2 + \frac{1}{2\varepsilon}|b|^2$ , triangle and Cauchy's inequalities, cf. [46], [47], we end up with the following estimate

$$\int_{\Omega} |u_{x_i x_j}|^2 dS =: \|u_{xx}\|_{\mathcal{L}_2(\Omega)}^2 \leq C_1 \|\Delta_{\mathbf{x}} u\|_{\mathcal{L}_2(\Omega)}^2 + C_2 \|u\|_{\mathcal{W}_2^1(\Omega)}^2 + C_3 \|g\|_{\mathcal{W}_2^1(\partial\Omega)}^2, \quad (3.45)$$

where  $C_1 = \frac{1}{1-C\varepsilon}$ ,  $C_2 = (1-C\varepsilon)^{-1} \left( \sigma_2 \varepsilon_1 + \frac{1}{\varepsilon_1} \sigma_2 + 2\sigma_1 + \varepsilon_2 + \sigma_2 + \frac{2}{\varepsilon_3} \sigma_1 \right)$ ,  $C_3 = \frac{1}{(1-C\varepsilon)\varepsilon_2}$ ,  $C = \max(\sigma_2, \sigma_1)$  and  $\varepsilon = \varepsilon_1^2 + 2\varepsilon_3$ . Here,  $\varepsilon_1, \varepsilon_2$  and  $\varepsilon_3$  are any numbers from  $\mathbb{R}_+$ ,  $\sigma_1 = \operatorname{ess\,max}_{\partial\Omega} |\sigma|$  and  $\sigma_2 = \operatorname{ess\,max}_{\partial\Omega} |\sigma_x| = \operatorname{ess\,max}_{\partial\Omega} |\nabla_{\mathbf{T}} \sigma|$ .

Using the fact that  $\sqrt{a+b} \leq \sqrt{a} + \sqrt{b}$  we get

$$\|u\|_{\mathcal{W}_2^2(\Omega)} \leq \tilde{C}_1 \|\Delta_{\mathbf{x}} u\|_{\mathcal{L}_2(\Omega)} + \tilde{C}_2 \|u\|_{\mathcal{W}_2^1(\Omega)} + \tilde{C}_3 \|g\|_{\mathcal{W}_2^1(\partial\Omega)}. \quad (3.46)$$

Remembering that the problem (3.1), (3.2) has a unique solution in  $\mathcal{W}_2^1(\Omega)$  for Lipschitz domain  $\Omega$ , for  $f, \sigma$  and  $g$  from appropriate classes, cf. Section 3.2, we apply the inequality (3.31), i.e.

$$\begin{aligned} \|u\|_{\mathcal{W}_2^1(\Omega)} &\leq \tilde{C} (\|f\|_{\mathcal{L}_2(\Omega)} + \|g\|_{\mathcal{L}_2(\partial\Omega)}) \\ &\leq \tilde{C} \left( \|f\|_{\mathcal{L}_2(\Omega)} + \|g\|_{\mathcal{W}_2^1(\partial\Omega)} \right) \\ &= \tilde{C} \left( \|\Delta_{\mathbf{x}} u + \lambda u\|_{\mathcal{L}_2(\Omega)} + \|g\|_{\mathcal{W}_2^1(\partial\Omega)} \right). \end{aligned} \quad (3.47)$$

The next estimate is also true

$$\begin{aligned} \|\Delta_{\mathbf{x}} u\|_{\mathcal{L}_2(\Omega)} &= \|\Delta_{\mathbf{x}} u + \lambda u - \lambda u\|_{\mathcal{L}_2(\Omega)} \\ &\leq \|\Delta_{\mathbf{x}} u + \lambda u\|_{\mathcal{L}_2(\Omega)} + \|\lambda u\|_{\mathcal{L}_2(\Omega)} \\ &\leq \left( 1 + |\lambda| \tilde{C} \right) \|\Delta_{\mathbf{x}} u + \lambda u\|_{\mathcal{L}_2(\Omega)} + \tilde{C} |\lambda| \|g\|_{\mathcal{W}_2^1(\partial\Omega)}. \end{aligned} \quad (3.48)$$

Substituting the expressions (3.47) and (3.48) into (3.46) we get the desired result, cf. (3.41). ■

**Remark 3.4.4** Let us note that the second fundamental quadratic form  $\mathcal{B}(\boldsymbol{\xi}, \boldsymbol{\eta})$  is uniformly bounded on  $\partial\Omega \in \mathcal{C}^2$  (or even  $\partial\Omega \in \mathcal{C}^{1,1}$ , cf. [34]), i.e.  $|\mathcal{B}(\boldsymbol{\xi}, \boldsymbol{\eta})| \leq \varsigma |\boldsymbol{\xi}| |\boldsymbol{\eta}|$ . The constant  $\varsigma$  represents the curvature.

We formulate (without proof) similar theorem for the case of non-convex domains which we will use in the sequel, i.e.

**Theorem 3.4.5** *Let  $\Omega$  be a non-convex, bounded open subset of  $\mathbb{R}^3$  with a  $\mathcal{C}^2$  boundary  $\partial\Omega$ . Then we have*

$$\|u\|_{\mathcal{W}_2^2(\Omega)} \leq \hat{C}_1 \|\Delta_{\mathbf{x}} u + \lambda u\|_{\mathcal{L}_2(\Omega)} + \hat{C}_2 \|g\|_{\mathcal{W}_2^1(\partial\Omega)}, \quad (3.49)$$

for all  $u \in \mathcal{W}_2^2(\Omega)$  such that  $\frac{\partial u}{\partial \mathbf{n}} + \sigma u = g$  on  $\partial\Omega$ , for all  $g \in \mathcal{W}_2^1(\partial\Omega)$  and  $\sigma \in \mathcal{W}_\infty^1(\partial\Omega)$ . Here  $\hat{C}_1$  and  $\hat{C}_2$  depend on the curvature of the concave parts of the boundary  $\partial\Omega$ .

Here, the only thing we have to worry about is the term

$$- \int_{\partial\Omega} \mathcal{B}(\nabla_{\mathbf{T}} u|_{\partial\Omega}, \nabla_{\mathbf{T}} u|_{\partial\Omega}) + \text{tr}(\mathcal{B})(-\sigma u + g)^2 dS.$$

Using the uniform boundedness of  $\mathcal{B}$  it can be shown that the constants  $\hat{C}_1$  and  $\hat{C}_2$  will depend on the upper bound  $\max_{\mathbf{x} \in \partial\Omega} \zeta(\mathbf{x})$  of  $\mathcal{B}$ . Let us consider, for example, the domain  $\Omega$  depicted in the Fig.3.1b. Obviously, the maximal value of  $\zeta$  can be achieved on the parts of the boundary  $\partial\Omega$  which are concave. The curvature here is positive and, hence, exactly these parts will influence the values of the constants  $\hat{C}_1$  and  $\hat{C}_2$  in the estimate (3.49).

### 3.5 Solvability of the Helmholtz Boundary Value Problem in $\mathcal{W}_2^2(\Omega)$

In this section, we show that, if certain conditions on the ‘‘input’’ functions and on the boundary are fulfilled, then any generalized solution of the Helmholtz boundary value problem (3.1), (3.2), which is in  $\mathcal{W}_2^1(\Omega)$ , is also the element of  $\mathcal{W}_2^2(\Omega)$ . We assume that  $\partial\Omega$  and  $g$  satisfy the same hypotheses used in the proof of the second fundamental inequality in Section 3.4 and  $\sigma \in \mathcal{C}_0^{0,1}(\partial\Omega) \cap \mathcal{W}_\infty^1(\partial\Omega)$ .

#### 3.5.1 Solvability in $\mathcal{W}_2^2(\Omega)$ with $\partial\Omega \in \mathcal{C}^2$

Let us consider the problem (3.1), (3.2), i.e.

$$-\Delta_{\mathbf{x}} u - \lambda u = -f \text{ in } \Omega, \quad (3.50)$$

$$\frac{\partial u}{\partial \mathbf{n}} + \sigma u = g \text{ on } \partial\Omega, \quad (3.51)$$

where  $f \in \mathcal{L}_2(\Omega)$ ,  $g \in \mathcal{W}_2^1(\partial\Omega)$ ,  $\sigma \in \mathcal{C}_0^{0,1}(\partial\Omega) \cap \mathcal{W}_\infty^1(\partial\Omega)$  and  $\partial\Omega \in \mathcal{C}^2$ .

We know that this problem has a unique solution  $u \in \mathcal{W}_2^1(\Omega)$ . Let us rewrite the weak form of this problem here

$$\int_{\Omega} \langle \nabla_{\mathbf{x}} u, \nabla_{\mathbf{x}} \bar{\eta} \rangle d\mathbf{x} + \int_{\partial\Omega} \sigma u \bar{\eta} dS = \lambda \int_{\Omega} u \bar{\eta} d\mathbf{x} + \int_{\partial\Omega} g \bar{\eta} dS - \int_{\Omega} f \bar{\eta} d\mathbf{x}, \quad (3.52)$$

where  $\bar{\eta} \in \mathcal{W}_2^1(\Omega)$ . Adding to both sides of the equation (3.52) the term  $\lambda_0 u$  and substituting the function  $(\lambda + \lambda_0)u - f$  by  $f_u$  and  $-\sigma u + g$  by  $g_u$  one gets the equivalent form of the equation (3.52)

$$a(u, \eta) = \int_{\Omega} f_u \bar{\eta} d\mathbf{x} + \int_{\partial\Omega} g_u \bar{\eta} dS, \quad (3.53)$$

where  $a(u, \eta)$  is defined as  $\int_{\Omega} \langle \nabla_{\mathbf{x}} u, \nabla_{\mathbf{x}} \bar{\eta} \rangle + \lambda_0 u \bar{\eta} \, d\mathbf{x}$ <sup>3</sup>. Let us show that the functions  $f_u$  and  $g_u$  belong to the function spaces  $\mathcal{L}_2(\Omega)$  and  $\mathcal{W}_2^{\frac{1}{2}}(\partial\Omega)$ , respectively<sup>4</sup>. Obviously,  $f_u := (\lambda + \lambda_0)u - f$  belongs to  $\mathcal{L}_2(\Omega)$  because the function  $u$  is in  $\mathcal{W}_2^1(\Omega) \subset \mathcal{L}_2(\Omega)$  and  $f \in \mathcal{L}_2(\Omega)$ . In order to show that the function  $g_u := -\sigma u + g$  belongs to the space  $\mathcal{W}_2^{\frac{1}{2}}(\partial\Omega)$  we first mention one useful theorem, cf. [25]

**Theorem 3.5.1** *Let the domain  $\Omega \subset \mathbb{R}^n$  be Lipschitz and  $\frac{1}{2} < s \leq 1$  then the trace operator  $\gamma|_{\partial\Omega} : \mathcal{W}_2^s(\Omega) \rightarrow \mathcal{W}_2^{s-\frac{1}{2}}(\partial\Omega)$  is continuous and the following estimate holds*

$$\|\gamma|_{\partial\Omega} u\|_{\mathcal{W}_2^{s-\frac{1}{2}}(\partial\Omega)} \leq C \|u\|_{\mathcal{W}_2^s(\Omega)}. \quad (3.54)$$

Applying this theorem to the function  $u$  we see that the function  $\gamma|_{\partial\Omega} u =: u$  is well defined and belongs to the space  $\mathcal{W}_2^{\frac{1}{2}}(\partial\Omega)$ . The product of two functions  $u \in \mathcal{W}_2^{\frac{1}{2}}(\partial\Omega)$  and  $\sigma \in \mathcal{C}_0^{0,1}(\partial\Omega) \cap \mathcal{W}_2^1(\partial\Omega)$  will belong to the space  $\mathcal{W}_2^{\frac{1}{2}}(\partial\Omega)$ . But to show this we use one useful theorem

**Theorem 3.5.2** *Let  $s = k + \delta$  for  $\delta \in [0, 1)$  and let  $U$  and  $V \subset \mathbb{R}^3$  be open sets. Let the function  $\Upsilon$  is in  $\mathcal{C}_0^{k,1}(V)$ , i.e.  $\text{supp}\Upsilon \in V$  and  $\Upsilon \in \mathcal{C}^{k,1}(\mathbb{R}^3)$ . Then, if  $w$  belongs to  $\mathcal{W}_2^s(U)$ , it follows that  $\Upsilon w \in \mathcal{W}_2^s(V \cap U)$  and, hence,  $\|\Upsilon w\|_{\mathcal{W}_2^s(U \cap V)} \leq C_{\sigma} \|w\|_{\mathcal{W}_2^s(U)}$ .*

Cf. [44] for the proof. Assume that the sets  $U$  and  $V$  contain the boundary  $\partial\Omega$ ,  $\Upsilon|_{\partial\Omega} = \sigma$  and  $w|_{\partial\Omega} = u|_{\partial\Omega}$ . Hence, we are able to conclude

$$\|\sigma u\|_{\mathcal{W}_2^{\frac{1}{2}}(\partial\Omega)} \leq C_{\sigma} \|u\|_{\mathcal{W}_2^{\frac{1}{2}}(\partial\Omega)}. \quad (3.55)$$

The function  $g$  is assumed to be from  $\mathcal{W}_2^1(\partial\Omega) \subset \mathcal{W}_2^{\frac{1}{2}}(\partial\Omega)$ . Hence,  $g_u \in \mathcal{W}_2^{\frac{1}{2}}(\partial\Omega)$ . Now we show that the bilinear form  $a(u, \eta)$  is  $\mathcal{W}_2^1(\Omega)$ -coercive.

**Definition 3.5.3** *The bilinear form  $\tilde{a}(u, \eta) := \int_{\Omega} a_{ij} u_{x_i} \bar{\eta}_{x_j} + a_i u_i \bar{\eta} \, d\mathbf{x}$  is called strongly elliptic if there is a constant  $c_0 > 0$  such that*

$$\Re(a_{ij} \xi_i \bar{\xi}_j) \geq c_0 |\xi_i|^2, \quad \boldsymbol{\xi} = (\xi_1, \dots, \xi_n) \in \mathbb{C}^n, \quad \mathbf{x} \in \Omega, \quad (3.56)$$

here  $a_{ij}$  and  $a_i$  are from  $\mathcal{L}_{\infty}(\Omega)$ , cf. [56].

In our case the bilinear form  $a(u, \eta)$  is strongly elliptic<sup>5</sup>.

<sup>3</sup>Such a definition of the bilinear form  $a(u, \eta)$  will lead to the  $\mathcal{W}_2^1(\Omega)$ -coercivity of  $a(u, \eta)$ , cf. Theorem 3.5.4.

<sup>4</sup>The spaces  $\mathcal{W}_2^s(\Omega \subset \mathbb{R}^n)$ ,  $n \in \mathbb{N}$  for fractional  $s \geq 0$  are defined in [2], [35].

<sup>5</sup>One can choose  $c_0$  equal to 1.

**Theorem 3.5.4** *Let the bilinear form  $a(u, \eta)$  be strongly elliptic. Then there is a  $\lambda_0 \in \mathbb{R}$  such that for every  $\lambda > \lambda_0$ , the form*

$$a(u, \eta) + \lambda \int_{\Omega} u \bar{\eta} \, d\mathbf{x} \quad (3.57)$$

is  $\mathcal{W}_2^1(\Omega)$  coercive<sup>6</sup>.

Let us count the facts we proved above

- 1. The problem (3.1), (3.2) is written in the form of the equation (3.53), where the solution  $u$  belongs to  $\mathcal{W}_2^1(\Omega)$ .
- 2. The functions  $f_u$  and  $g_u$  belong to  $\mathcal{L}_2(\Omega)$  and  $\mathcal{W}_2^{\frac{1}{2}}(\partial\Omega)$ , respectively.
- 3. The bilinear form  $a(u, \eta)$  is  $\mathcal{W}_2^1(\Omega)$ -coercive.

By the Theorems (9.1.17) and (9.1.15) from [35], which say that if all three conditions above are satisfied and  $\partial\Omega \in \mathcal{C}^2$ , then the solution  $u$  belongs to the space  $\mathcal{W}_2^2(\Omega)$  and the second fundamental inequality holds, cf. Section 3.4.

**Remark 3.5.5** Under some additional conditions on the smoothness of the functions  $f, g, \sigma$  and  $\partial\Omega$  one is able to use the Theorems (9.1.17) and (9.1.15) to get more regular solution  $u$ , i.e.  $u \in \mathcal{W}_2^3\Omega$ ,  $u \in \mathcal{W}_2^4(\Omega)$ , etc.<sup>7</sup>

**Remark 3.5.6** If one is confused about the presence of the inhomogeneous parts in the boundary conditions, then one is able to homogenize them via substitution  $\tilde{u} = u - U$ , where the function  $U \in \mathcal{W}_2^2(\Omega)$  is known and satisfy condition  $\frac{\partial U}{\partial \mathbf{n}} + \sigma U = g$ .

### 3.5.2 Solvability in $\mathcal{W}_2^2(\Omega)$ for $\partial\Omega \in \mathcal{C}^2$ piecewise

In order to prove the solvability of the problem (3.1), (3.2) in  $\mathcal{W}_2^2(\Omega)$ , where  $\partial\Omega$  has convex corners (i.e. the inner angle between two edges is less than  $\pi$ ), we have to remind that the constants in the second fundamental inequality, considered above, are independent of the curvature of convex parts of the boundary  $\partial\Omega$ . They may depend on the curvature of concave parts. And it can be chosen as the upper bound for the second fundamental quadratic form  $\mathcal{B}$ .

Let us choose some sequence  $\Omega_k$ ,  $k = 1, 2, \dots$  of open sets of  $\mathbb{R}^3$  with  $\mathcal{C}^2$  boundaries  $\partial\Omega_k$  such that  $\Omega_k \subseteq \Omega$  and  $d(\partial\Omega, \partial\Omega_k)$  tends to zero as  $k \rightarrow \infty$ , where  $d(\partial\Omega, \partial\Omega_k)$  denotes the distance from  $\partial\Omega$  to  $\partial\Omega_k$ , cf. [34]. Assume that the concave parts of boundaries  $\partial\Omega$  and  $\partial\Omega_k$  coincide almost everywhere, cf. Fig. 3.2. We consider the Robin problem in  $\Omega_k$ , i.e.

<sup>6</sup>Cf. [56] for the proof.

<sup>7</sup>In order to get more regular solution  $u$  one has to use another theorem about the traces instead of the Theorem 3.5.1, it can be found, for example, in [35].

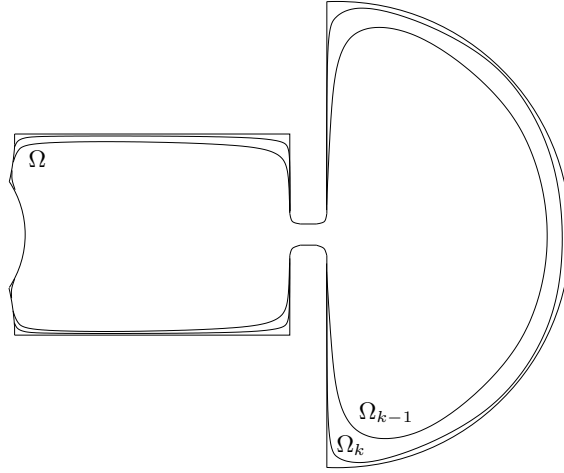


Figure 3.2: Sequences of the domains, 2D cut.

$$\Delta_{\mathbf{x}} u_k + \lambda u_k = \tilde{f}, \quad \text{in } \Omega_k \quad (3.58)$$

$$\frac{\partial u_k}{\partial \mathbf{n}} + \sigma_k u_k = g_k, \quad \text{on } \partial\Omega_k. \quad (3.59)$$

The functions  $\sigma_{k_m}$  and  $g_{k_m}$  on the  $\partial\Omega_{k_m}$  are defined as the restrictions  $G|_{\partial\Omega_{k_m}} = g_{k_m}$  and  $\Upsilon|_{\partial\Omega_{k_m}} = \sigma_{k_m}$ , where the functions  $G$  and  $\Upsilon$  belong to the spaces

$$\mathcal{G} := \left\{ \tilde{u} \in \mathcal{C}^1(\mathbb{R}^3 \setminus \partial\Omega) \mid \tilde{T}_{\partial\Omega} \tilde{u} \in \mathcal{W}_2^1(\partial\Omega) \right\}$$

and

$$\mathcal{F} := \left\{ \tilde{u} \in \mathcal{C}^1(\mathbb{R}^3 \setminus \partial\Omega) \mid \tilde{T}_{\partial\Omega} \tilde{u} \in \mathcal{C}_0^{0,1}(\partial\Omega) \cap \mathcal{W}_\infty^1(\partial\Omega) \right\},$$

respectively, and  $G|_{\partial\Omega} = g$  and  $\Upsilon|_{\partial\Omega} = \sigma$ . Here,  $\tilde{T}$  denotes a bounded projection. Obviously,  $\tilde{f} := f|_{\Omega_k} \in \mathcal{L}_2(\Omega_k)$ ,  $g_k \in \mathcal{W}_2^1(\partial\Omega_k)$ ,  $\sigma_k \in \mathcal{C}_0^{0,1}(\partial\Omega_k) \cap \mathcal{W}_\infty^1(\partial\Omega_k)$ . Hence  $u_k$  exists and belong to  $\mathcal{W}_2^2(\Omega_k)$  space by the theorems above.

From the fact that the functions  $g_k$  and  $\sigma_k$  are the restrictions of  $G$  and  $\Upsilon$ , respectively, and, hence, are bounded and by the Theorem 3.4.5 it follows that there exists a constant  $C$  independent of  $k$  such that

$$\|u_k\|_{\mathcal{W}_2^2(\Omega_k)} \leq C. \quad (3.60)$$

By the Theorem (1.4.3.1) in [34], which says that for a bounded open subsets  $\Omega \subset \mathbb{R}^n$  with a Lipschitz boundary and for every  $s > 0$  there exists a continuous linear operator  $P_s$  from  $\mathcal{W}_p^s(\Omega)$  into  $\mathcal{W}_p^s(\mathbb{R}^n)$  such that  $P_s u|_\Omega = u$ , one is able to consider a sequence  $P_2 u_k|_\Omega$  in  $\mathcal{W}_2^2(\Omega)$ . This sequence, due to (3.60) and due to continuity and linearity of  $P_2$ , is bounded. Hence, there exists an increasing sequence of integers  $k_m$  and a function  $P_2 u|_\Omega \in \mathcal{W}_2^2(\Omega)$  such that

$$u_{k_m}^\Omega := P_2 u_{k_m}|_\Omega \xrightarrow[k_m \rightarrow \infty]{} P_2 u|_\Omega = u \quad \text{weakly in } \mathcal{W}_2^2(\Omega). \quad (3.61)$$

We now have to show that  $u =: u_{\text{sol}}$  indeed is a solution of the weak form of the problem (3.1), (3.2), i.e.

$$\int_{\Omega} \langle \nabla_{\mathbf{x}} u_{\text{sol}}, \nabla_{\mathbf{x}} v \rangle d\mathbf{x} + \int_{\partial\Omega} \sigma u_{\text{sol}} v dS = \lambda \int_{\Omega} u_{\text{sol}} v d\mathbf{x} + \int_{\partial\Omega} g v dS - \int_{\Omega} f v d\mathbf{x}, \quad (3.62)$$

where  $v \in \mathcal{W}_2^1(\Omega)$ . We define a function  $V \in \mathcal{C}^1(\mathbb{R}^3)$  such that  $V|_{\Omega} = v$ . It is clear that  $V|_{\Omega_k} \in \mathcal{W}_2^1(\Omega_k)$  and from (3.58) and (3.59) we deduce

$$\begin{aligned} \int_{\Omega_{k_m}} \langle \nabla_{\mathbf{x}} u_{k_m}, \nabla_{\mathbf{x}} V \rangle d\mathbf{x} + \int_{\partial\Omega_{k_m}} \sigma_{k_m} u_{k_m} V dS &= \lambda \int_{\Omega_{k_m}} u_{k_m} V d\mathbf{x} + \int_{\partial\Omega_{k_m}} g_{k_m} V dS \\ &- \int_{\Omega_{k_m}} \tilde{f} V d\mathbf{x}. \end{aligned} \quad (3.63)$$

We have to consider the limit of the equality (3.63) when  $k \rightarrow \infty$ . We have first

$$\begin{aligned} \int_{\Omega} uv d\mathbf{x} - \int_{\Omega_{k_m}} u_{k_m} V d\mathbf{x} &= \int_{\Omega} uv d\mathbf{x} - \int_{\Omega_{k_m}} u_{k_m}^{\Omega} V d\mathbf{x} \\ &= \int_{\Omega \setminus \Omega_{k_m}} uv d\mathbf{x} + \int_{\Omega_{k_m}} (u - u_{k_m}^{\Omega}) V d\mathbf{x}. \end{aligned} \quad (3.64)$$

Hence,

$$\begin{aligned} \left| \int_{\Omega} uv d\mathbf{x} - \int_{\Omega_{k_m}} u_{k_m} V d\mathbf{x} \right| &\leq \|u\|_{\mathcal{L}_2(\Omega)} \left( \int_{\Omega \setminus \Omega_{k_m}} V^2 d\mathbf{x} \right)^{\frac{1}{2}} \\ &+ \|u - u_{k_m}^{\Omega}\|_{\mathcal{L}_2(\Omega)} \|V\|_{\mathcal{L}_2(\Omega)}. \end{aligned} \quad (3.65)$$

The right hand side of this inequality converges to zero due to the compactness of the embedding of  $\mathcal{W}_2^2(\Omega)$  in  $\mathcal{L}_2(\Omega)$ . Analogously,

$$\begin{aligned} \left| \int_{\Omega} \nabla_{\mathbf{x}} u \cdot \nabla_{\mathbf{x}} v d\mathbf{x} - \int_{\Omega_{k_m}} \nabla_{\mathbf{x}} u_{k_m} \cdot \nabla_{\mathbf{x}} V d\mathbf{x} \right| &\leq \|u\|_{\mathcal{W}_2^1(\Omega)} \left( \int_{\Omega \setminus \Omega_{k_m}} (\nabla_{\mathbf{x}} V)^2 d\mathbf{x} \right)^{\frac{1}{2}} \\ &+ \|u - u_{k_m}^{\Omega}\|_{\mathcal{W}_2^1(\Omega)} \|V\|_{\mathcal{W}_2^1(\Omega)}. \end{aligned} \quad (3.66)$$

The right hand side converges to zero, as in the previous case, due to the compactness of the embedding of  $\mathcal{W}_2^2(\Omega)$  in  $\mathcal{W}_2^1(\Omega)$ , cf. [2], [34] or [13].

Obviously, the last term in (3.63) converges to the last term of (3.62), i.e.

$$\left| \int_{\Omega} f v d\mathbf{x} - \int_{\Omega_{k_m}} \tilde{f} V d\mathbf{x} \right| \leq \|f\|_{\mathcal{L}_2(\Omega)} \left( \int_{\Omega \setminus \Omega_{k_m}} V^2 d\mathbf{x} \right)^{\frac{1}{2}} + \|f - \tilde{f}\|_{\mathcal{L}_2(\Omega)} \|V\|_{\mathcal{L}_2(\Omega)}. \quad (3.67)$$

Let us consider now the term  $\int_{\partial\Omega_{k_m}} (-\sigma_{k_m} u_{k_m} + g_{k_m}) V dS$ . We have to show that

$$\int_{\partial\Omega_{k_m}} (-\sigma_{k_m} u_{k_m} + g_{k_m}) V dS \xrightarrow{k_m \rightarrow \infty} \int_{\partial\Omega} (-\sigma u + g) V dS. \quad (3.68)$$

First of all we choose the covering  $\mathcal{V}_l$ ,  $1 \leq l \leq \tilde{l}$  of the boundary  $\partial\Omega_{k_m}$  for each  $k_m$ . Here  $\mathcal{V}_l$  is defined as follows

$$\mathcal{V}_l := \{(y_1^l, y_2^l, y_3^l) \mid -a_j^l < y_j^l < a_j^l, 1 \leq j \leq 3\},$$

where  $(y_1^l, y_2^l, y_3^l)$  are some local coordinates. Next, we fix a partition of unity  $(\theta_l, 1 \leq l \leq \tilde{l})$  on  $\partial\Omega$  and  $\partial\Omega_{k_m}$  corresponding to the covering  $\mathcal{V}_l$ .

Obviously, that

$$\sum_{l=1}^{\tilde{l}} \int_{\partial\Omega_{k_m}} \theta_l (-\sigma_{k_m} u_{k_m} + g_{k_m}) dS = \int_{\partial\Omega_{k_m}} (-\sigma_{k_m} u_{k_m} + g_{k_m}) dS$$

and

$$\sum_{l=1}^{\tilde{l}} \int_{\partial\Omega} \theta_l (-\sigma u + g) dS = \int_{\partial\Omega} (-\sigma u + g) dS.$$

To make our life easier we consider all the limits in local coordinates. The desired limit (3.68) will follow from the last two summations above. We consider separately

$$\mathcal{I}_1 := \int_{\partial\Omega_{k_m}} -\theta_l V(\sigma_{k_m} u_{k_m} - \Upsilon u) + \theta_l V(g_{k_m} - G) dS \quad (3.69)$$

and

$$\mathcal{I}_2 := \int_{\partial\Omega_{k_m}} \theta_l V(-\Upsilon u + G) dS - \int_{\partial\Omega} \theta_l V(-\sigma u + g) dS. \quad (3.70)$$

Consider the expression (3.69) <sup>8</sup>

$$\begin{aligned} |\mathcal{I}_1| &\leq C_1 \int_{\partial\Omega_{k_m} \cap \mathcal{V}_l} |u_{k_m} - u| dS + C_2 \int_{\partial\Omega_{k_m} \cap \mathcal{V}_l} |g_{k_m} - g_{k_m}| dS \\ &= C_1 \int_{\mathcal{V}_l'} |u_{k_m} - u|(z, \varphi_{k_m}(z)) \sqrt{1 + (\varphi'_{k_m}(z))^2} dz, \end{aligned} \quad (3.71)$$

<sup>8</sup>Let us note that we are able to choose the covering  $\mathcal{V}_l$  in such a way that the boundaries  $\partial\Omega_{k_m}$  and  $\partial\Omega$  can be represented as  $\mathcal{C}^2$  functions  $\varphi_{k_m}$  and  $\varphi$ , respectively. The function, which is defined, for example, on the boundary  $\partial\Omega_{k_m}$  in local coordinates, will depend on two variables, i.e.  $g = g(z^l, \varphi_{k_m}(z^l))$ , where  $\{z = (y_1^l, y_2^l) \mid -a_j^l < y_j^l < a_j^l, j = 1, 2\} =: \mathcal{V}_l'$ .



where  $C_1$  does not depend on  $k_m$ . Let us use the fact (we will prove it further) that  $|\nabla\varphi_{k_m}^l(z^l)|, |\nabla\varphi^l(z^l)| \leq L \in \mathbb{R}$  for every  $z^l \in \mathcal{V}_l'$ , i.e.

$$\begin{aligned}
|\mathcal{I}_1| &\leq C_1 \sqrt{1+L^2} \left\{ \int_{\mathcal{V}_l'} |u_{k_m}^\Omega - u|(z, \varphi(z)) dz \right. \\
&\quad \left. + \int_{\mathcal{V}_l'} |(u_{k_m} - u)(z, \varphi_{k_m}(z)) - (u_{k_m}^\Omega - u)(z, \varphi(z))| dz \right\} \\
&\leq \tilde{C}_1 \|u_{k_m}^\Omega - u\|_{\mathcal{L}_2(\partial\Omega)} + C_1 \sqrt{1+L^2} \int_{\mathcal{V}_l'} \left| \int_{\varphi(z)}^{\varphi_{k_m}(z)} D_y(u_{k_m}^\Omega - u)(z, y) dy \right| dz \\
&\leq \tilde{C}_1 \|u_{k_m}^\Omega - u\|_{\mathcal{L}_2(\partial\Omega)} + \tilde{C}_1 \max_{z \in \mathcal{V}_l'} |\varphi_{k_m}(z) - \varphi(z)|^{\frac{1}{2}} \|u_{k_m}^\Omega - u\|_{\mathcal{W}_2^1(\partial\Omega_{k_m})}.
\end{aligned} \tag{3.72}$$

Hence,

$$\int_{\partial\Omega_{k_m}} -\theta_l V(\sigma_{k_m} u_{k_m} - \Upsilon u) + \theta_l V(g_{k_m} - G) dS \xrightarrow[k_m \rightarrow \infty]{} 0 \tag{3.73}$$

since  $u_{k_m}^\Omega \rightarrow u$  weakly in  $\mathcal{W}_2^2(\Omega)$  and  $\varphi_{k_m} \rightarrow \varphi$  uniformly in  $\mathcal{V}_l'$ <sup>9</sup>.

Let us attack the second expression (3.70). Obviously,  $-(\theta_l V \Upsilon)(z, \varphi_{k_m}(z))$  and  $(\theta_l V G)(z, \varphi_{k_m}(z))$  converge uniformly to  $-(\theta_l V \sigma)(z, \varphi(z))$  and  $(\theta_l V g)(z, \varphi(z))$ , respectively. We also have

$$\begin{aligned}
|u(z, \varphi(z)) - u(z, \varphi_{k_m}(z))| &\leq \int_{\varphi_{k_m}(z)}^{\varphi(z)} |D_y u(z, y)| dy \\
&\leq |\varphi(z) - \varphi_{k_m}(z)|^{\frac{1}{2}} \left\{ \int_{-a_3}^{a_3} |D_y u(z, y)|^2 dy \right\}^{\frac{1}{2}} \tag{3.74}
\end{aligned}$$

and consequently  $u(z, \varphi_{k_m}(z))$  converges to  $u(z, \varphi(z))$  almost everywhere in  $\mathcal{V}_l'$ . This shows that the integrand of the first integral in (3.70) has a limit almost everywhere in  $\mathcal{V}_l'$ . In addition we have

$$|u(z, \varphi_{k_m}(z))| \leq |u(z, \varphi(z))| + |\varphi_{k_m}(z) - \varphi(z)|^{\frac{1}{2}} \left\{ \int_{-a_3}^{a_3} |D_y u(z, y)|^2 dy \right\}^{\frac{1}{2}}. \tag{3.75}$$

It means that the sequence  $\{u(z, \varphi_{k_m}(z))\}_{k_m}$  is bounded by a fixed integrable function on  $\mathcal{V}_l'$ . The same follows for the sequence  $\{g_{k_m}(z, \varphi_{k_m}(z))\}_{k_m}$ . By the

<sup>9</sup>This fact we will prove further.

Lebesgue's Dominated Convergence Theorem, cf. [15], one concludes that

$$\int_{\partial\Omega_{k_m}} \theta_l V(-\sigma_{k_m} u + g_{k_m}) dS \rightarrow \int_{\partial\Omega} \theta_l V(-\sigma u + g) dS. \quad (3.76)$$

The desired limit (3.68) follows from (3.73) and (3.76).

By this we proved the following theorem

**Theorem 3.5.7** *Let  $\Omega$  be a bounded open subset of  $\mathbb{R}^3$  such that all corners are convex and the boundary  $\partial\Omega$  is piecewise  $\mathcal{C}^2$ . Then for each  $f \in \mathcal{L}_2(\Omega)$  there exists a unique  $u \in \mathcal{W}_2^2(\Omega)$  which is a solution of the equation (3.62) for all  $v \in \mathcal{W}_2^1(\Omega)$ ,  $g \in \mathcal{W}_2^1(\partial\Omega)$  and  $\sigma \in \mathcal{C}_0^{0,1}(\partial\Omega) \cap \mathcal{W}_\infty^1(\partial\Omega)$ .*

In order to finish the proof of the Theorem 3.5.7 we have to show that  $|\nabla\varphi_{k_m}^l(z^l)|$ ,  $|\nabla\varphi^l(z^l)| \leq L \in \mathbb{R}$  for every  $z^l \in \mathcal{V}_l'$  and  $\varphi_{k_m} \rightarrow \varphi$  uniformly in  $\mathcal{V}_l'$ . The second property follows from the fact that the distance from  $\partial\Omega$  to  $\partial\Omega_k$  converges to zero as  $k \rightarrow \infty$ . Hence, the distance from the graph  $\varphi^l$  to the graph  $\varphi_k^l$  tends to zero. This means that  $\varphi_k^l$  converges uniformly to  $\varphi^l$ .

The boundedness of the terms  $|\nabla\varphi_{k_m}^l(z^l)|$  and  $|\nabla\varphi^l(z^l)|$  follows from the fact that these functions are from  $\mathcal{C}^2$  in each  $\mathcal{V}_l$  (at least we are free to choose such a covering for piecewise  $\mathcal{C}^2$  boundaries).

**Remark 3.5.8** All this theory, what we have done until now, is sufficient even in the case, when some functions are not smooth enough. For example, in our case we assume that the function  $\sigma$  is from  $\mathcal{C}_0^{0,1}(\partial\Omega) \cap \mathcal{W}_\infty^1(\partial\Omega)$  space. But in the reality it is only from  $\mathcal{L}_\infty(\partial\Omega)$  space. Numerically there will be no difference between these two cases because solvers on robust discretization will make some approximation of all input data we provide. However, from the theoretical point of view it will be nice to know exactly how regular our solution  $u$  is.

### 3.5.3 Solvability of the Helmholtz Boundary Value Problem in $\mathcal{W}_2^2(\Omega)$ Under Condition $\sigma \in \mathcal{L}_\infty(\partial\Omega)$

In previous section we used the fact that the function  $\sigma$  belongs to  $\mathcal{C}_0^{0,1}(\partial\Omega) \cap \mathcal{W}_\infty^1(\partial\Omega)$ . Unfortunately, in our case, cf. Table 3.1, the boundary conditions are not so nice, i.e. there some discontinuities take the place. Hence,  $\sigma \notin \mathcal{C}_0^{0,1}(\partial\Omega) \cap \mathcal{W}_\infty^1(\partial\Omega)$  and the second fundamental inequality (3.49) is no longer true because the constants (at least one of them) are not bounded. We need some another way to prove that under some conditions on the "input" functions  $f$ ,  $g$ ,  $\sigma$  and the boundary  $\partial\Omega$  the solution  $u$  belongs to  $\mathcal{W}_2^2(\Omega)$ .

The problem (3.1), (3.2) has the solution  $u \in \mathcal{W}_2^1(\Omega)$ , which is unique, cf. Section 3.2. Therefore, we are able to consider some equivalent to (3.1), (3.2) prob-

lem

$$\begin{aligned} \Delta_{\mathbf{x}}u &= f - \lambda u = f_u, & \text{in } \Omega, \\ \frac{\partial u}{\partial \mathbf{n}} &= g_u, & \text{on } \partial\Omega, \end{aligned} \quad (3.77)$$

where the index  $u$  refers to the dependence of the right hand sides on the solution  $u$ . For the sake of simplicity we introduce new unknown function  $\tilde{u} = u - U$ ,

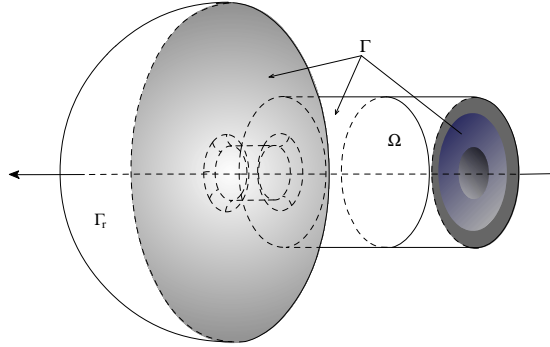


Figure 3.3: Plane part of  $\partial\Omega$  (light-gray artificial boundary)

where  $U \in \mathcal{W}_2^2(\Omega)$  is some known function such that  $\frac{\partial U}{\partial \mathbf{n}}|_{\partial\Omega} = g_u$ . We note that such a function  $U$  exists in our case. We focus on the plane part of the boundary  $\partial\Omega$  depicted by light-gray, cf. Fig. 3.3. The right hand side of the boundary condition (3.2) on this part of  $\partial\Omega$  is homogeneous<sup>10</sup>. It means that if we choose  $U = U(|\mathbf{x}|)$ , then the boundary condition (2.74) will be satisfied, i.e.  $\frac{\partial U}{\partial \mathbf{n}} = 0 = \frac{\partial u}{\partial \mathbf{n}}$  on this part of  $\partial\Omega$ . On the other hand we always can find  $U(|\mathbf{x}|)$  such that the condition  $\frac{\partial U}{\partial \mathbf{n}} = g_u = \sigma u$  is satisfied on  $\Gamma_r$ <sup>11</sup>.

As a consequence, the problem (3.77) reduces to the following one

$$\begin{aligned} \Delta_{\mathbf{x}}\tilde{u} &= \tilde{f}_u, & \text{in } \Omega, \\ \frac{\partial \tilde{u}}{\partial \mathbf{n}} &= 0, & \text{on } \partial\Omega, \end{aligned} \quad (3.78)$$

where  $\tilde{f}_u := f_u - \Delta_{\mathbf{x}}U$ . Obviously, the solution  $\tilde{u}$  of this problem is in  $\mathcal{W}_2^1(\Omega)$ , this is only some shifting of the solution  $u$  by function  $U$ .

We know that the domain  $\Omega$  has the boundary  $\partial\Omega$  with some convex corners and smooth concave parts. Applying analogous theory from the Sections 3.4 and 3.5 to the problem (3.78) one is able to conclude that the solution  $\tilde{u}$  (and, hence, the solution  $u$  of the problem (3.1), (3.2)) belongs to the space  $\mathcal{W}_2^2(\Omega)$ <sup>12</sup>.

<sup>10</sup>Cf. (2.73) and (2.74) under conditions that the curvature is equal to zero and the boundary does not oscillate, i.e.  $\nu = \mathbf{0}$ .

<sup>11</sup>We note that the function  $u$  on the boundary  $\Gamma_r$  is assumed to depend only on the distance  $|\mathbf{x}|$ , cf. Subsection 2.5.3.

<sup>12</sup>One can imagine that the solution  $u$  may belong also to  $\mathcal{W}_2^m(\Omega)$  for  $m \geq 3$  under certain conditions on input data and  $\partial\Omega$ .

**Remark 3.5.9** The theory above does not say anything about the solvability of the problem (2.36), (2.77) and (2.102). The solvability of this problem highly depends on the regularity of the  $p_1$  function. Unfortunately, it is not enough to have  $p_1$  from  $\mathcal{W}_2^2(\Omega)$  space to show the existence of the  $p_2$  solution. On the other hand, it is not a trivial task to find conditions under which  $p_1$  can be more regular. By the Sobolev embedding theorem, cf. [2], one finds that, if the bounded domain  $\Omega \subset \mathbb{R}^3$  has the local Lipschitz property, then there exists the following embedding

$$\mathcal{W}_2^{j+\frac{3}{2}+\varepsilon}(\Omega) \hookrightarrow \mathcal{C}^{j,\alpha}(\bar{\Omega}) \subset \mathcal{C}^j(\bar{\Omega}), \quad (3.79)$$

where  $0 < \alpha \leq \varepsilon$  and  $\varepsilon > 0$ . Assume that  $j = 2$  and the function  $p_1$  belong to the space  $\mathcal{W}_2^{\frac{7}{2}+\varepsilon}(\Omega)$ . Hence, the right hand sides of the equation (2.36) and of the boundary condition (2.77) belong to the spaces  $\mathcal{L}_2(\Omega)$  and  $\mathcal{L}_2(\partial\Omega)$ , respectively. By the Fredholm alternative the problem (2.36), (2.77) and (2.102) has the unique solution which belongs to the space  $\mathcal{W}_2^1(\Omega)$ .

Here, we stop to consider the case of the bounded domain  $\Omega$  and try to establish similar results in the case of the exterior domain  $\Omega^+$ .

### 3.6 The Case of the Exterior Domain $\Omega^+$

We are interested to investigate the properties of the solution  $u$  of the problem

$$\Delta_{\mathbf{x}}u + \lambda u = f \quad \text{in } \Omega^+, \quad (3.80)$$

$$\frac{\partial u}{\partial \mathbf{n}} = g \quad \text{on } \partial\Omega^+, \quad (3.81)$$

$$\lim_{\mathbf{r} \rightarrow \infty} \mathbf{r} \left( u_{\mathbf{r}} + i\sqrt{\lambda}u \right) = 0 \quad \text{uniformly in both spherical angles,} \quad (3.82)$$

where  $\partial\Omega^+$  is the boundary of the loudspeaker, cf. Fig.3.4. The boundary condition "at infinity", (3.82), is the Sommerfeld radiation condition in 3D. To show that the solution  $u$  of the problem (3.80)–(3.82) exists and is regular enough, we split the problem (3.80) – (3.82) into two problems: one of them we denote by interior problem, but another by exterior one, i.e.

$$\Delta_{\mathbf{x}}u_{\text{int}} + \lambda u_{\text{int}} = f_{\text{int}} \quad \text{in } \Omega_{\text{int}}^+, \quad (3.83)$$

$$\frac{\partial u_{\text{int}}}{\partial \mathbf{n}} = g \quad \text{on } \partial\Omega_{\text{int}}^+, \quad (3.84)$$

and

$$\Delta_{\mathbf{x}}u_{\text{ext}} + \lambda u_{\text{ext}} = f_{\text{ext}} \quad \text{in } \Omega_{\text{ext}}^+, \quad (3.85)$$

$$\frac{\partial u_{\text{ext}}}{\partial \mathbf{n}} = g_{\Gamma_r} \quad \text{on } \Gamma_r, \quad (3.86)$$

$$\lim_{\mathbf{r} \rightarrow \infty} \mathbf{r} \left( \frac{\partial u_{\text{ext}}}{\partial \mathbf{r}} + i\sqrt{\lambda}u_{\text{ext}} \right) = 0 \quad \text{uniformly in both spherical angles.} \quad (3.87)$$

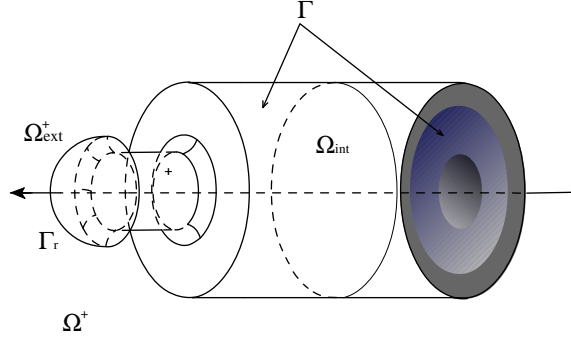


Figure 3.4: Truncated domain  $\Omega_{\text{tr}}^+$  of the exterior domain  $\Omega^+$ .

Here,  $\overline{\Omega}_{\text{int}}^+ \cup \overline{\Omega}_{\text{ext}}^+ = \overline{\Omega}^+$ ,  $\Gamma_r = \overline{\Omega}_{\text{int}}^+ \cap \overline{\Omega}_{\text{ext}}^+$  and  $g|_{\Gamma_r} = g_{\Gamma_r}|_{\Gamma_r}$ , cf. Fig. 3.4. The boundary condition (3.84) defined on  $\Gamma_r$  is an approximation of the Sommerfeld radiation condition on  $\Gamma_r$ . We have to note that the function  $g|_{\Gamma_r} = g_{\Gamma_r}$  has the following form

$$g|_{\Gamma_r} = -i\sqrt{\lambda}u_{\text{int}} + u_{\text{int}}^*, \quad (3.88)$$

where the function  $u_{\text{int}}^* = \mathcal{O}\left(\frac{1}{r^2}\right)$  is unknown function.

As we showed in the previous sections, cf. Sections 3.2–3.5, the solution  $u_{\text{int}}$ , under appropriate smoothness conditions on the boundary  $\partial\Omega_{\text{int}}^+$  and on the boundary condition (3.84), belongs to the corresponding space, i.e.  $\mathcal{W}_2^1(\Omega_{\text{int}}^+)$ ,  $\mathcal{W}_2^2(\Omega_{\text{int}}^+)$ , etc.

The domain  $\Omega_{\text{ext}}^+$  is constructed in such a way that it is exterior with respect to a spherical boundary  $\Gamma_r$ . The problem (3.85)–(3.87) is called by Exterior Neumann Problem, cf. [20]. The existence of the solution  $u_{\text{ext}}$  of such a problem guaranteed by the following theorem, cf. [20]

**Theorem 3.6.1** *The exterior Neumann problem has a unique solution and the solution depends continuously on the boundary data and free term with respect to uniform convergence of the solution on  $\Omega_{\text{ext}}^+$  and all its derivatives on closed subsets of  $\Omega_{\text{ext}}^+$ .*

In the case when  $g_{\Gamma_r} \in \mathcal{C}^{0,\alpha}(\Gamma_r)$ , one is able to find that the solution  $u_{\text{ext}}$  belongs to  $\mathcal{C}^{1,\alpha}(\Gamma_r)$ . The boundary values  $u_{\text{ext}}$  on  $\Gamma_r$  are given by

$$u = Bg_{\Gamma_r}, \quad (3.89)$$

where  $B : \mathcal{C}^{0,\alpha} \rightarrow \mathcal{C}^{1,\alpha}$  is the so-called Dirichlet to Neumann map which is bounded.

Instead of looking for classical solutions in the spaces of continuous or Hölder continuous functions one can also pose and solve the boundary value problems for the Helmholtz equation in a weak formulation for the boundary condition either

in an  $\mathcal{L}_2$  sense or in a Sobolev space setting. This then leads to the existence results under weaker regularity assumptions on the given boundary data and to continuous dependence in different norms. The weak formulation of the problem also gives a possibility to weaken the regularity of the boundary  $\Gamma_r$ , i.e. it allows to consider the so-called Lyapunov boundaries<sup>13</sup> instead of  $\mathcal{C}^2$  boundaries.

### 3.7 The Main Results of Chapter 3

In this section, we summarize all results we have got in this chapter. First of all we have to conclude that the solution in a bounded domain  $\Omega$  exists and is unique due to Fredholm alternative. This theorem shows that under certain conditions on the boundary  $\partial\Omega$ , on the boundary data and on the right hand side of the Helmholtz equation, the solution is unique and it belongs to the Sobolev space  $\mathcal{W}_2^1(\Omega)$ . Next, we derived the Second Fundamental Inequality which means that if the function  $u$  belongs to the space  $\mathcal{W}_2^2(\Omega)$ , then its  $\mathcal{W}_2^2$ -norm is bounded in a special way, cf. (3.49), where the boundary  $\partial\Omega$  is supposed to be from the class  $\mathcal{C}^2$ . This result has been used to show that the solution of the problem (3.1), (3.2) belongs to the space  $\mathcal{W}_2^2(\Omega)$  under appropriate assumptions on the input data, where the boundary  $\partial\Omega$  assumed to be from  $\mathcal{C}^2$ . Further, the assumption on the boundary has been weakened, i.e. we assumed that  $\partial\Omega \in \mathcal{C}^2$  piecewise. Very remarkable property has been established, i.e. the convex corners do not affect the regularity of the solution but the concave corners are critical. Next, we showed that the conditions on the boundary data can also be weakened without any loss of the regularity of the solution  $u$ . We have to note that all the theory, what we derived here, is based on the results which can be found in [46] and [34]. Of course, some certain adaptation is needed.

In the case of an exterior domain  $\Omega^+$  the existence and uniqueness of the solution  $u$  of the problem (3.80)–(3.82) is guaranteed by the Theorem 3.6.1.

Therefore, the solutions in both cases of bounded and unbounded domains exist and are unique. Thus, we can say that the problems<sup>14</sup> defined in Chapter 2, under appropriate assumptions, are well-posed and the numerical techniques can be applied to find corresponding solutions.

---

<sup>13</sup>The boundary is said to satisfy a Lyapunov condition if at each point  $x \in \Gamma_r$  the normal vector  $\mathbf{n}$  to the surface exists and if there are positive constants  $L$  and  $\alpha$  such that for the angle  $\beta(x, y)$  between the normal vectors at  $x$  and  $y$  there holds  $\beta(x, y) \leq L|x - y|^\alpha$ .

<sup>14</sup>In the case of bounded domain  $\Omega$  and in the case of unbounded domain  $\Omega^+$ .



## Chapter 4

# Numerical Method and Simulations

In previous chapters we derived the model which describes the physical phenomenon, i.e. we defined the governing equations, the computational domain and the boundary conditions. Also, we showed that under certain conditions on the input data and on the boundary of the computational domain one is able to prove the existence and uniqueness of the solution of the mathematical problem. Certain regularity results were also derived and presented. A natural stage of the mathematical modeling is the simulation of a physical process. Therefore, we continue with the searching of the solutions  $p_1$  and  $p_2$ . Obviously, the only way to find  $p_1$  and  $p_2$  functions is to use a certain numerical method. An analytical approach will not work here because of the rather complicated geometry of the computational domain, cf. Fig. 2.1, 2.4 and 2.6.

The most popular numerical techniques to solve steady-state acoustic problems within a closed cavity are element based methods (FEM, cf. [64], [13], [8], BEM, cf. [7], [18], [8]). In order to use finite elements (FEM) one has to discretize the computational domain. On each small element certain shape functions of certain order have to be defined. Further, we are able to construct a usually symmetric, frequency independent, real, sparse matrix to solve a linear algebraic system. There exist a lot of direct and iterative solvers which deal with such systems. However, if the frequency increases in our model, then we have to increase the discretization of the computational domain in order to achieve a proper accuracy of the numerical solution of the problem. Such a procedure leads to extremely large matrices and, hence, the computational time and memory requirements also increase. This is why finite element methods can be applied only in the cases of low frequencies, i.e. up to 2kHz, where the computational domain has dimensions of the bass loudspeaker, cf. Fig. 2.5.

The boundary element methods (BEM) are based on solving boundary integral equations. The main advantage of this method is the reduction of the



dimension of the problem. One has to discretize only the boundary of the computational domain. This leads to rather small matrices which are, unfortunately, fully populated, frequency dependent and complex. Hence, one has to apply special solvers to that linear algebraic system. Moreover, the calculation of entries of such a matrix is a non-trivial task. This is a consequence of single and double layer potentials presence in the integral equation, which are singular, cf. [18]. Again, if we would like to increase the frequency in our model, then we have to increase the discretization of the boundary. Hence, the computational costs will increase.

There are several spectral methods, cf. [12], [31], which use global smooth functions (Fourier functions, Chebyshev polynomials, Legendre polynomials, etc.) to approximate the solution of a given problem.

All these methods express the solution in terms of simple functions which do not necessarily solve the investigated partial differential equation. The shape functions do not satisfy any equation of a given problem. This is why we have to take a sufficient amount of the shape functions to achieve a proper accuracy. By the increasing of the frequency in the model the number of the shape functions also increases. This leads to rather large matrices and, hence, to rather big amount of memory and computational time requirements.

Recently, a new numerical method for solving the steady-state acoustic problems has been developed. This method can be applied in the cases of mid-frequency range. It is based on the indirect Trefftz approach, i.e. it does not use simple shape functions to approximate the solution but the exact solutions of the governing differential equations, cf. [58]. This is why the method is called *Wave Based Method* (WBM), i.e. each “wave” is a solution of the homogeneous Helmholtz equation, cf. [23], [24], [37], [38]. This allows to avoid the discretization of the domain. In [24] and [37] one can find certain validation examples which show that the Wave Based Method is faster and much accurate than the Finite Element Method. The authors used two different car-like cavities, where the pressure field has been simulated. From the results of numerical simulations (using WBM and FEM) compared to the measurements one can conclude that starting from certain frequency, WBM better predicts the pressure field than FEM. The speed of the convergence of two numerical methods also has been compared.

The Wave Based Method, however, has some application restrictions. Theory, so far, allowed to apply this method only in cases, where the domain may be subdivided into convex subdomains, cf. [23], [24], [37], [38]. Unfortunately, numerous subdivision of the domain leads to an ineffective procedure to get the numerical solution of the problem. Another disadvantage is the fact that there is no theoretical convergence proof of the WBM solution to the exact one in the

case of concave domains. However, in the last time the hybridization of the wave based method and the finite element method has been investigated, cf. [53], [59], [60]. This hybrid method may be applied to quite arbitrary geometries.

In this chapter, we present the possibility to use pure WBM technique in some cases of concave domains without any hybridization. So far, only convex domains have been considered. Afterwards, we will show that the WBM can be applied to the inhomogeneous Helmholtz equation with rather general right hand side. In the literature one can find only special cases of the right hand side of the Helmholtz equation, which represents the point source. The particular solution in this case can be expressed in rather simple way, cf. [23].

We also present the methodology (based on the Wave Based Technique) to solve homogeneous (or inhomogeneous) Helmholtz equation in an external to a spherical boundary surface, unbounded domain, i.e.  $\Omega^+ = \mathbb{R}^3 \setminus B_r(0)$ , where  $r > 0$  is some fixed radius. This allows to avoid any additional construction of an artificial boundary, cf. Chapters 2 and 3.

All the results presented below in this chapter will allow to apply Wave Based Method to our problem, i.e. to solve the equations (2.35) and (2.36) of Helmholtz type in an unbounded domain with partially concave boundary, cf. Fig. 2.6.

## 4.1 The Main Principles of the Wave Based Method

In order to apply the Wave Based Method to find the functions  $p_1$  and  $p_2$  we have to show first the main ideas of this method. However, all the details in this section can be found in [23].

One simple example may show the concept of this method. Consider the homogeneous Helmholtz equation for a scalar function  $u$ , i.e.

$$\Delta_{\mathbf{x}}u + \kappa^2u = 0 \quad (4.1)$$

in a bounded open subset fitting into a rectangle of size  $L_x \times L_y$ <sup>1</sup>, i.e.  $\Omega \subseteq [0, L_x] \times [0, L_y] \subset \mathbb{R}^2$ , with the Neumann type boundary condition

$$\frac{\partial u}{\partial \mathbf{n}} = v \quad (4.2)$$

on  $\partial\Omega$ <sup>2</sup>. Now, as we already mentioned, we approximate the solution  $u$  of (4.1) by a truncated series, i.e.

$$u(x, y) \approx \sum_{n=0}^N c_n \Phi_n(x, y), \quad N \in \mathbb{N}_0, \quad (4.3)$$

---

<sup>1</sup>The parameters  $L_x$  and  $L_y$  represent the sizes of the smallest rectangle, which circumscribes a given domain  $\Omega$ . However, the term ‘‘smallest rectangle’’ might be changed to just ‘‘rectangle’’, i.e. we are able to consider also rectangles, which circumscribe given domain  $\Omega$  and are not ‘‘the smallest’’ ones.

<sup>2</sup>Everything can be applied to 3D case.

where the functions  $\Phi_n(x, y)$  solve the homogeneous Helmholtz equation (4.1) exactly, i.e.

$$\Phi_n(x, y) = e^{-i(\kappa_{x_j}x + \kappa_{y_j}y)}.$$

The components  $(\kappa_{x_j}, \kappa_{y_j})$ ,  $j \in \{1, 2\}$ , are any complex valued numbers which satisfy the restriction

$$\kappa_{x_j}^2 + \kappa_{y_j}^2 = \kappa^2. \quad (4.4)$$

It means that we are able to define the wave functions in infinitely many ways, and it is proposed to choose (in 2D) the following components, cf. [23], [24]

$$(\kappa_{x_{1n}}, \kappa_{y_{1n}}) = \left( \frac{n\pi}{L_x}, \pm \sqrt{\kappa^2 - \left(\frac{n\pi}{L_x}\right)^2} \right), \quad (4.5)$$

$$(\kappa_{y_{2n}}, \kappa_{x_{2n}}) = \left( \frac{n\pi}{L_y}, \pm \sqrt{\kappa^2 - \left(\frac{n\pi}{L_y}\right)^2} \right), \quad n \in \mathbb{N}_0. \quad (4.6)$$

Thus, the wave functions set  $\{\Phi_n\}_n$  can be rewritten as follows

$$\begin{aligned} \Phi_{2n}(x, y) &= \cos \kappa_{x_{1n}} x e^{-i\kappa_{y_{1n}} y} \\ \Phi_{2n+1}(x, y) &= \cos \kappa_{y_{2n}} y e^{-i\kappa_{x_{2n}} x}. \end{aligned} \quad (4.7)$$

Approximation of the solution (4.3) satisfies the Helmholtz equation (4.1) exactly, no matter how the unknown constants  $c_n$  look like. Therefore, the determination of  $c_n$  depends only on the boundary condition (4.2). Obviously, the boundary condition (4.2), in general, cannot be satisfied exactly because the number of terms in the expansion (4.3) is finite. Thus, one proposes to satisfy it in an average integral sense. We multiply both sides of (4.2) by a test function  $\aleph$  and integrate over the boundary  $\partial\Omega$

$$\int_{\partial\Omega} \aleph(\mathbf{x}) \frac{\partial u}{\partial \mathbf{n}}(\mathbf{x}) dS = \int_{\partial\Omega} \aleph(\mathbf{x}) v(\mathbf{x}) dS. \quad (4.8)$$

This is so-called weighted residual formulation, cf. [23]. Inserting the expansion (4.3) into the latter expression we get the equation with respect to unknowns  $c_n$ . In order to construct a linear algebraic system we choose the test function  $\aleph$  equal to  $\Phi_j$ . Running the index  $j$  from 0 to  $N$  we get  $N + 1$  equations for  $N + 1$  unknowns  $c_n$ ,  $n = \overline{0, N}$ . The corresponding linear algebraic system looks as

$$\mathbf{A} \mathbf{c} = \mathbf{b}, \quad (4.9)$$

where

$$\mathbf{A} : \int_{\partial\Omega} \Phi_j(\mathbf{x}) \frac{\partial \Phi_n}{\partial \mathbf{n}}(\mathbf{x}) d\mathbf{S} \quad (4.10)$$

and

$$\mathbf{b} = \int_{\partial\Omega} \Phi_j(\mathbf{x}) \mathbf{v}(\mathbf{x}) d\mathbf{S}, \quad (4.11)$$

$j, n = \overline{0, N}$ . The matrix  $\mathbf{A}$  is rather small<sup>3</sup> and, hence, the system (4.9) can be solved relatively fast, cf. [24] and [37], where the details of the convergence speed are presented.

To show that the Wave Based Method really works, we present a trivial example. The homogeneous Helmholtz equation (4.1) has been solved numerically in the box  $\Pi := [0, 1] \times [0, 1]$ . Here, we used rather simple boundary conditions, cf. Fig.4.1.

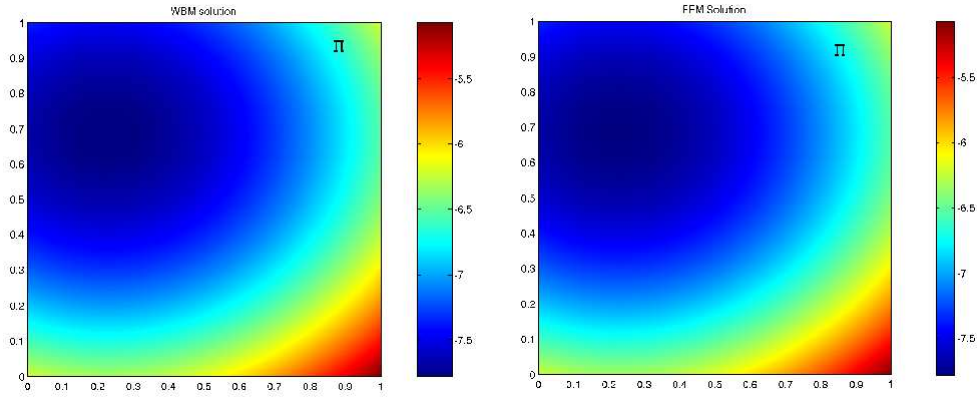


Figure 4.1: Comparison of the WBM (left) and FEM (right) solutions (real parts) of the problem (4.1), (4.2), where  $v|_{x=0} = 1$ ,  $v|_{y=1} = 2$ ,  $v|_{x=1} = 3$  and  $v|_{y=0} = 4$ .

**Remark 4.1.1** Note that the Wave Based Method can be applied also in the cases of Dirichlet, Robin or mixed type boundary conditions, cf. [23] for the details.

## 4.2 On the Convergence of the Wave Based Method

So far we did not investigate the convergence of WBM solution (4.3). The necessary condition for the convergence of the WBM solution is that the normal numerical velocity on the boundary  $\partial\Omega$  converges to the exact normal velocity, i.e.

$$\lim_{N \rightarrow \infty} \sum_{n=0}^N c_n \frac{\partial \Phi_n}{\partial \mathbf{n}}(\mathbf{x}) \Big|_{\partial\Omega} = v(\mathbf{x}). \quad (4.12)$$

This condition is also sufficient, cf. [23]. The only thing we have to show is that the wave functions set (or sets)  $\{\Phi_n\}_n$  exists, that it is complete and can

<sup>3</sup>However, the main disadvantage is that  $\mathbf{A}$  is fully populated. Yet, the components of  $\mathbf{A}$  are complex valued and frequency dependent.

approximate a homogeneous scalar field<sup>4</sup>  $u =: u_\Omega$  with an arbitrary normal velocity on the boundary  $\partial\Omega$ . Obviously, if the domain  $\Omega$  is just a rectangle (cuboid), then such a wave functions set  $\{\Phi_n\}_n$  exists and it looks exactly (in 2D case) like it was written above, cf. (4.7), [23], [24]. Fortunately, the same wave functions set can be applied in the case of a non-rectangular (non-cuboidal) domain  $\Omega$ .

There are several restrictions on the use of the WBM technique. In particular, there seems to be a lack of theoretical results on the applicability of the WBM to smooth non-convex domains. Only polygon-shaped (polyhedron-shaped) domains were considered. Such domains, clearly, can be subdivided into several *convex* subdomains, cf. [23], [24], [37], [38]. The theory, so far, says nothing about the cases of domains with concave parts<sup>5</sup>. Of course, we are able to approximate such kind of domain with aid of a polygon (polyhedron), but then we already create some error into our solution via shape approximation. Fortunately, there are some non-convex domains for which the WBM solution converges to the exact one, i.e. the scalar field  $u_\Omega$  in such a non-convex domain is homogeneous and it can be represented as a linear combination of the wave functions of the circumscribed rectangular (in 2D) domain, cf. (4.7). In [23] it is already mentioned that such domains may exist. But there was no detailed description what they are and how to classify them. In this section, we are filling this gap.

#### 4.2.1 Classification of the Problems

From now on we subdivide the class of the problems of type (4.1), (4.2) into three subclasses:

1. the domain  $\Omega$  is convex;
2. the domain  $\Omega$  is non-convex (concave) and concave parts<sup>6</sup> of the boundary  $\partial\Omega$  are Lipschitz continuous. The angle between any two tangents of a connected concave segment of the boundary  $\partial\Omega$ <sup>7</sup> is greater than or equal

---

<sup>4</sup>By the homogeneous scalar field we understand the function which solves the homogeneous Helmholtz equation.

<sup>5</sup>Here, we do not consider cases, when the computational domain  $\Omega$  is non-convex and the boundary conditions on  $\partial\Omega$  are chosen in such a way that the scalar field  $u_\Omega$  by the construction is homogeneous, cf. [23]. In other words, the representation (4.3) satisfies both the equation (4.1) and the condition (4.2). Let us consider one small example. Assume that we have rectangular domain  $\Pi$  and boundary conditions on  $\partial\Pi$ :  $\frac{\partial u_\Pi}{\partial \mathbf{n}} \Big|_{\partial\Pi} = 1$ . One is able analytically find the solution  $u_\Pi$ . Now inside the domain  $\Pi$  we construct some subdomain  $\Omega$  in the way depicted in Fig. 4.2a. On  $\partial\Omega$  we define the boundary condition  $\frac{\partial u_\Omega}{\partial \mathbf{n}} \Big|_{\partial\Omega} = \frac{\partial u_\Pi}{\partial \mathbf{n}} \Big|_{\partial\Omega}$ . Obviously,  $u_\Omega$  will be only some restriction of  $u_\Pi$ , i.e.  $u_\Omega = u_\Pi|_\Omega$ .

<sup>6</sup>The number of concave parts of  $\partial\Omega$  and, hence, convex parts of  $\partial\Omega$  is finite. This is to avoid the consideration of certain domains with uncontrollable oscillating boundaries.

<sup>7</sup>For example, we do not look at the angle between the tangents  $T_1$  and  $T_3$ , cf. Fig. 4.2b.

to  $\frac{\pi}{2}$ , cf. Fig. 4.2b. Here, we have to clarify which angle exactly we have to consider. Assume for the moment that the tangent has two sides<sup>8</sup>: one of them sticks to the boundary, but another one is “looking outside”. The angle of interest has to be measured between two “outside looking” sides of the tangents, cf. Fig. 4.2b. For the sake of simplicity let us call such domains by “SL”–domains (“S”–smooth, “L”–L-shaped);

3. the domain  $\Omega$  can be subdivided into a finite number parts which belong to the first or second subclasses defined here, cf. Fig.4.2c.

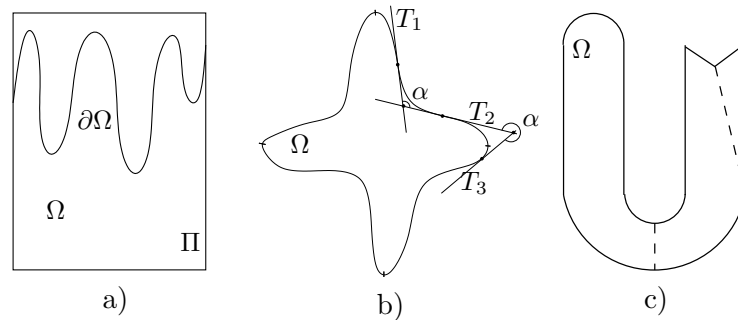


Figure 4.2: a) General concave domain circumscribed by a rectangle; b) concave domain (second subclass); the angle  $\alpha$  between two tangents  $T_1$  and  $T_2$  is minimal and greater than  $\frac{\pi}{2}$ ; c) domain of the third subclass.

We will focus only on the domains of the second subclass, cf. Fig. 4.2b.

#### 4.2.2 Convergence of the WBM Solution in a Non-Convex Domain

The convergence proof of the WBM solution of the problem (4.1), (4.2) in a domain of “SL”–type is completely the same as in [23]. We only repeat all steps of the proof and apply them to the case what we are interested in. Because these steps are not new, cf. [23], we only shortly show the main idea.

One wants to use wave functions set (4.7) to approximate homogeneous scalar field  $u_\Omega$ . It means that we have to show that  $u_\Omega$  can be extended to a homogeneous scalar field  $u_\Pi$  defined in the smallest<sup>9</sup> rectangular domain, which circumscribes  $\Omega$ . As it is done in [23] we construct additional domain  $D$ . This domain  $D$  is defined as  $(\Pi \setminus \Omega) \cup \left( \bigcup_{j=1}^M \Omega \cap \Pi_j \right)$  where  $\Pi_j$ ,  $j = 1, 2, 3, \dots$  are gray rectangles, cf. Fig. 4.3. Doing the same procedure as in [23], i.e. solving in each small rectangle initial value problem and getting homogeneous scalar field  $u_{\Pi_j}$  in each such a small rectangle and, hence, the global homogeneous scalar

<sup>8</sup>One has to think about some board, which has two wide sides.

<sup>9</sup>In general, this rectangular domain can be bigger.

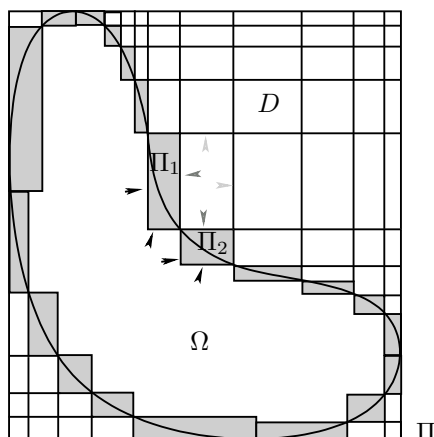


Figure 4.3: Extention of the homogeneous scalar field  $u_\Omega$ . Black arrows show the sides, where  $u_\Omega$  and normal velocity fields are given (for all gray rectangles); gray arrows show the sides, where  $u_\Omega$  and normal velocity fields are determined. Further, this data is used to determine the appropriate information on the sides indicated with light-gray arrows (in each small white rectangle). And so on, until we reach the boundary of the domain  $\Pi$ .

field, we are able to conclude that there exists an extension  $u_\Pi$  of  $u_\Omega$ <sup>10</sup> in  $\Pi$ . Obviously,  $u_\Pi$  is also homogeneous. The restriction of  $u_\Pi$  on  $\Omega$  gives exactly  $u_\Omega$ . Consequently, we can use the wave functions set of the circumscribing rectangle  $\Pi$  to approximate the pressure field  $u_\Omega$ . This approximation for  $N \rightarrow \infty$  is convergent since the wave functions set  $\{\Phi_n\}_n$  is complete, cf. [23]. In order to summarize these results we formulate a small proposition:

**Proposition 4.2.1** *Consider the problem*

$$\Delta_{\mathbf{x}}u + \kappa^2u = 0 \quad \text{in } \Omega \subset \mathbb{R}^2, \quad (4.13)$$

$$\frac{\partial u}{\partial \mathbf{n}} = v(\mathbf{x}) \quad \text{on } \partial\Omega, \quad (4.14)$$

where the domain  $\Omega$  is non-convex, cf. Fig. 4.2b and Fig. 4.3. Moreover, if the minimal angle between any two tangents, which belong to the same concave part of  $\partial\Omega$ , is greater than or equal to  $\frac{\pi}{2}$ , then the WBM solution of such a problem is homogeneous and convergent to the exact one, i.e.

$$\lim_{N \rightarrow \infty} \left| \sum_{n=0}^N c_n \Phi_n(\mathbf{x}) - u(\mathbf{x}) \right| = 0 \quad \forall \mathbf{x} \in \Omega \subset \mathbb{R}^2.$$

**Remark 4.2.1** The condition on the minimal angle between two tangent lines has been chosen in order to avoid the case discussed in [23], i.e. if the angle of interest is smaller than  $\frac{\pi}{2}$ , then we get certain inconsistency on boundaries of small rectangles  $\Pi_j$ ,  $j = 1, 2, 3, \dots$ , cf. [23], Fig. 4.4a.

<sup>10</sup>It is obvious that in the intersections of the domain  $\Omega$  with any small gray rectangle  $\Pi_j$ , cf. Fig. 4.3, the solution  $u_\Omega$  coincides with the solution  $u_{\Pi_j}$ , which is defined only in  $j$ -th small rectangle. Otherwise we would get non-uniqueness of the solution  $u_\Omega$ . The proof is rather obvious.

**Remark 4.2.2** To illustrate how the rectangular covering has to be chosen for certain domain of “SL”-type (as it is done in Fig. 4.3) we do the following in order to show the convergency of WBM solution: we choose two coverings, i.e. one of them leads to a contradiction and, hence, the convergence cannot be proven in general; the other leads to the convergence of WBM solution.

First consider smooth concave domain depicted in Fig. 4.4a. Choose an arbitrary (convenient for us) rectangular covering, i.e. the sides of the rectangles are parallel to the axes of the Cartesian coordinate system. Such a covering leads to the contradiction: as we mentioned above, we solve in each small rectangle initial value problem, where the initial values and initial velocities are given. If we consider two gray rectangles depicted in Fig. 4.4a, then solving the initial value problem in the left rectangle gives certain values along the side denoted by  $s$ . On the other hand, solving the initial value problem in the right rectangle also gives certain values along  $s$ . In general, these values do not coincide. And as a consequence we cannot show convergence using this covering.

Second example considers the same domain  $\Omega$ . First, we try to draw two tangents in such a way that the angle  $\alpha$  between them is as small as possible. Then, we define our rectangles such that one side of them is parallel to one of the tangents we have constructed<sup>11</sup>. Solving the initial value problems in each such rectangle we will not get any contradiction and the convergence of the WBM solution can be shown, cf. Fig. 4.4b.

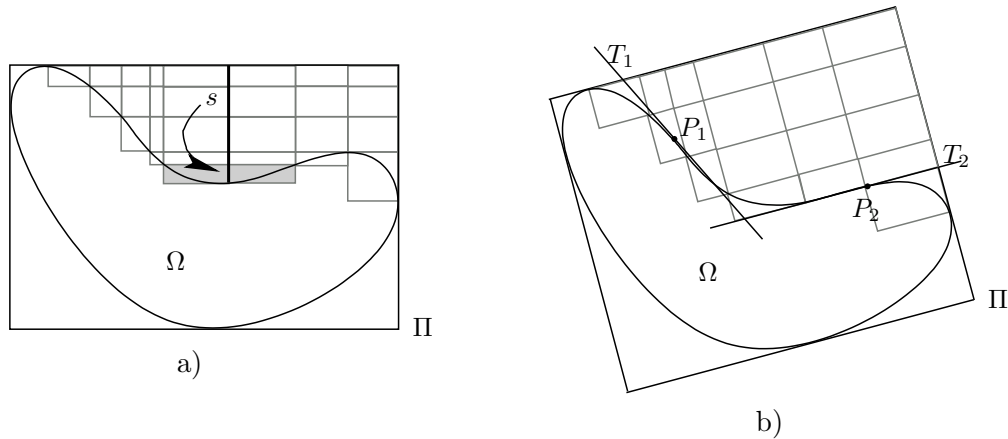


Figure 4.4: a) Wrong orientation of the rectangles; b) correct orientation of the rectangles.

**Remark 4.2.3** We also have to take care about the domains of “SL”-type, which have several concave parts. Let us consider one example. Certain domain  $\Omega$  is given, where  $\partial\Omega$  has two concave parts, cf. Fig. 4.5. Obviously, we are able

<sup>11</sup>The correct covering of the rectangles is not unique. We are able to allow certain deviation



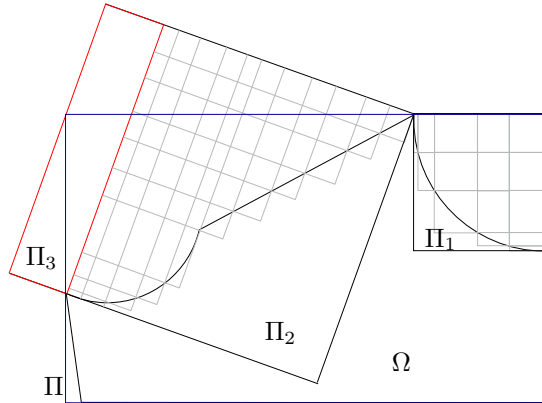


Figure 4.5: The part of the possible covering of the concave domain of “SL” type

to subdivide  $\Omega$  into several subdomains and prove the convergence of the WBM solutions in each subdomain using methodology described above, cf. Remark 4.2.2. But we choose another way. For each concave part we define two separate coverings, where the orientation of small rectangles is different, cf. Fig. 4.5. These two coverings define two disjoint rectangles  $\Pi_1$  and  $\Pi_2$ , where the solution  $u_\Omega$  can be extended. Further, one is able to extend the solution defined in  $\Pi_2$  up to rectangle  $\Pi_2 \cup \Pi_3$ . Obviously, on each side “ $j$ ” of the rectangle  $\Pi$ <sup>12</sup>, which circumscribes the domain  $\Omega$ , we are able to define function  $v_j$ . Solving the boundary value problem in  $\Pi$  with Neumann data  $v_j$  on  $\partial\Pi$  one defines an extended solution  $u_\Pi$ , where  $u_\Pi|_\Omega = u_\Omega$ . Consequently, the convergence of the WBM solution in  $\Omega$  can be shown.

One is able to extend the proposition 4.2.1 to 3D case. Although, 3D case has certain special features, the main idea remains the same as in 2D case.

### 4.2.3 Numerical Examples

In order to corroborate the theory above we present several simple 2D examples.

We consider concave domain  $\Omega$ , which can be circumscribed with the rectangle  $1\text{m} \times 1\text{m}$ . The boundary of this domain satisfies the requirements of the proposition 4.2.1, i.e. the minimal angle between any two tangents of the same concave part of  $\partial\Omega$  is not less than  $\frac{\pi}{2}$ . Fig. 4.6 presents two numerical solutions obtained using WBM (left) and FEM (right). In order to find WBM solution 24 (i.e.  $N = 5$ ) wave functions were used.  $\kappa = 1.1899$ , which corresponds to the angular frequency  $\omega = 130\pi$  Hz.

in the orientation of the rectangles. This deviation, clearly, depends on the minimal angle between two tangents, cf. Subsection 4.2.1

<sup>12</sup>Blue rectangle in Fig. 4.5.

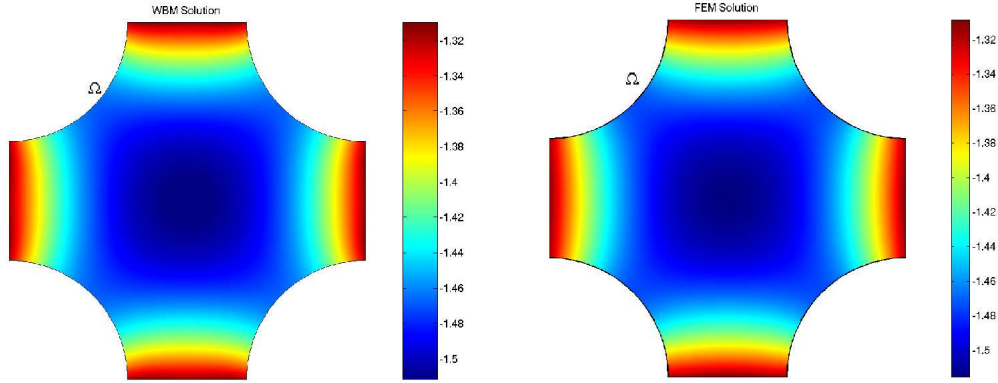


Figure 4.6: Numerical solutions (real parts) of the problem (4.1), (4.2) with the normal velocity  $v = 1$  on the straight parts of  $\partial\Omega$  and  $v = 0$  on the curved parts of  $\partial\Omega$ : WBM (left) and FEM (right).

Fig. 4.7 presents the same domain  $\Omega$  and two numerical solutions obtained using WBM (left) and FEM (right). The boundary conditions in this case are the following: on the straight parts  $v = 0$  and on the curved parts  $v = 1$ , cf. Fig. 4.7. As in the previous case, to find WBM solution only 24 (i.e.  $N = 5$ ) wave functions were used.

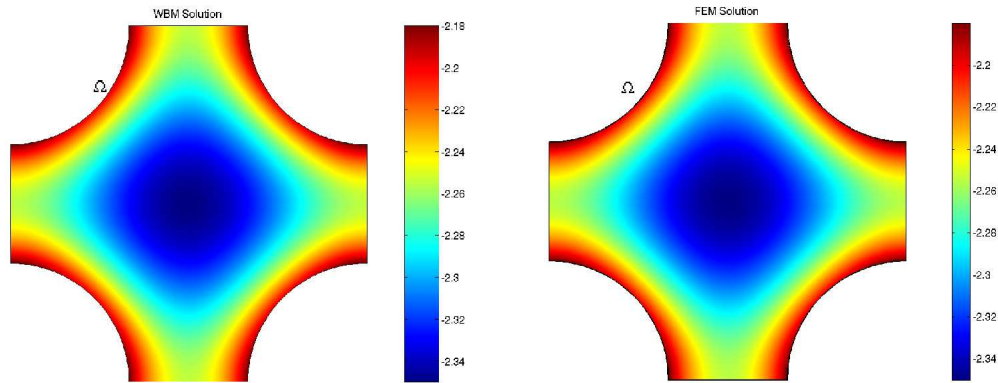


Figure 4.7: Numerical solutions (real parts) of the problem (4.1), (4.2) with the normal velocity  $v = 0$  on the straight parts of  $\partial\Omega$  and  $v = 1$  on the curved parts of  $\partial\Omega$ : WBM (left) and FEM (right).

Third example presents two numerical solutions, namely WBM and FEM solutions, respectively. The domain  $\Omega$  looks similar to the domain discussed in Remark 4.2.3. The rectangle  $\Pi$  circumscribing  $\Omega$  has dimensions  $1\text{m} \times 2.1294\text{m}$ . The wave number stays the same, i.e.  $\kappa = 1.1899$ .  $N$  in this case is equal to 13, i.e. 56 wave functions were used.

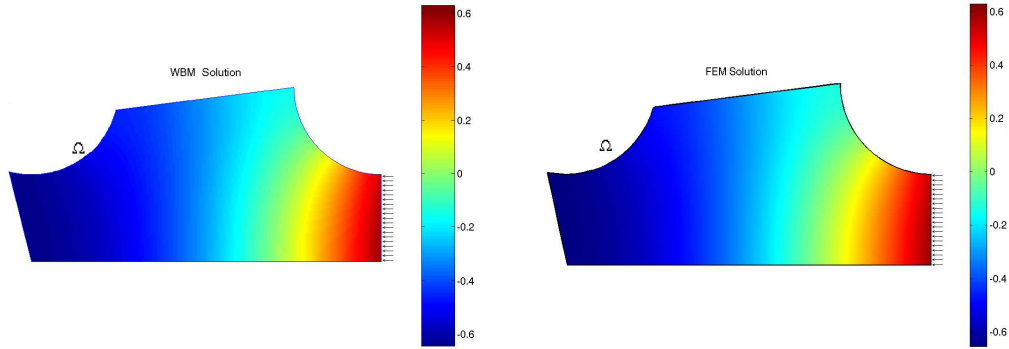


Figure 4.8: Numerical solutions (real parts) of the problem (4.1), (4.2) with the normal velocity  $v = 1$  on the right straight part of  $\partial\Omega$  and  $v = 0$  otherwise: WBM (left) and FEM (right).

### 4.3 WBM in the Case of Inhomogeneous Helmholtz Equation

One is able to notice that the equation (2.36) is the inhomogeneous Helmholtz differential equation. Therefore, we have to investigate the differential equation of Helmholtz type with non-zero function  $f$  on the right hand side together with appropriate boundary conditions, i.e.

$$\Delta_{\mathbf{x}}u + \kappa^2u = f, \text{ in } \Omega, \quad (4.15)$$

$$\frac{\partial u}{\partial \mathbf{n}} = g, \text{ on } \partial\Omega. \quad (4.16)$$

In the literature we found several results, where the right hand side is assumed to be a point-source. Therefore, the analytical solution in such cases can be found, cf. [23], [24], [37], etc. Here, we are interested to consider the case of rather smooth source function  $f$ . Thus, the wave functions set  $\{\Phi_n\}_n$  cannot solve the equation (4.15) at all. To apply WBM to the problem (4.15), (4.16) we find a simple trick.

Consider the problem (4.15), (4.16) in the case of 2D domain  $\Omega$ . We know that the solution  $u$  can be split into its homogeneous and particular parts, i.e.  $u = u_h + u_p$ . This can always be done because of the superposition principle, which is possible for linear problems. Thus, we have to find a particular solution  $u_p$ , which corresponds to the right hand side  $f$ . Then we are able to solve the problem

$$\Delta_{\mathbf{x}}u_h + \kappa^2u_h = 0, \quad \text{in } \Omega, \quad (4.17)$$

$$\frac{\partial u_h}{\partial \mathbf{n}} = g - \frac{\partial u_p}{\partial \mathbf{n}} \quad \text{on } \partial\Omega, \quad (4.18)$$

using Wave Based Method. Assume that free term  $f$  is regular enough and it vanishes outside the domain  $\Omega$ . Thus we are able to approximate it by the 2D

Fourier series, i.e.

$$\begin{aligned} f(x, y) &= \sum_{j,k=0}^{\infty} f_{jk}^{\text{ac}} \cos \frac{\pi j}{L_x} x \cos \frac{\pi k}{L_y} y + f_{jk}^{\text{as}} \sin \frac{\pi j}{L_x} x \cos \frac{\pi k}{L_y} y \\ &+ f_{jk}^{\text{bc}} \cos \frac{\pi j}{L_x} x \sin \frac{\pi k}{L_y} y + f_{jk}^{\text{bs}} \sin \frac{\pi j}{L_x} x \sin \frac{\pi k}{L_y} y, \end{aligned} \quad (4.19)$$

where the coefficients  $f_{jk}^{\text{ac}}$ ,  $f_{jk}^{\text{as}}$ ,  $f_{jk}^{\text{bc}}$  and  $f_{jk}^{\text{bs}}$  are 2D Fourier coefficients which can easily be found using appropriate well-known formulae. On the other hand, we assume that the solution  $u_p$  can also be presented in Fourier series form, i.e.

$$\begin{aligned} u_p(x, y) &= \sum_{j,k=0}^{\infty} a_{jk}^{\text{c}} \cos \frac{\pi j}{L_x} x \cos \frac{\pi k}{L_y} y + a_{jk}^{\text{s}} \sin \frac{\pi j}{L_x} x \cos \frac{\pi k}{L_y} y \\ &+ b_{jk}^{\text{c}} \cos \frac{\pi j}{L_x} x \sin \frac{\pi k}{L_y} y + b_{jk}^{\text{s}} \sin \frac{\pi j}{L_x} x \sin \frac{\pi k}{L_y} y, \end{aligned} \quad (4.20)$$

where  $a_{jk}^{\text{c}}$ ,  $a_{jk}^{\text{s}}$ ,  $b_{jk}^{\text{c}}$  and  $b_{jk}^{\text{s}}$  are unknown coefficients, yet. Inserting the above given relations (4.19) and (4.20) into the equation  $\Delta_{\mathbf{x}} u_p + \kappa^2 u_p = f$  we get the equation for unknowns  $a_{jk}^{\text{c,s}}$  and  $b_{jk}^{\text{c,s}}$ ,  $j, k = 0, 1, \dots$ , i.e.

$$\begin{aligned} \sum_{j,k=0}^{\infty} &\left[ \left( \kappa^2 - \left( \frac{\pi j}{L_x} \right)^2 - \left( \frac{\pi k}{L_y} \right)^2 \right) a_{jk}^{\text{c}} - f_{jk}^{\text{ac}} \right] \cos \frac{\pi j}{L_x} x \cos \frac{\pi k}{L_y} y + \\ &\left[ \left( \kappa^2 - \left( \frac{\pi j}{L_x} \right)^2 - \left( \frac{\pi k}{L_y} \right)^2 \right) a_{jk}^{\text{s}} - f_{jk}^{\text{as}} \right] \sin \frac{\pi j}{L_x} x \cos \frac{\pi k}{L_y} y + \\ &\left[ \left( \kappa^2 - \left( \frac{\pi j}{L_x} \right)^2 - \left( \frac{\pi k}{L_y} \right)^2 \right) b_{jk}^{\text{c}} - f_{jk}^{\text{bc}} \right] \cos \frac{\pi j}{L_x} x \sin \frac{\pi k}{L_y} y + \\ &\left[ \left( \kappa^2 - \left( \frac{\pi j}{L_x} \right)^2 - \left( \frac{\pi k}{L_y} \right)^2 \right) b_{jk}^{\text{s}} - f_{jk}^{\text{bs}} \right] \sin \frac{\pi j}{L_x} x \sin \frac{\pi k}{L_y} y = 0. \end{aligned} \quad (4.21)$$

Obviously, the relation (4.21) is true only in the case when all the coefficients vanish. Hence, we find the coefficients

$$a_{jk}^{\text{c,s}} = \frac{f_{jk}^{\text{ac,as}}}{\kappa^2 - \left( \frac{\pi j}{L_x} \right)^2 - \left( \frac{\pi k}{L_y} \right)^2}, \quad (4.22)$$

$$b_{jk}^{\text{c,s}} = \frac{f_{jk}^{\text{bc,bs}}}{\kappa^2 - \left( \frac{\pi j}{L_x} \right)^2 - \left( \frac{\pi k}{L_y} \right)^2}, \quad (4.23)$$

and the solution  $u_p$  can be found. Next, we are able to use the Wave Based Method to find the numerical solution  $u_h$  of the problem (4.17), (4.18). And, finally, we find the starting solution  $u$  of the problem (4.15), (4.16).

We present one small 2D example, which finalizes this section. Consider the problem (4.15), (4.16) in 2D domain depicted in Fig. 4.9. The right hand side

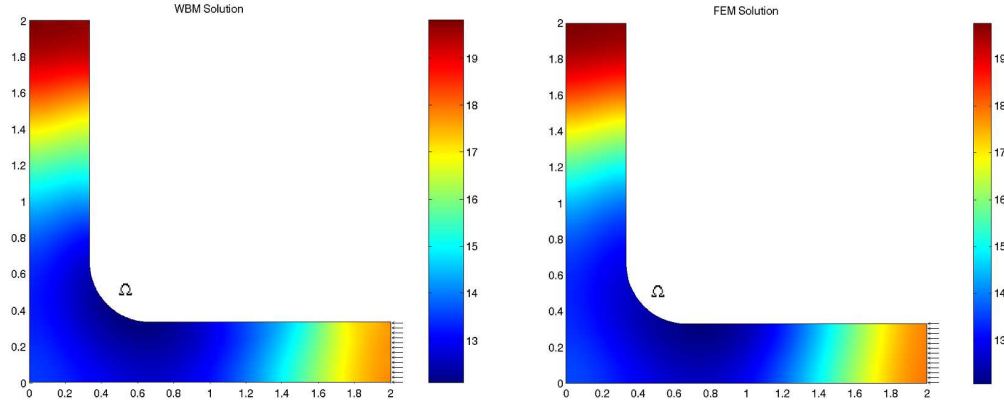


Figure 4.9: Numerical solutions (real parts) of the problem (4.15), (4.16) with the normal velocity  $v = 1$  on the right straight part of  $\partial\Omega$  and  $v = 0$  otherwise: WBM (left) and FEM (right).

of (4.15) is given as  $f = 100(2x - x^2)(2y - y^2)$ . The boundary conditions are of Neumann type, i.e.  $\frac{\partial u}{\partial \mathbf{n}}|_{x=2, y \in [0, 1/3]} = 1$ ,  $\frac{\partial u}{\partial \mathbf{n}}|_{\text{otherwise}} = 0$ .

**Remark 4.3.1** Let us note that the approximation of the right hand side  $f$  by Fourier series is rather expensive procedure. Therefore, one has to think about another (cheaper) possibility to find  $u_p$ . For example, with the aid of Fast Fourier Transform this problem can be resolved.

#### 4.4 WBM in an Unbounded 3D Domain

This section describes the applicability of the Wave Based Technique (WBT) to solve homogeneous Helmholtz equation in the case of a 3D unbounded exterior domain. As we already mentioned in Chapter 2, the domain  $\Omega^+$  has two parts, i.e.  $\overline{\Omega^+} = \overline{\Omega_{\text{int}}} \cup \overline{\Omega_{\text{ext}}}$ . We recall from the Chapter 2 that in each subdomain of  $\Omega^+$  the following boundary value problems have to be solved

$$\Delta_{\mathbf{x}} u_{\text{int}} + \kappa^2 u_{\text{int}} = 0 \quad \text{in } \Omega_{\text{int}}, \quad (4.24)$$

$$\frac{\partial u_{\text{int}}}{\partial \mathbf{n}} = g_{\text{int}} \quad \text{on } \partial\Omega_{\text{int}} \setminus \Gamma_r \quad (4.25)$$

and

$$\Delta_{\mathbf{x}} u_{\text{ext}} + \kappa^2 u_{\text{ext}} = 0 \quad \text{in } \Omega_{\text{ext}}, \quad (4.26)$$

$$\lim_{\mathbf{r} \rightarrow \infty} \mathbf{r} \left( \frac{\partial u_{\text{ext}}}{\partial \mathbf{r}} + i\kappa u_{\text{ext}} \right) = 0. \quad (4.27)$$

The Sommerfeld radiation condition has to be satisfied uniformly in both spherical angles. Note that on the interface  $\Gamma_r$  the coupling conditions on  $u_{\text{int}}$  and  $u_{\text{ext}}$  have to be defined, i.e.

$$u_{\text{int}}|_{\Gamma_r} = u_{\text{ext}}|_{\Gamma_r} \quad (4.28)$$

and

$$\left. \frac{\partial u_{\text{int}}}{\partial \mathbf{n}_{\text{int}}} \right|_{\Gamma_r} = - \left. \frac{\partial u_{\text{ext}}}{\partial \mathbf{n}_{\text{ext}}} \right|_{\Gamma_r}. \quad (4.29)$$

The main principles of the coupling can be found in [37] or in Subsection 4.5. Within a bounded subdomain  $\Omega_{\text{int}}$ , cf. Fig. 2.6, we use usual Wave Based Method to approximate the solution  $u_{\text{int}}$  as in the cases described above <sup>13</sup>. In an unbounded subdomain  $\Omega_{\text{ext}}$  we approximate the solution  $u_{\text{ext}}$  by the wave functions, which solve the homogeneous Helmholtz equation (4.26) <sup>14</sup> and behave as an outgoing spherical wave, i.e. it has to satisfy the Sommerfeld radiation condition at infinity (4.27). Here,  $\Omega_{\text{ext}}$  is an unbounded domain exterior to a spherical boundary surface, unbounded domain, cf. Chapters 2 and 3.

We know, cf. [29] and [1], that in the spherical coordinate system  $(r, \alpha, \beta)$  <sup>15</sup> the general solution of the homogeneous Helmholtz equation can be written as follows

$$u_{\text{ext}}(r, \alpha, \beta) = \sum_{n=0}^{\infty} \sum_{m=0}^n \left[ c_n^{(1)} h_n^{(1)}(\kappa r) + c_n^{(2)} h_n^{(2)}(\kappa r) \right] \times \\ \left[ c_m^{(3)} e^{im\alpha} + c_m^{(4)} e^{-im\alpha} \right] \times \\ \left[ c_{nm}^{(5)} P_n^m(\cos \beta) + c_{nm}^{(6)} Q_n^m(\cos \beta) \right], \quad (4.30)$$

where  $h_n^{(1)}$  and  $h_n^{(2)}$  are the so-called spherical Hankel functions of order  $n$  of the first and second kind, respectively;  $P_n^m$  and  $Q_n^m$  are the so-called Legendre functions of the first and second kind, respectively. To simplify a little the expression above we investigate the properties of the summands. We know that

<sup>13</sup>Of course, we have to apply the wave functions set designed for 3D, cf. [37], [38]. These wave functions can be defined in the following way

$$\begin{aligned} \Phi_{n,m}^1 &= \cos \kappa_{x_{1n,m}} x \cos \kappa_{y_{1n,m}} y e^{-i\kappa_{z_{1n,m}} z}, \\ \Phi_{n,m}^2 &= \cos \kappa_{y_{2n,m}} y \cos \kappa_{z_{2n,m}} z e^{-i\kappa_{x_{2n,m}} x}, \\ \Phi_{n,m}^3 &= \cos \kappa_{x_{3n,m}} x \cos \kappa_{z_{3n,m}} z e^{-i\kappa_{y_{3n,m}} y}, \quad n \in \mathbb{N}_0, \end{aligned}$$

where

$$\begin{aligned} (\kappa_{x_{1n,m}}, \kappa_{y_{1n,m}}, \kappa_{z_{1n,m}}) &= \left( \frac{n\pi}{L_x}, \frac{m\pi}{L_y}, \pm \sqrt{\kappa^2 - \left(\frac{n\pi}{L_x}\right)^2 - \left(\frac{m\pi}{L_y}\right)^2} \right), \\ (\kappa_{y_{2n,m}}, \kappa_{z_{2n,m}}, \kappa_{x_{2n,m}}) &= \left( \frac{n\pi}{L_y}, \frac{m\pi}{L_z}, \pm \sqrt{\kappa^2 - \left(\frac{n\pi}{L_y}\right)^2 - \left(\frac{m\pi}{L_z}\right)^2} \right), \\ (\kappa_{x_{3n,m}}, \kappa_{z_{3n,m}}, \kappa_{y_{3n,m}}) &= \left( \frac{n\pi}{L_x}, \frac{m\pi}{L_z}, \pm \sqrt{\kappa^2 - \left(\frac{n\pi}{L_x}\right)^2 - \left(\frac{m\pi}{L_z}\right)^2} \right). \end{aligned}$$

Obviously, the condition  $\kappa^2 = \kappa_{x_{in,m}}^2 + \kappa_{y_{in,m}}^2 + \kappa_{z_{in,m}}^2$ ,  $i \in \{1, 2, 3\}$ , is satisfied.

<sup>14</sup>The equation (4.26) has to be transformed into spherical coordinates first.

<sup>15</sup> $\alpha$  is the azimuth,  $\beta$  is the zenith.

the Legendre function of the second kind  $Q_n^m$  is unbounded at points  $-1$  and  $1$  for any  $n, m$ . Therefore, the only possibility to get bounded solution  $u_{\text{ext}}$  is to set all  $c_{nm}^{(6)}$  equal to zero.

As we mentioned before, the solution  $u_{\text{ext}}$  has to satisfy “outgoing wave” property. Let us note that the spherical Hankel functions  $h_n^{(1,2)}(\kappa r)$  are similar to  $\cos \kappa r \pm i \sin \kappa r$  and behave as  $\frac{1}{\kappa r} e^{\pm i(\kappa r - \frac{\pi(n+1)}{2})}$  for  $\kappa r \gg 1$ , respectively, cf. [1]. Thus, we conclude that the function  $h_n^{(2)}$  represents the “outgoing wave”. And, hence, all  $c_n^{(1)}$  are set to zero. Obviously, the Sommerfeld radiation condition (4.27) is thus satisfied. The final representation of the solution  $u_{\text{ext}}$  might be expressed as follows

$$u_{\text{ext}}(r, \alpha, \beta) = \sum_{n=0}^{\infty} \sum_{m=0}^n h_n^{(2)}(\kappa r) P_n^m(\cos \beta) (c_{nm}^c \cos m\alpha + c_{nm}^s \sin m\alpha) \quad (4.31)$$

or

$$u_{\text{ext}}(r, \alpha, \beta) = \sum_{n=0}^{\infty} \sum_{m=-n}^n c_{nm} h_n^{(2)}(\kappa r) Y_n^m(\beta, \alpha), \quad (4.32)$$

where  $Y_n^m(\beta, \alpha)$  are the spherical harmonics, cf. [14], [27]. Now, if we assume that on the boundary  $\Gamma_r$  the boundary condition

$$\left. \frac{\partial u_{\text{ext}}}{\partial \mathbf{n}} \right|_{\Gamma_r} = g_r \quad (4.33)$$

is given and the function  $g_r(\alpha, \beta)$  on  $\Gamma_r$  can be represented by

$$g_r(\alpha, \beta) = \sum_{n=0}^{\infty} \sum_{m=-n}^n \tilde{c}_{nm} Y_n^m(\beta, \alpha), \quad (4.34)$$

then the orthogonality properties of  $Y_n^m(\beta, \alpha)$  functions result in the following relationship between the coefficients in the solution  $u_{\text{ext}}$  and the coefficients in (4.34)

$$c_{nm} = - \frac{\tilde{c}_{nm}}{\left. \frac{\partial h_n^{(2)}(\kappa r)}{\partial r} \right|_{\Gamma_r}}. \quad (4.35)$$

Hence, the solution can be determined through the boundary condition (4.33).

To approximate the solution  $u_{\text{ext}}$  of the problem (4.26)–(4.27) in an exterior domain  $\Omega_{\text{ext}}$  we take only truncated part of the solution (4.31), namely, we consider the expression

$$u_{\text{ext}}(r, \alpha, \beta) \approx \sum_{n=0}^N \sum_{m=-n}^n c_{nm} \Phi_{nm}(r, \alpha, \beta), \quad (4.36)$$

where  $N \geq 0$  and the wave functions  $\Phi_{nm}$  are the following

$$\Phi_{nm}(r, \alpha, \beta) = h_n^{(2)}(\kappa r) Y_n^m(\beta, \alpha), \quad n, m = 1, 2, \dots \quad (4.37)$$

Because the functions in the summations (4.31) and (4.36) form the complete set of functions, cf. [39], [27], the solution  $u_{\text{ext}}$  is well defined and the truncated series (4.36) converges for  $N \rightarrow \infty$ . The unknowns  $c_{nm}$  have to be determined using the boundary condition (4.33) by following the same idea described above, cf. Section 4.1.

To show that the idea above really works in practice we present two trivial examples. Consider a 3D domain  $\Omega_{\text{ext}} = \{(r, \alpha, \beta) \mid r \in (r_0, \infty), \alpha \in [0, 2\pi], \beta \in [0, \pi]\}$ , exterior to a spherical boundary surface  $\Gamma_{r_0}$  of radius  $r_0 = 1$ [m]. First, on the surface  $\Gamma_{r_0}$  we define the boundary condition of Neumann type, i.e.

$$\left. \frac{\partial u_{\text{ext}}}{\partial r} \right|_{r=r_0} = -1. \quad (4.38)$$

The analytical solution can easily be found, i.e.

$$u_{\text{ext}}^{\text{an}} = - \left[ \frac{(\kappa r_0 - i)e^{-i\kappa r_0}}{\kappa r_0^2} \right]^{-1} h_0^{(2)}(\kappa r) = -i \left[ \frac{(\kappa r_0 - i)e^{-i\kappa r_0}}{\kappa r_0^2} \right]^{-1} \frac{e^{-i\kappa r}}{r}. \quad (4.39)$$

Both results, numerical and analytical, are depicted in Fig. 4.10. Next, we define

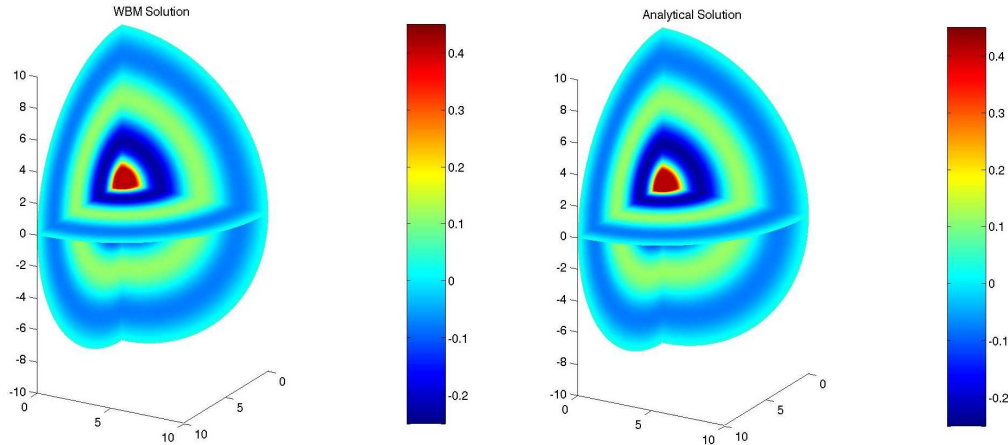


Figure 4.10: WBM (left) and analytical (right) solutions (real parts) of the problem (4.26)–(4.27) with the boundary condition  $\frac{\partial u_{\text{ext}}}{\partial r} = -1$  on  $\Gamma_{r_0}$ .  $\kappa = 1.1899$ .

another boundary condition, which depends on the angle  $\beta$ , i.e.  $\frac{\partial u_{\text{ext}}}{\partial \mathbf{n}} = \sin^2 \beta$ . The analytical solution in this case can be found by the following formula

$$\begin{aligned} u_{\text{ext}}^{\text{an}} &= -\frac{2}{3} \left[ \left. \frac{\partial h_0^{(2)}(\kappa r)}{\partial r} \right|_{r=r_0} \right]^{-1} h_0^{(2)}(\kappa r) \\ &+ \frac{1}{3} \left[ \left. \frac{\partial h_2^{(2)}(\kappa r)}{\partial r} \right|_{r=r_0} \right]^{-1} h_2^{(2)}(\kappa r) (3 \cos^2 \beta - 1). \end{aligned} \quad (4.40)$$

The results are depicted in Fig. 4.11. We have to mention that the WBM solutions in the examples coincides exactly with the analytical ones, cf. Fig. 4.10 and 4.11.



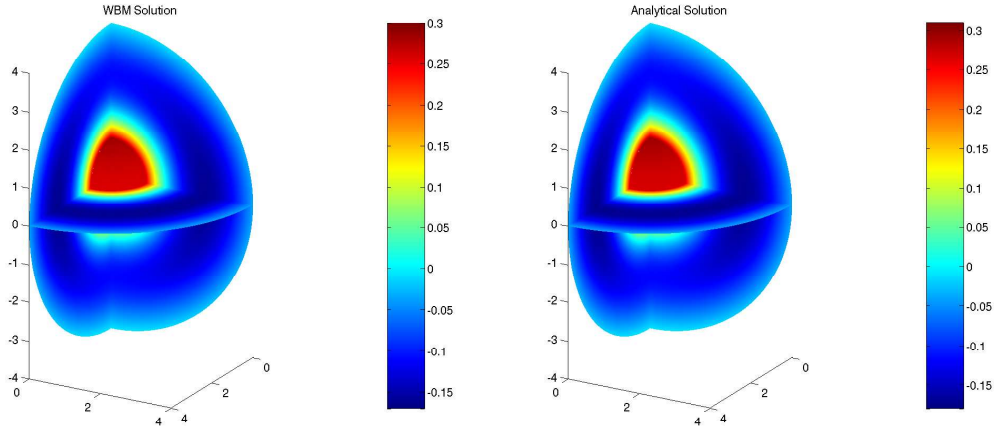


Figure 4.11: WBM (left) and analytical (right) solutions (real parts) of the problem (4.26)–(4.27) with the boundary condition  $\frac{\partial u_{\text{ext}}}{\partial r} = \sin^2 \beta$  on  $\Gamma_{r_0}$ .  $\kappa = 1.1899$ .

## 4.5 Interface Continuity Conditions

As we already mentioned above, in the cases, when the computational domain has complicated non-convex geometry, we are not able to apply Wave Based Method directly. An appropriate subdivision of the domain  $\Omega$  is needed, where all the subdomains satisfy conditions of the proposition 4.2.1 (in 2D case). In each subdomain the Wave Based Method can be applied. On common interface  $\Gamma_i := \bar{\Omega}_1 \cap \bar{\Omega}_2$ <sup>16</sup> the function and normal velocity continuity conditions are enforced, i.e.

$$u_{\Omega_1}|_{\Gamma_i} = u_{\Omega_2}|_{\Gamma_i}, \quad (4.41)$$

$$\frac{\partial u_{\Omega_1}}{\partial \mathbf{n}_1} \Big|_{\Gamma_i} = - \frac{\partial u_{\Omega_2}}{\partial \mathbf{n}_2} \Big|_{\Gamma_i}. \quad (4.42)$$

Thus, in order to solve a coupled linear system  $\mathbf{A}\mathbf{c} = \mathbf{b}$  we have to define the matrix  $\mathbf{A}$  and the right hand side  $\mathbf{b}$ , which look a little different as in the case of a simple convex domain, cf. Section 4.1. The structure of the matrix  $\mathbf{A}$  and of the right hand side  $\mathbf{b}$  can be found in [37], where 3D computational domain has been subdivided into two subdomains. Obviously, the sizes of  $\mathbf{A}$  and  $\mathbf{b}$  will increase together with the number of subdomains of  $\Omega$ .

In this section, we would like to present the structure of  $\mathbf{A}$  and  $\mathbf{b}$  in the case of 3D unbounded open domain  $\Omega^+$ , which has two main parts, i.e. interior subdomain  $\Omega_{\text{int}}$  and exterior subdomain  $\Omega_{\text{ext}}$ . Moreover, the subdomain  $\Omega_{\text{int}}$  is supposed to be non-convex, and, yet, it can be subdivided into two subdomains  $\Omega_{\text{int}}^1$  and  $\Omega_{\text{int}}^2$ . We assume that the classical Wave Based Method, cf. [23], [37], [38], etc., in these two domains can be applied. In the exterior domain

<sup>16</sup>Where, for example,  $\bar{\Omega} = \bar{\Omega}_1 \cup \bar{\Omega}_2$ .

$\Omega_{\text{ext}}$  we will apply the method derived in Section 4.4. We denote the interface  $\bar{\Omega}_{\text{int}}^1 \cap \bar{\Omega}_{\text{int}}^2$  by  $\Gamma_i$  and the interface  $\bar{\Omega}_{\text{int}} \cap \bar{\Omega}_{\text{ext}}$  by  $\Gamma_r$ . On these two surfaces we enforce appropriate continuity conditions on the solutions and on their normal derivatives, cf. (4.41), (4.42), (4.28) and (4.29).

First of all we define the unknown vector  $c$ , i.e.

$$c = \left( c_1^{(1)}, c_2^{(1)}, c_3^{(1)}, \dots, c_1^{(2)}, c_2^{(2)}, c_3^{(2)}, \dots, c_1^{(3)}, c_2^{(3)}, c_3^{(3)}, \dots \right)^T,$$

where  $c_i^{(j)}$  are unknown coefficients of an appropriate approximation of the solutions  $u_{\Omega_{\text{int}}^1}$ ,  $u_{\Omega_{\text{int}}^2}$  or  $u_{\Omega_{\text{ext}}}$ ,  $i = 3$  corresponds to the external subdomain of  $\Omega^+$ , i.e. to  $\Omega_{\text{ext}}$ . Hence, the matrix  $\mathbf{A}$  looks as follows

$$\mathbf{A} = \begin{pmatrix} \mathbf{A}^{(1)} + \mathbf{C}^{(11)} & \mathbf{C}^{(12)} & \mathbf{0} \\ \mathbf{C}^{(21)} & \mathbf{A}^{(2)} + \mathbf{C}_1^{(22)} + \mathbf{C}_2^{(22)} & \mathbf{C}^{(23)} \\ \mathbf{0} & \mathbf{C}^{(32)} & \mathbf{A}^{(3)} + \mathbf{C}^{(33)} \end{pmatrix}, \quad (4.43)$$

where the components of the appropriate matrices are defined as

$$\begin{aligned} \mathbf{A}^{(1)} &: \int_{\partial\Omega_{\text{int}}^1 \setminus \Gamma_i} \Phi_{j_1 k_1}^1 \frac{\partial \Phi_{n_1 m_1}^1}{\partial \mathbf{n}_1} dS, & \mathbf{A}^{(2)} &: \int_{(\partial\Omega_{\text{int}}^2 \setminus \Gamma_i) \setminus \Gamma_r} \Phi_{j_2 k_2}^2 \frac{\partial \Phi_{n_2 m_2}^2}{\partial \mathbf{n}_2} dS, \\ \mathbf{A}^{(3)} &: \int_{\partial\Omega_{\text{ext}} \setminus \Gamma_r} \Phi_{j_3 k_3}^3 \frac{\partial \Phi_{n_3 m_3}^3}{\partial \mathbf{n}_3} dS, & \mathbf{C}^{(11)} &: \int_{\Gamma_i} \Phi_{j_1 k_1}^1 \frac{\partial \Phi_{n_1 m_1}^1}{\partial \mathbf{n}_1} dS, \\ \mathbf{C}^{(12)} &: \int_{\Gamma_i} \Phi_{j_1 k_1}^1 \frac{\partial \Phi_{n_2 m_2}^2}{\partial \mathbf{n}_2} dS, & \mathbf{C}^{(21)} &: \int_{\Gamma_i} \Phi_{n_1 m_1}^1 \frac{\partial \Phi_{j_2 k_2}^2}{\partial \mathbf{n}_2} dS, \\ \mathbf{C}_1^{(22)} &: - \int_{\Gamma_i} \Phi_{n_2 m_2}^2 \frac{\partial \Phi_{j_2 k_2}^2}{\partial \mathbf{n}_2} dS, & \mathbf{C}_2^{(22)} &: - \int_{\Gamma_r} \Phi_{n_2 m_2}^2 \frac{\partial \Phi_{j_2 k_2}^2}{\partial \mathbf{n}_2} dS, \\ \mathbf{C}^{(23)} &: \int_{\Gamma_r} \Phi_{n_3 m_3}^3 \frac{\partial \Phi_{j_2 k_2}^2}{\partial \mathbf{n}_2} dS, & \mathbf{C}^{(32)} &: \int_{\Gamma_r} \Phi_{j_3 k_3}^3 \frac{\partial \Phi_{n_2 m_2}^2}{\partial \mathbf{n}_2} dS, \\ \mathbf{C}^{(33)} &: \int_{\Gamma_r} \Phi_{j_3 k_3}^3 \frac{\partial \Phi_{n_3 m_3}^3}{\partial \mathbf{n}_3} dS. \end{aligned}$$

Here  $\Phi_{jk}^1$ ,  $\Phi_{jk}^2$  and  $\Phi_{jk}^3$  denote the wave functions defined in the subdomains  $\Omega_{\text{int}}^1$ ,  $\Omega_{\text{int}}^2$  and  $\Omega_{\text{ext}}$ , respectively. The indices  $j_i$ ,  $k_i$ ,  $n_i$  and  $m_i$  run from 0 till  $N_i \geq 0$ ,  $i \in \{1, 2, 3\}$ .  $\mathbf{n}_i$  denotes the outer normal vector to appropriate domain,  $i \in \{1, 2, 3\}$ .

The vector  $\mathbf{b}$  can be found similarly, i.e.

$$\mathbf{b} = \begin{pmatrix} \int_{\Omega_{\text{int}}^1 \setminus \Gamma_i} \Phi_{j_1 k_1}^1 g_{\text{int}} dS \\ \int_{(\Omega_{\text{int}}^2 \setminus \Gamma_i) \setminus \Gamma_r} \Phi_{j_2 k_2}^2 g_{\text{int}} dS \\ \int_{\Omega_{\text{ext}} \setminus \Gamma_r} \Phi_{j_3 k_3}^3 g_{\text{ext}} dS \end{pmatrix}. \quad (4.44)$$

Therefore, the coupled linear system  $\mathbf{A}\mathbf{c} = \mathbf{b}$  is defined, and we are able to search for a solution  $\mathbf{c}$ .

## 4.6 Numerical Simulations

### 4.6.1 First Order Correction Function $p_1$

In this subsection, we present the simulation results of the first order correction function  $p_1$ . We use two different numerical methods to solve an appropriate problem, i.e. we apply Wave Based Method in the case of unbounded domain  $\Omega^+$ , and we apply Finite Element Method in the case of bounded computational domain  $\Omega$ , cf. Chapter 2. Of course, the results are not comparable because of different boundary conditions at infinity in the first case and on the artificial boundary  $\Gamma_r$  in the second one. But we claim that the boundary condition on the artificially constructed boundary  $\Gamma_r$  rather well approximates the Sommerfeld radiation condition at infinity. Hence, the results have to be similar to each other.

#### Wave Based Method

All the theory we presented above in this chapter, was developed to apply it to the Helmholtz type equations (both homogeneous and inhomogeneous) together with appropriate boundary conditions in special computational domains, i.e. in bounded domain  $\Omega$  and in unbounded external domain  $\Omega^+$ . Let us once more thoroughly write the complete problem for the first order correction function  $p_1$ , i.e. find the unknown solution  $p_1$ , which satisfies

$$\Delta_{\mathbf{x}} p_1 + \kappa^2 p_1 = 0 \quad \text{in } \Omega^+, \quad (4.45)$$

$$\frac{\partial p_1}{\partial \mathbf{n}} = \langle \mathbf{n}, \kappa \boldsymbol{\nu} \rangle \quad \text{on } \partial\Omega^+ \setminus \Gamma_\infty, \quad (4.46)$$

$$\lim_{\mathbf{r} \rightarrow \infty} \mathbf{r} \left( \frac{\partial p_1}{\partial \mathbf{n}} + i\kappa p_1 \right) = 0, \quad (4.47)$$

where the Sommerfeld radiation condition (4.47) is valid uniformly in both angular directions, and  $\Gamma_\infty$  denotes “the boundary at infinity”. Obviously, the boundary condition (4.46) on the membrane and cap parts is inhomogeneous. In all other cases the boundary condition (4.46) is the reflective one.

The domain  $\Omega^+$  can be split into three parts, i.e.  $\bar{\Omega}^+ = \bar{\Omega}_{\text{int}}^1 \cup \bar{\Omega}_{\text{int}}^2 \cup \bar{\Omega}_{\text{ext}}$ , where the open subdomains  $\Omega_{\text{int}}^1$  and  $\Omega_{\text{int}}^2$  are such that the WBM solution converges pointwise (theoretically) to the true solution, cf. Section 4.2. Therefore, there are two interfaces  $\Gamma_{\text{i}} := \bar{\Omega}_{\text{int}}^1 \cap \bar{\Omega}_{\text{int}}^2$  and  $\Gamma_{\text{r}} := \bar{\Omega}_{\text{int}}^2 \cap \bar{\Omega}_{\text{ext}}$ , where the continuity conditions on the function and its normal derivative are enforced. In the subdomain  $\Omega_{\text{ext}}$  we use the Wave Based Method designed for spherical domains, cf. Section 4.4. Thus, the coupled system  $\mathbf{A}\mathbf{c} = \mathbf{b}$  has to be solved. The matrix  $\mathbf{A}$  and the vectors  $\mathbf{b}$  and  $\mathbf{c}$  look exactly as in Section 4.5.

In Fig. 4.12 and 4.13 the results of the numerical simulation of the first order correction function  $p_1$  are presented. These pictures present the real part of the function  $p_1$ . The angular frequency  $\omega$  is equal to  $130\pi$  [Hz] (i.e. usual frequency is equal to 65 [Hz]). This corresponds to the wave number  $\kappa = 1.1899$ .

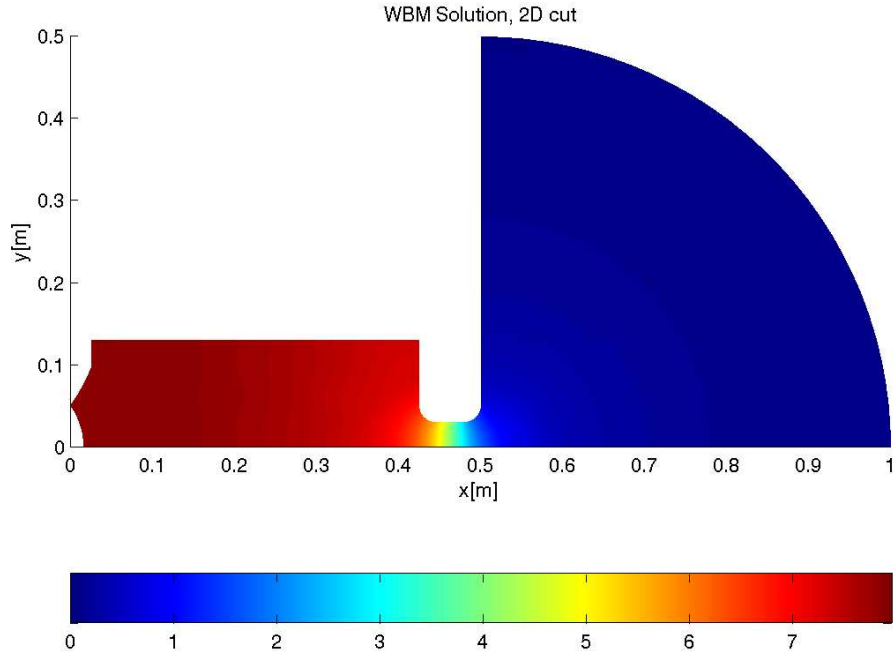


Figure 4.12: Numerical simulation (WBM) of the first order correction function  $p_1$ , 2D slice view, real part.

The numerical WBM simulation of the function  $p_1$ , which solves the problem (4.45)–(4.47), looks rather smooth on the interfaces  $\Gamma_{\text{i}}$  and  $\Gamma_{\text{r}}$ . It means that the algebraic system  $\mathbf{A}\mathbf{c} = \mathbf{b}$  has been correctly constructed, especially on the above

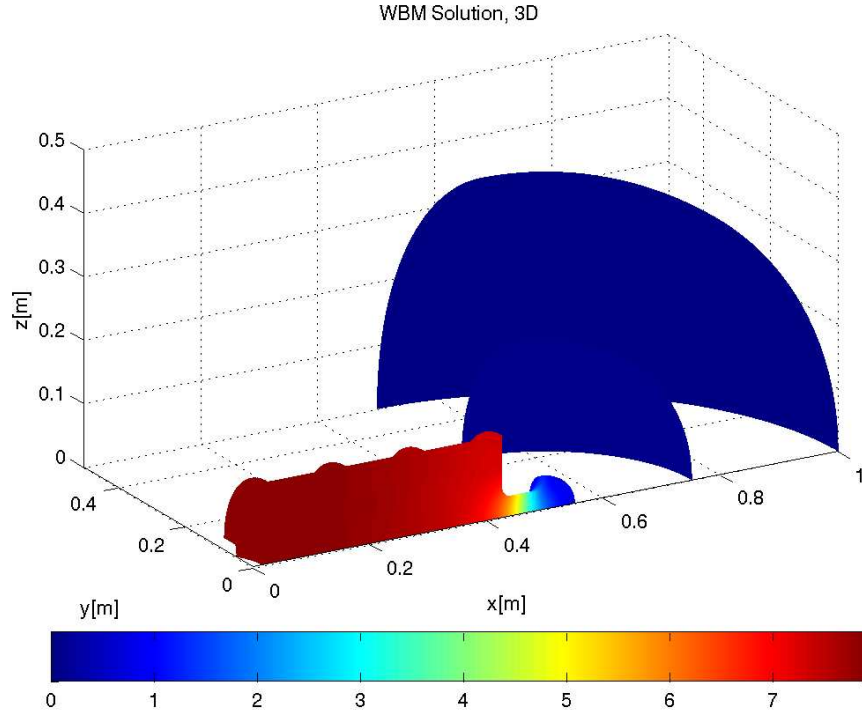


Figure 4.13: Numerical simulation (WBM) of the first order correction function  $p_1$ , 3D view, real part.

mentioned interfaces. Of course, it would be nice to compare WBM results<sup>17</sup> to another numerical method. This comparison will be done further.

### Finite Element Method

The main problem with the Finite Element Method in our case is that we have to consider bounded computational domain. Therefore, we consider the following problem, i.e. find the unknown solution  $p_1$ , which satisfies

$$\Delta_{\mathbf{x}} p_1 + \kappa^2 p_1 = 0 \quad \text{in } \Omega, \quad (4.48)$$

$$\frac{\partial p_1}{\partial \mathbf{n}} = \langle \mathbf{n}, \kappa \boldsymbol{\nu} \rangle \quad \text{on } \partial\Omega \setminus \Gamma_r, \quad (4.49)$$

$$\frac{\partial p_1}{\partial \mathbf{n}} = - \left( i\kappa + \frac{1}{R} \right) p_1 \quad \text{on } \Gamma_r, \quad (4.50)$$

where  $R$  is a given radius of  $\Gamma_r$ , cf. Chapter 2. Obviously, the radiation boundary condition (4.50) approximates the Sommerfeld radiation condition (4.47) which is valid at infinity. The numerical result of FEM simulation, therefore, looks a little different than the WBM solution<sup>18</sup>.

<sup>17</sup>At least visually.

<sup>18</sup>Compare the color bars.

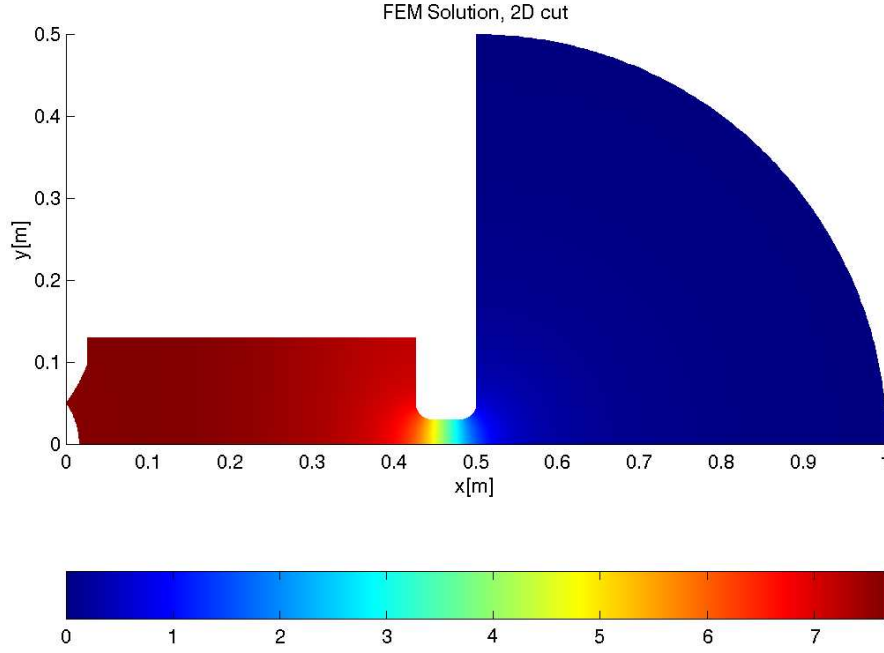


Figure 4.14: Numerical simulation (FEM) of the first order correction function  $p_1$ , 2D slice view, real part.

#### 4.6.2 Second Order Correction Function $p_2$

As in the previous case, cf. Subsection 4.6.1, we would like to present the results of the numerical simulations for the second order correction function  $p_2$ . Similarly to the Subsection 4.6.1 we use two numerical methods WBM and FEM in the case of unbounded and bounded domains, respectively.

##### Wave Based Method

Again, we formulate the problem for the second order correction function  $p_2$ , i.e.

$$\Delta_{\mathbf{x}} p_2 + 4\kappa^2 p_2 = \left(\gamma - \frac{1}{2}\right) \kappa^2 p_1^2 + \frac{3}{2\kappa^2} \left(\frac{\partial^2 p_1}{\partial x_j \partial x_k}\right)^2 \quad \text{in } \Omega^+, \quad (4.51)$$

$$\begin{aligned} \frac{\partial p_2}{\partial \mathbf{n}} &= \frac{1}{4} \frac{\partial}{\partial \mathbf{n}} \left( p_1^2 + \frac{1}{\kappa^2} (\nabla_{\mathbf{x}} p_1)^2 \right) \\ &+ \frac{1}{\kappa^2 r} (\nabla_{\mathbf{x}} p_1 - \kappa \boldsymbol{\nu})^2 \quad \text{on } \partial\Omega^+ \setminus \Gamma_\infty, \end{aligned} \quad (4.52)$$

$$\lim_{\mathbf{r} \rightarrow \infty} \mathbf{r} \left( \frac{\partial p_2}{\partial \mathbf{n}} + 2i\kappa p_2 \right) = 0, \quad (4.53)$$

where  $j, k \in \{1, 2, 3\}$ . In order to apply WBM to the problem (4.51)–(4.53) we have to split the solution  $p_2$  into homogeneous  $p_2^{\text{h}}$  and particular  $p_2^{\text{p}}$  solutions and

rewrite above problem as follows

$$\Delta_{\mathbf{x}} p_2^{\text{h}} + 4\kappa^2 p_2^{\text{h}} = 0 \quad \text{in } \Omega^+, \quad (4.54)$$

$$\begin{aligned} \frac{\partial p_2^{\text{h}}}{\partial \mathbf{n}} &= \frac{1}{4} \frac{\partial}{\partial \mathbf{n}} \left( p_1^2 + \frac{1}{\kappa^2} (\nabla_{\mathbf{x}} p_1)^2 \right) \\ &+ \frac{1}{\kappa^2 r} (\nabla_{\mathbf{x}} p_1 - \kappa \boldsymbol{\nu})^2 - \frac{\partial p_2^{\text{p}}}{\partial \mathbf{n}} \quad \text{on } \partial\Omega^+ \setminus \Gamma_{\infty}, \end{aligned} \quad (4.55)$$

$$\lim_{r \rightarrow \infty} \mathbf{r} \left( \frac{\partial p_2^{\text{h}}}{\partial \mathbf{n}} + 2i\kappa p_2^{\text{h}} \right) = 0 \quad (4.56)$$

and

$$\Delta_{\mathbf{x}} p_2^{\text{p}} + 4\kappa^2 p_2^{\text{p}} = \left( \gamma - \frac{1}{2} \right) \kappa^2 p_1^2 + \frac{3}{2\kappa^2} \left( \frac{\partial^2 p_1}{\partial x_j \partial x_k} \right)^2 \quad \text{in } \Omega^+, \quad (4.57)$$

where  $j, k \in \{1, 2, 3\}$ . Hence, we have to find the particular solution  $p_2^{\text{p}}$  first and then use it to find the homogeneous solution  $p_2^{\text{h}}$ .

Unfortunately, it seems to be expensive to find the particular solution  $p_2^{\text{p}}$  using similar procedure described above, cf. Section 4.3. Therefore, we use another approach. Namely, we approximate the  $p_1$  function using the Bézier interpolation in 3D, cf. [54], i.e. we subdivide the computational domain into blocks, where at each corner point of the block  $j$  the values of the  $p_1$  function are given. Thus, the values of the right hand side, cf. (4.57), are also given. We construct 3D polynomial, say  $\mathcal{P}_j(t_1, t_2, t_3)$ , of third order which approximates the right hand side in the block  $j$ . Exactly these polynomials we use to find the particular solution  $p_2^{\text{p}}$ . We assume that the solution  $p_2^{\text{p}}$  in each block can be represented by some polynomial  $\mathcal{R}_j(t_1, t_2, t_3)$  of the same third order. Inserting this representation into the equation (4.57) and solving an appropriate linear system we find the unknown constants of the representative polynomial  $\mathcal{R}_j(t_1, t_2, t_3)$ . The procedure is rather simple, therefore we omit all details.

In Fig. 4.15 the results of the numerical simulation of the second order correction function  $p_2$  are presented. This picture presents the real part of the function  $p_2$ . The angular frequency  $\omega$  is equal to  $130\pi$  [Hz] (i.e. usual frequency is equal to 65 [Hz]). This corresponds to the wave number  $\kappa = 1.1899$ .

### Finite Element Method

Again, consider the following problem, i.e. find the unknown solution  $p_2$ , which satisfies

$$\Delta_{\mathbf{x}} p_2 + 4\kappa^2 p_2 = f \quad \text{in } \Omega, \quad (4.58)$$

$$\frac{\partial p_2}{\partial \mathbf{n}} = g \quad \text{on } \partial\Omega \setminus \Gamma_r, \quad (4.59)$$

$$\frac{\partial p_2}{\partial \mathbf{n}} = - \left( 2i\kappa + \frac{1}{R} \right) p_1 \quad \text{on } \Gamma_r, \quad (4.60)$$

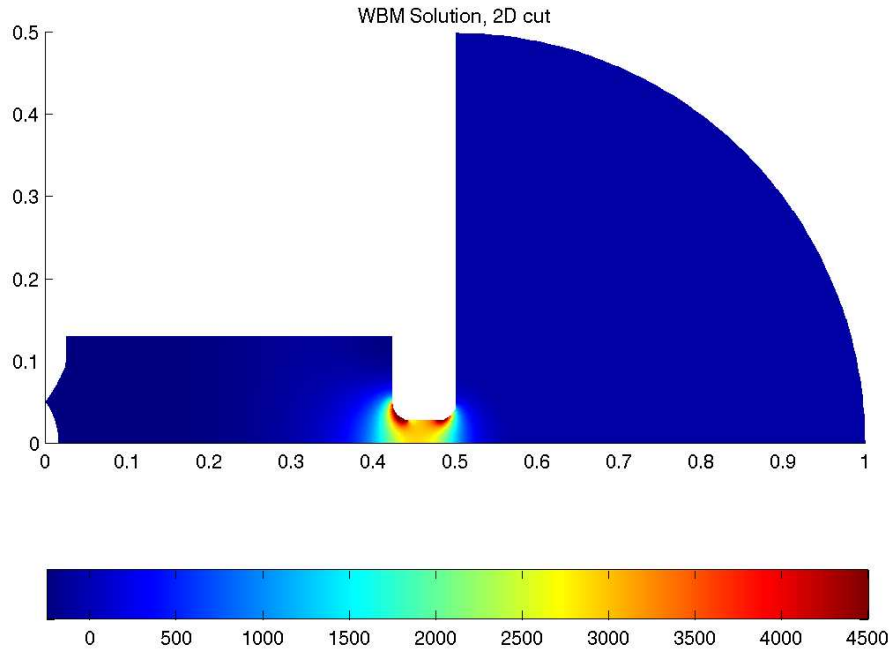


Figure 4.15: Numerical simulation (WBM) of the second order correction function  $p_2$ , 2D slice view, real part.

The numerical result of FEM simulation is presented in Fig. 4.16. As one is able to conclude, the results of WBM and FEM simulations are similar, but not, obviously, the same. We notice that the color bars in both cases are the same.

## 4.7 The Main Results of Chapter 4

Here, we finalize all the results we have got in this chapter.

In order to simulate the mathematical problems stated in the Chapter 2 we used modern numerical method, i.e. Wave Based Method. This method is based on the indirect Trefftz approach and approximates the exact solution using special shape functions which solve the governing homogeneous Helmholtz equations exactly. However, the boundary conditions are satisfied in a weak sense. The theory, which can be found in the literature, so far, allowed to apply WBM only in the cases of convex domains. In this chapter, we found the criterion<sup>19</sup> which allows to apply the WBM in some cases of non-convex domains. In the case of 2D problems we summarize this criterion as the Proposition 4.2.1. With the aid of this proposition one is able to subdivide arbitrary 2D domains such that the number of subdomains is minimal, WBM may be applied in each subdomain and the geometry is not altered, e.g. via polygonal approximation. Further, the same principles have been used in the case of 3D problem, cf. Section

<sup>19</sup>This is the first benefit of this chapter.



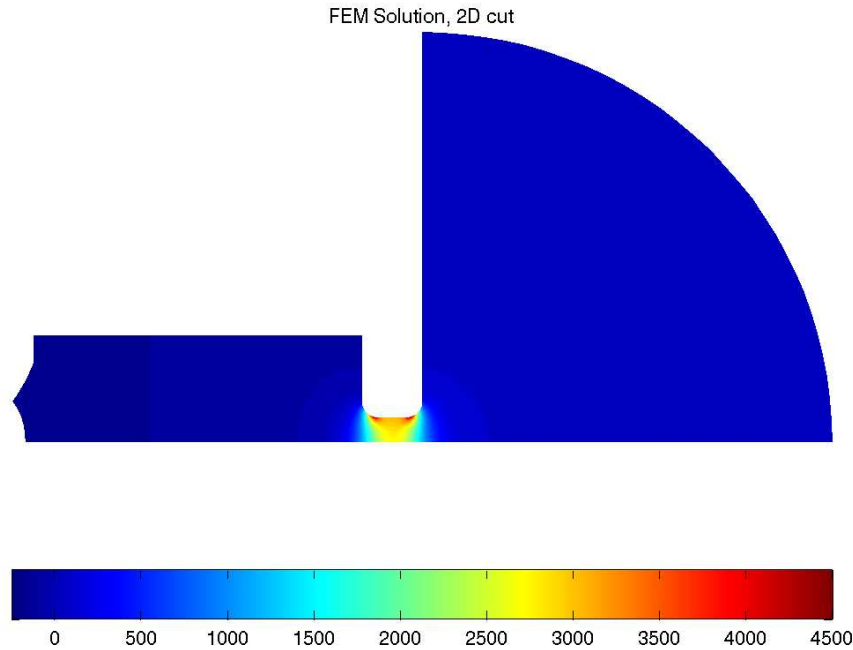


Figure 4.16: Numerical simulation (FEM) of the second order correction function  $p_2$ , 2D slice view, real part.

4.6. However, the formulation of a similar proposition in cases of 3D problems has to be done, yet.

Next, we showed a simple procedure to solve an inhomogeneous Helmholtz equation. This procedure, however, is rather computationally expensive and can probably be improved. Several examples have been also presented.

Further, we presented the possibility to apply the Wave Based Technique to solve steady-state acoustic problems in the case of an unbounded 3D domain<sup>20</sup>. The main principle of the classical WBM, cf. [23], has been extended to the case of an external domain. We used the spherical Hankel functions of second kind and the spherical harmonics to approximate the exact solution of the homogeneous Helmholtz equation, which has been transformed into spherical coordinates first. Also, two numerical examples have been presented.

In order to apply the WBM to our problems, cf. Chapter 2, we had to subdivide the computational domain  $\Omega^+$  into three subdomains. Therefore, on the interfaces certain coupling conditions have been defined.

Finally, we had the necessary, specially developed theory at hand to find the

<sup>20</sup>This is the second benefit of this chapter.

---

numerical WBM solutions, i.e.  $p_1$  and  $p_2$  functions. In order to be sure that WBM gives appropriate results we compared them to the numerical results calculated using FEM. However, the starting problems did not coincide completely, cf. Subsections 4.6.1 and 4.6.2, the results are similar.

We have to mention that the results of this chapter partially have been presented on the ISMA2006 Conference and published as proceedings, cf. [41] and [42].



## Chapter 5

# Optimization

In this chapter, we come to the last stage, i.e. to the optimization. All the theory described in previous chapters has been derived in order to simulate the behaviour of the acoustic pressure functions  $p_1$  and  $p_2$ . These two functions will play an important role in an optimization process. Such an optimization process usually is called by optimal shape design. Let us define what does it mean. Let  $u$  be the solution of a partial differential equation in a domain  $\Omega$

$$u(x) \in \mathbb{R}^m \quad \forall x \in \Omega \subset \mathbb{R}^n, \quad (5.1)$$

where  $m$  and  $n$  are certain positive integer numbers. Let  $J(u, \Omega)$  be a real valued function of  $u$  and  $\Omega$ . We may say that we have an optimal shape design problem to solve if we find  $\Omega$ , in class  $\mathfrak{D}$  of admissible domains, to minimize  $J$ . Formally, we may write

$$\min_{\Omega \in \mathfrak{D}} \{J(u, \Omega) : A(\Omega, u) = 0\}, \quad (5.2)$$

where  $A$  is an unbounded operator which defines a unique  $u$  for every  $\Omega \in \mathfrak{D}$ . Also, certain additional constraints can be considered.

In reality, this definition is too restrictive. We use the term *optimal shape design* whenever a function is to be minimized with respect to a particular geometric element appearing in a partial differential equation.

### 5.1 Formulation of the Optimization Problem

Let us formulate the optimization problem in details. The main task is to minimize the first harmonic, i.e.  $p_2$ , influence on the sound with respect to the key note, i.e.  $p_1$ , by the reflex tube optimization. Several additional conditions are also imposed, i.e. the volume of the reflex tube is always preserved and the key note remains unchanged. It means that the resonance frequency remains the same. In the sequel, we fix the resonance frequency  $f_{\text{res}}$  equal to 60[Hz]. The "working" frequency  $f_0$ , i.e. the frequency which we use to simulate  $p_1$  and  $p_2$ ,

has been chosen as 65[Hz].  $f_{\text{res}}$  differs from  $f_0$  because in this case small changes of the domain  $\Omega$  will slightly move the resonance.

Obviously, one is able to construct the functional

$$J(p_1, p_2, \Omega) := \int_{\Gamma_r} \left( \frac{p_2}{p_1} \right)^2 dS, \quad (5.3)$$

which has to be minimized with respect to  $\Omega^1$ . Here, the boundary  $\Gamma_r$  is a spherical surface of the radius  $R$  which is given and is equal to 0.5[m]. In other words, we have to consider the behaviour of the fraction  $\left( \frac{p_2}{p_1} \right)^2$  in certain surrounding area only. For the sake of simplicity, we would like to replace the surface integral

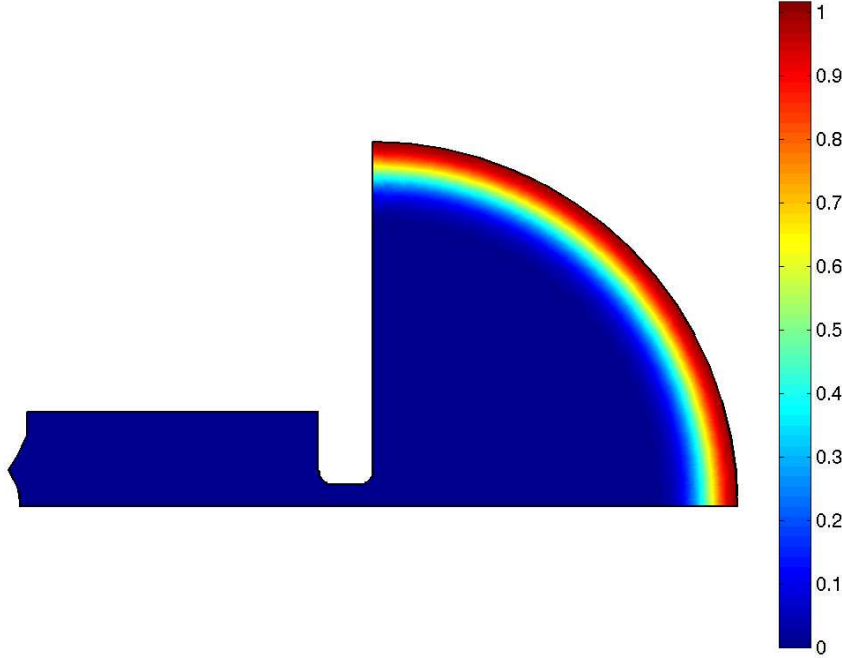


Figure 5.1:  $\zeta$  function.

above with the following one, i.e.

$$J(p_1, p_2, \Omega) := \int_{\Omega} \left( \frac{p_2}{p_1} \right)^2 \zeta d\mathbf{x}, \quad (5.4)$$

where the function  $\zeta$  is equal to 1 on  $\Gamma_r$  and it smoothly vanishes when  $\mathbf{x} \in \Omega$  goes away from  $\Gamma_r$ , cf. Fig. 5.1. The reason of such a replacement will be shown later on.

Obvious constraints of the shape design are the Helmholtz type differential equations together with the boundary conditions for the functions  $p_1$  and  $p_2$ , cf.

<sup>1</sup>In the following, we will denote the computational domain by  $\Omega$ , however it can be also changed to  $\Omega^+$ , e.g.  $J = J(p_1, p_2, \Omega^+)$ .

Chapter 2. Yet, the conservations of the volume of the reflex tube<sup>2</sup> and of the resonance frequency have to be fulfilled, i.e.

$$\text{vol}(\Omega) = \int_{\Omega} d\mathbf{x} = \text{const}, \quad (5.5)$$

$$\Delta_{\mathbf{x}}u + \kappa_0^2 u = 0 \quad \text{in } \Omega, \quad (5.6)$$

$$\frac{\partial u}{\partial \mathbf{n}} = 0 \quad \text{on } \partial\Omega \setminus \Gamma_r, \quad (5.7)$$

$$\frac{\partial u}{\partial \mathbf{n}} = -\left(i\kappa_0 + \frac{1}{R}\right)u \quad \text{on } \Gamma_r, \quad (5.8)$$

where the function  $u(\mathbf{x})$  is a non-trivial solution of the problem above and the appropriate eigenvalue  $\kappa_0^2$ , which corresponds to the resonance frequency  $f_{\text{res}}$ , is supposed to be constant.

**Remark 5.1.1 (On the existence and uniqueness of the optimal shape)**

No doubt, one has to think about the existence of an optimal shape  $\Omega^*$  in the set of admissible domains  $\mathfrak{D}$ . If the solution exists then we have to analyze under which conditions this optimum is unique. In practice, usually, the volume or perimeter constraint to the optimization problem is added. This is rather natural condition which guarantees the existence. For example, if we would omit the constraints (5.5)–(5.8) in our case and during the optimization process for each iteration step the volume of the reflex tube would increase, then the value of the objective functional (5.4), obviously, would decrease. In the next iteration the previous value of (5.4) can also be decreased by the further increase of the volume of the reflex tube. Such kind of problem will not have any solution. Therefore, the volume constraint is an important condition for the existence of the optimum.

The uniqueness of the optimal solution can be investigated using so-called Kuhn–Tucker conditions in the case of constraint optimization. Moreover, if the objective function and all constraint functions are convex, then the design space is convex, and the Kuhn–Tucker conditions are sufficient to guarantee that  $\Omega^*$  is a global optimum (i.e. the solution  $\Omega^*$  is unique), cf. [61], etc. In general, for engineering problems, the design space is not convex.

In order to be sure that the solution of the optimization problem exists, we add to the functional (5.4) a term which is proportional to the volume of the domain  $\Omega$ , i.e.

$$J(p_1, p_2, \Omega) := \int_{\Omega} \left(\frac{p_2}{p_1}\right)^2 \zeta d\mathbf{x} + \ell \int_{\Omega} d\mathbf{x}, \quad (5.9)$$

---

<sup>2</sup>The volume of the computational domain  $\Omega$ , obviously, does not change if the volume of the reflex tube is constant.

where  $\ell > 0$  is fixed Lagrange multiplier.

Therefore, we end up with the optimization problem: find an optimal shape of the reflex tube such that the functional (5.9) is minimal under additional constraints that  $p_1$  is the solution of (2.35), (2.76),  $p_2$  is the solution of (2.36), (2.77)<sup>3</sup>, the resonance frequency is assumed to be constant, cf. (5.5) and (5.6).

## 5.2 Optimization Procedure

In order to find an optimal shape of the reflex tube we have to construct an algorithm. Popular methods to solve the shape optimization problems are so-called shape sensitivity analysis or the gradient method, cf. [6], [4], [3], etc, topological gradient method, cf. [28], [5], [4], etc. The topological gradient method seems to be not applicable in our case because it requires to investigate the sensitivity of the objective function with respect to certain hole creation inside the computational domain. Obviously, the hole (or the obstacle) inside the reflective tube of the loudspeaker will increase the influence of the first harmonic on the sound. However, if the hole creation can be done in certain "smart" way exactly on the boundary such that the curvature of the "hole" is small and the boundary remains smooth enough, then the topological gradient method can be applied.

To avoid the difficulties connected with special control of the hole creation (in the case of topological gradient method), we apply the gradient method to find the optimal shape of the reflective tube. This method is based exactly on the boundary variations and, therefore, is much suitable in our case. The idea of this method is based on the fact that one is able to consider the changes of the objective function with respect to the shape changes, i.e. we define so-called classical shape derivative  $J'$  of the objective function  $J$  and analyze its behaviour. We use new numerical method based on the combination of the classical shape derivative and of the level set method, cf. [55], for front propagation (boundary transition), cf. [4]. Running forward, we mention that the shape derivative is used as the normal velocity of the tube boundary which is moved during the optimization process. Front (boundary of the tube) propagation is performed by solving the Hamilton–Jacobi equation for a level set function.

### 5.2.1 Shape Derivative

To apply the shape sensitivity analysis to minimize the function (5.9) we recall a classical notion of shape derivative. This notion goes back, at least, to Hadamard,

---

<sup>3</sup>In the case of bounded computational domain  $\Omega$  we define the radiative boundary conditions (2.101) and (2.106) for  $p_1$  and  $p_2$ , respectively. In the case of unbounded computational domain  $\Omega^+$  we define the boundary conditions (2.104) and (2.105) at infinity for  $p_1$  and  $p_2$ , respectively.

and many have contributed to its development, cf. [52], [57], etc. Starting from a smooth reference open set  $\Omega$ , we consider domains of the type

$$\Omega_{\boldsymbol{\theta}} = (\mathbf{I} + \boldsymbol{\theta})(\Omega) \quad (5.10)$$

with  $\mathbf{I}$  the identity mapping from  $\mathbb{R}^3$  into  $\mathbb{R}^3$  and  $\boldsymbol{\theta}$  is a vector field in  $\mathcal{W}_{\infty}^1(\mathbb{R}^3, \mathbb{R}^3)$ . It is well known that, for sufficiently small  $\boldsymbol{\theta}$ ,  $(\mathbf{I} + \boldsymbol{\theta})$  is a diffeomorphism in  $\mathbb{R}^3$ , i.e. the map  $(\mathbf{I} + \boldsymbol{\theta})$  is differentiable and has differentiable inverse. We remark that no change of topology is possible with this method of shape variation.

**Definition 5.2.1** The shape derivative of  $J(\Omega)$  at  $\Omega$  is defined as the Fréchet derivative in  $\mathcal{W}_{\infty}^1(\mathbb{R}^3, \mathbb{R}^3)$  at 0 of the application  $\boldsymbol{\theta} \rightarrow J((\mathbf{I} + \boldsymbol{\theta})(\Omega))$ , i.e.

$$J((\mathbf{I} + \boldsymbol{\theta})(\Omega)) = J(\Omega) + J'(\Omega)(\boldsymbol{\theta}) + o(\boldsymbol{\theta}), \quad (5.11)$$

with  $\lim_{\boldsymbol{\theta} \rightarrow 0} \frac{|o(\boldsymbol{\theta})|}{\|\boldsymbol{\theta}\|} = 0$ , where  $J'(\Omega)$  is a continuous linear form on  $\mathcal{W}_{\infty}^1(\mathbb{R}^3, \mathbb{R}^3)$ .

Although, the definition above gives certain concept about the shape derivative, it does not help to find this derivative. In order to calculate  $J'$  we present two useful lemmas

**Lemma 5.2.2** Let  $\Omega$  be a smooth bounded open set and  $\phi(x) \in \mathcal{W}_1^1(\mathbb{R}^3)$ . Define

$$J_1(\Omega) := \int_{\Omega} \phi(x) \, dx. \quad (5.12)$$

Then  $J_1$  is differentiable at  $\Omega$  and

$$J_1'(\Omega)(\boldsymbol{\theta}) = \int_{\partial\Omega} \langle \boldsymbol{\theta}(x), \mathbf{n}(x) \rangle \phi(x) \, dS \quad (5.13)$$

for any  $\boldsymbol{\theta} \in \mathcal{W}_{\infty}^1(\mathbb{R}^3, \mathbb{R}^3)$ .

**Lemma 5.2.3** Let  $\Omega$  be a smooth bounded open set and  $\phi(x) \in \mathcal{W}_1^2(\mathbb{R}^3)$ . Define

$$J_2(\Omega) := \int_{\partial\Omega} \phi(x) \, dS. \quad (5.14)$$

Then  $J_2$  is differentiable at  $\Omega$  and

$$J_2'(\Omega)(\boldsymbol{\theta}) := \int_{\partial\Omega} \langle \boldsymbol{\theta}(x), \mathbf{n}(x) \rangle \left( \frac{\partial\phi}{\partial\mathbf{n}} + \phi \operatorname{div}\mathbf{n} \right) dS \quad (5.15)$$

for any  $\boldsymbol{\theta} \in \mathcal{W}_{\infty}^1(\mathbb{R}^3, \mathbb{R}^3)$ , where  $\operatorname{div}\mathbf{n}$  is the mean curvature of  $\partial\Omega$ . Furthermore, this result still holds true if one replaces  $\partial\Omega$  by  $\Gamma$ , a smooth open subset of  $\partial\Omega$ , and assumes that  $\phi = 0$  on the surface boundary  $\partial\Omega \setminus \Gamma$ .



These two results can be found in [4]. We will use these two lemmas to calculate the shape derivative of the functional (5.9). In particular, Lemma 5.2.2 is useful in order to calculate the shape derivative of a volume constraint (5.5). Indeed, we have

$$\text{vol}(\Omega) = \int_{\Omega} d\mathbf{x} \longrightarrow \text{vol}'(\Omega)(\boldsymbol{\theta}) = \int_{\partial\Omega} \langle \boldsymbol{\theta}(\mathbf{x}), \mathbf{n}(\mathbf{x}) \rangle dS. \quad (5.16)$$

Let us assume for the moment that the constraints (5.6)–(5.8) are omitted<sup>4</sup>. Then we formulate a small theorem which determines the shape derivative of the objective functional (5.9).

**Theorem 5.2.4** *Let  $\Omega$  be a smooth bounded open set and  $\boldsymbol{\theta} \in \mathcal{W}_{\infty}^1(\mathbb{R}^3, \mathbb{R}^3)$ . Assume that the right hand side of the equation (2.36), denoted by  $f_2$ , belongs to the space  $\mathcal{W}_2^1(\Omega)$ ; the right hand sides of the boundary conditions (2.76) and (2.77), denoted by  $g_1$  and  $g_2$ , respectively, belong to  $\mathcal{W}_2^2(\Omega)$ ; the solutions  $p_1$  and  $p_2$  of the equations (2.35) and (2.36), respectively, belong to the space  $\mathcal{W}_2^2(\Omega)$ . The shape derivative of the functional (5.9) can be found by*

$$\begin{aligned} J'(\Omega)(\boldsymbol{\theta}) &= \int_{\partial\Omega} \langle \boldsymbol{\theta}, \mathbf{n} \rangle \left[ \left( \frac{p_2}{p_1} \right)^2 \zeta + \ell + \langle \nabla_{\mathbf{x}} p_1, \nabla_{\mathbf{x}} q_1 \rangle - \kappa^2 p_1 q_1 \right. \\ &\quad + \langle \nabla_{\mathbf{x}} p_2, \nabla_{\mathbf{x}} q_2 \rangle - 4\kappa^2 p_2 q_2 - f_2 q_2 \\ &\quad \left. - \frac{\partial}{\partial \mathbf{n}} (g_1 q_1 + g_2 q_2) + \text{div} \mathbf{n} (g_1 q_1 + g_2 q_2) \right] dS, \end{aligned} \quad (5.17)$$

where  $q_1$  and  $q_2$  are so-called adjoint states which assumed to be smooth, i.e.  $q_1, q_2 \in \mathcal{W}_2^2(\Omega)$ . They are defined as the solutions of the linearized<sup>5</sup> problems

$$\Delta_{\mathbf{x}} q_1 + \kappa^2 q_1 = -2 \frac{p_2^2}{p_1^3} \quad \text{in } \Omega, \quad (5.18)$$

$$\frac{\partial q_1}{\partial \mathbf{n}} = 0 \quad \text{on } \partial\Omega \quad (5.19)$$

and

$$\Delta_{\mathbf{x}} q_2 + 4\kappa^2 q_2 = 2 \frac{p_2}{p_1^2} \quad \text{in } \Omega, \quad (5.20)$$

$$\frac{\partial q_2}{\partial \mathbf{n}} = 0 \quad \text{on } \partial\Omega. \quad (5.21)$$

**Proof** In order to show a short, albeit formal proof due to [4], we consider the objective function (5.9) for which we introduce the Lagrangian defined for

<sup>4</sup>These constraints will be included into optimization process in iterative manner, cf. Subsection 5.2.3

<sup>5</sup>In general, the problem for the function  $q_1$  is much complicated, see the proof.

$(u_1, u_2, w_1, w_2)$  by the following expression, cf. [4]

$$\begin{aligned} \mathfrak{L}(\Omega, u_1, u_2, w_1, w_2) &= \int_{\Omega} \left( \frac{u_2}{u_1} \right)^2 \zeta \, d\mathbf{x} + \ell \int_{\Omega} \mathbf{x} \\ &+ \int_{\Omega} \langle \nabla_{\mathbf{x}} u_1, \nabla_{\mathbf{x}} w_1 \rangle - \kappa^2 u_1 w_1 \, d\mathbf{x} - \int_{\partial\Omega} g_1 w_1 \, dS \\ &+ \int_{\Omega} \langle \nabla_{\mathbf{x}} u_2, \nabla_{\mathbf{x}} w_2 \rangle - (4\kappa^2 u_2 - f_2) w_2 \, d\mathbf{x} - \int_{\partial\Omega} g_2 w_2 \, dS, \end{aligned} \quad (5.22)$$

where  $u_1, u_2, w_1$  and  $w_2$  belong to the space  $\mathcal{W}_2^1(\mathbb{R}^3)$ . Here, the functions  $g_1, g_2$  and  $f_2$  are evaluated at the points  $u_1$  and  $u_2$ . It is worth to notice that the functions  $u_1, u_2, w_1$  and  $w_2$  do not depend on the domain  $\Omega$ . Therefore, we are able to apply the usual differentiation rule to the Lagrangian  $\mathfrak{L}$ . The stationarity of the Lagrangian is going to give the optimality conditions of the minimization problem. For a given  $\Omega$ , we denote by  $(p_1, p_2, q_1, q_2)$  such a stationary point. The partial derivatives of  $\mathfrak{L}$  with respect to  $w_1$  and  $w_2$  at the point  $(p_1, p_2, q_1, q_2)$  in the direction  $\phi \in \mathcal{W}_2^1(\mathbb{R}^3)$ , after integration by parts lead to

$$\begin{aligned} 0 = \left\langle \frac{\partial \mathfrak{L}}{\partial w_1}(\Omega, p_1, p_2, q_1, q_2), \phi \right\rangle &= - \int_{\Omega} (\Delta_{\mathbf{x}} p_1 + \kappa^2 p_1) \phi \, d\mathbf{x} \\ &+ \int_{\partial\Omega} \left( \frac{\partial p_1}{\partial \mathbf{n}} - g_1 \right) \phi \, dS \end{aligned} \quad (5.23)$$

and

$$\begin{aligned} 0 = \left\langle \frac{\partial \mathfrak{L}}{\partial w_2}(\Omega, p_1, p_2, q_1, q_2), \phi \right\rangle &= - \int_{\Omega} (\Delta_{\mathbf{x}} p_2 + 4\kappa^2 p_2 - f_2) \phi \, d\mathbf{x} \\ &+ \int_{\partial\Omega} \left( \frac{\partial p_2}{\partial \mathbf{n}} - g_2 \right) \phi \, dS. \end{aligned} \quad (5.24)$$

Thus, taking first  $\phi$  with compact support in  $\Omega$  gives the state equations (2.35) and (2.36) for the  $p_1$  and  $p_2$  functions, respectively. Then, by the variation of the trace function  $\phi$  on the boundary  $\partial\Omega$  gives the Neumann type boundary conditions (2.76) and (2.77).

On the other hand, to find the adjoint equations for the  $q_1$  and  $q_2$  functions we have to differentiate the Lagrangian  $\mathfrak{L}$  with respect to  $u_1$  and  $u_2$  (at the point  $(p_1, p_2, q_1, q_2)$ ), respectively, in the direction  $\phi$ . Let us first differentiate the Lagrangian with respect to  $u_2$ , i.e.

$$\begin{aligned} 0 = \left\langle \frac{\partial \mathfrak{L}}{\partial u_2}(\Omega, p_1, p_2, q_1, q_2), \phi \right\rangle &= - \int_{\Omega} \left( \Delta_{\mathbf{x}} q_2 + 4\kappa^2 q_2 - 2 \frac{p_2}{p_1^2} \right) \phi \, d\mathbf{x} \\ &+ \int_{\partial\Omega} \left( \frac{\partial q_2}{\partial \mathbf{n}} - g'_{2p_2} \right) \phi \, dS. \end{aligned} \quad (5.25)$$

Because the function  $g_2$  does not depend on  $p_2$ , we (by analogous variations of the function  $\phi$  and of the trace function of  $\phi$ ) define the adjoint problem for the function  $q_2$ , cf. (5.20), (5.21).

Obviously, in order to derive the adjoint problem for the function  $q_1$  we have to differentiate the Lagrangian  $\mathcal{L}$  with respect to  $u_1$  at the point  $(p_1, p_2, q_1, q_2)$  in the direction  $\phi$ . But before the derivation let us note first that the functions  $f_2$  and  $g_2$  depend on the function  $p_1$ , cf. (2.36) and (2.77). Remember, these two functions have been derived via asymptotical analysis, cf. Chapter 2. The function  $p_1$  and the functions  $f_2$  and  $g_2$  are defined on different scales. Therefore, we neglect them as the higher order terms. Thus, the differentiation gives the problem (5.18), (5.19).

We have found a well-posed boundary value problems for the adjoint functions  $q_1$  and  $q_2$ .

The shape derivative of the Lagrangian  $\mathcal{L}$  can be found using the Lemmas 5.2.2 and 5.2.3, i.e.

$$\begin{aligned} \frac{\partial \mathcal{L}}{\partial \Omega}(\Omega, p_1, p_2, q_1, q_2)(\boldsymbol{\theta}) &= \int_{\partial \Omega} \langle \boldsymbol{\theta}, \mathbf{n} \rangle \left[ \left( \frac{p_2}{p_1} \right)^2 \zeta + \langle \nabla_{\mathbf{x}} p_1, \nabla_{\mathbf{x}} q_1 \rangle - \kappa^2 p_1 q_1 \right. \\ &\quad + \langle \nabla_{\mathbf{x}} p_2, \nabla_{\mathbf{x}} q_2 \rangle - 4\kappa^2 p_2 q_2 - f_2 q_2 + \ell \\ &\quad \left. - \frac{\partial}{\partial \mathbf{n}}(g_1 q_1 + g_2 q_2) + \operatorname{div} \mathbf{n}(g_1 q_1 + g_2 q_2) \right] dS. \end{aligned} \quad (5.26)$$

So, we found the shape derivative of the Lagrangian  $\mathcal{L}$ . What does it give us? Obviously, the following relation is true

$$J(p_1(\Omega), p_2(\Omega), \Omega) = \mathcal{L}(\Omega, p_1(\Omega), p_2(\Omega), q_1(\Omega), q_2(\Omega)). \quad (5.27)$$

Indeed, if the functions  $p_1$ ,  $p_2$ ,  $q_1$  and  $q_2$  are the solutions of the above mentioned problems, then the last four integrals vanish, cf. (5.22), and we get the identity. Differentiation of both sides of the relation (5.27) with respect to the shape  $\Omega$  gives

$$J'(\Omega)(\boldsymbol{\theta}) = \frac{\partial \mathcal{L}}{\partial \Omega}(\Omega, p_1, p_2, q_1, q_2)(\boldsymbol{\theta}), \quad (5.28)$$

where the functions  $p_1$ ,  $p_2$ ,  $q_1$  and  $q_2$  have to be shape differentiable.

This proof is merely formal computation (in particular, it assumes that the functions  $p_1$ ,  $p_2$ ,  $q_1$  and  $q_2$  are differentiable with respect to the shape  $\Omega$ ) but it can be rigorously justified, cf. [4], [52], [57].

■

Let us denote the expression in the [ ] brackets in (5.26) by  $v$ . Then the shape derivative of the objective function (5.9) expresses as

$$J'(\Omega)(\boldsymbol{\theta}) = \frac{\partial \mathcal{L}}{\partial \Omega}(\Omega, p_1, p_2, q_1, q_2)(\boldsymbol{\theta}) = \int_{\partial \Omega} \langle \boldsymbol{\theta}, \mathbf{n} \rangle v dS, \quad (5.29)$$

In order to show that the value of the objective function can be decreased we choose the vector

$$\boldsymbol{\theta} = -v\mathbf{n}. \quad (5.30)$$

Next, we update the domain  $\Omega$  in the following way

$$\Omega_t = (\mathbf{I} + t\boldsymbol{\theta}) \Omega, \quad (5.31)$$

where  $t > 0$  is a small descent step. We obtain

$$J(\Omega_t) = J(\Omega) - t \int_{\partial\Omega} v^2 dS + \mathcal{O}(t^2), \quad (5.32)$$

which guarantees the decrease of the objective functional.

**Remark 5.2.5** It is also possible to consider the transitions of certain part of the boundary. In the case of the reflex tube optimization we have to allow to move only the part of the boundary  $\partial\Omega$  which describes the tube. Therefore, in such a case the vector field  $\boldsymbol{\theta}$  has to satisfy the constraint (or boundary condition)  $\langle \boldsymbol{\theta}, \mathbf{n} \rangle = 0$  on  $\Gamma_{\text{fixed}}$ .

**Remark 5.2.6** We have to note that from theoretical point of view there is no matter which domain (either  $\Omega$  or  $\Omega^+$ ) we consider. The shape of the reflex tube has to be optimized and it is the same in both cases.

### 5.2.2 Level Set Method

As we already mentioned above, for the transition of the boundary of the reflex tube,  $\Gamma_{\text{tube}}$ , we use the level set method. The main ideas of this method can be found in [55]. Here, we shortly explain the principles of the level set method which have been applied to find an optimal shape of the tube.

#### Definition of the Level Set Function

Let a bounded domain  $D \subset \mathbb{R}^3$  be the working domain in which all admissible shapes  $\Omega$  are included, i.e.  $\Omega \subset D$ . In numerical practice, the domain  $D$  will be uniformly meshed once and for all. We parameterize the boundary  $\partial\Omega$  ( $\Gamma_{\text{tube}}$ ) by means of the level set function  $\Psi$ , following the idea of [51], i.e. we define

$$\begin{cases} \Psi(\mathbf{x}) = 0 & \iff \mathbf{x} \in \partial\Omega \cap D, \\ \Psi(\mathbf{x}) < 0 & \iff \mathbf{x} \in \Omega, \\ \Psi(\mathbf{x}) > 0 & \iff \mathbf{x} \in (D \setminus \overline{\Omega}). \end{cases} \quad (5.33)$$

The normal  $\mathbf{n}$  to the shape  $\partial\Omega$  is presented as  $\frac{\nabla_{\mathbf{x}}\Psi}{|\nabla_{\mathbf{x}}\Psi|}$  and can be found numerically using the finite differences since the mesh is supposed to be uniform. We also remark that the values of the normal vector  $\mathbf{n}$  theoretically are defined only on

$\partial\Omega$ , but due to level set method it can be defined in the whole domain  $D$ , cf. [55].

As we already mentioned, the boundary propagation in time is described by the Hamilton–Jacobi equation. To be precise, assume that the shape  $\Omega_t$  evolves in time  $t \in \mathbb{R}_+$  with a normal velocity  $-v(t, \mathbf{x})$ . Then the boundary  $\partial\Omega_t$  of the domain  $\Omega_t$  can be found by

$$\Psi(t, \mathbf{x}(t)) = 0 \quad \text{for any } \mathbf{x}(t) \in \partial\Omega_t. \quad (5.34)$$

Differentiation of (5.34) with respect to the time variable  $t$  gives

$$\frac{\partial\Psi}{\partial t} + \langle \dot{\mathbf{x}}(t), \nabla_{\mathbf{x}}\Psi \rangle = \frac{\partial\Psi}{\partial t} - \langle v\mathbf{n}, \nabla_{\mathbf{x}}\Psi \rangle = 0. \quad (5.35)$$

Since  $\mathbf{n} = \frac{\nabla_{\mathbf{x}}\Psi}{|\nabla_{\mathbf{x}}\Psi|}$  we obtain

$$\frac{\partial\Psi}{\partial t} - v|\nabla_{\mathbf{x}}\Psi| = 0. \quad (5.36)$$

The initial shape, i.e.  $\Psi(0, \mathbf{x}(0))$ , is given. The Hamilton–Jacobi equation (5.36) is posed in the whole domain  $D$ , and not only on the boundary  $\partial\Omega$  if the velocity  $v$  is given everywhere.

### Numerical Scheme

In order to solve the initial value problem, i.e. the equation (5.36) together with the initial condition, one requires certain theoretical knowledges about the hyperbolic type equations and about the numerical schemes which deal with such kind of equations. The basic material can be found in [48], [55], etc. Here, we use an explicit in time, first order upwind numerical scheme (multidimensional version) presented in [55] and [4], i.e.

$$\Psi_{ijk}^{n+1} = \Psi_{ijk}^n - \Delta t \left[ \max(-v_{ijk}^n, 0)\nabla^+ + \min(-v_{ijk}^n, 0)\nabla^- \right], \quad (5.37)$$

where

$$\begin{aligned} \nabla^+ &:= \left[ \max\left(D_{ijk}^{-x_1}, 0\right)^2 + \min\left(D_{ijk}^{+x_1}, 0\right)^2 + \right. \\ &\quad \max\left(D_{ijk}^{-x_2}, 0\right)^2 + \min\left(D_{ijk}^{+x_2}, 0\right)^2 + \\ &\quad \left. \max\left(D_{ijk}^{-x_3}, 0\right)^2 + \min\left(D_{ijk}^{+x_3}, 0\right)^2 \right]^{1/2}, \\ \nabla^- &:= \left[ \max\left(D_{ijk}^{+x_1}, 0\right)^2 + \min\left(D_{ijk}^{-x_1}, 0\right)^2 + \right. \\ &\quad \max\left(D_{ijk}^{+x_2}, 0\right)^2 + \min\left(D_{ijk}^{-x_2}, 0\right)^2 + \\ &\quad \left. \max\left(D_{ijk}^{+x_3}, 0\right)^2 + \min\left(D_{ijk}^{-x_3}, 0\right)^2 \right]^{1/2} \end{aligned}$$

and

$$D_{ijk}^{+x_1} = D_{ijk}^{+x_1} u \equiv \frac{u(x_1 + h, x_2, x_3, t) - u(x_1, x_2, x_3, t)}{h},$$

$$D_{ijk}^{-x_1} = D_{ijk}^{-x_1} u \equiv \frac{u(x_1, x_2, x_3, t) - u(x_1 - h, x_2, x_3, t)}{h}.$$

Here, we use the uniform grid, i.e. the space step  $h$  in all directions is the same. Using this numerical method we find the level set function  $\Psi(t, \mathbf{x}(t))$  for every  $t \in \mathbb{R}_+$ . The zeroth level has to represent the boundary  $\partial\Omega_t$  of the domain  $\Omega_t$ .

**Remark 5.2.7** Obviously, the level set function  $\Psi(t, \mathbf{t})$  due to the numerical treatment has discrete nature. In order to use the Wave Based Method, cf. Chapter 4, to solve the appropriate equations one has to define certain continuous analogue of the level set function. It can be (and has been) done via interpolation using Bézier technique, cf. [54].

### Stability and the CFL Condition

There are natural time step  $\Delta t$  requirements in the above numerical scheme. This is so-called CFL condition which guarantees that the numerical solution stays stable and adequately predicts the shape transformations. Similarly to the advection equation, cf. [48], a rather rough estimate for the time step  $\Delta t$  in 3D would be

$$\max_D |v^n| \Delta t < \frac{h}{2\sqrt{3}}, \quad (5.38)$$

where the maximum is taken over the values for  $v$  at all possible grid points, not simply those corresponding to the zeroth level.

### 5.2.3 Optimization Algorithm

In this subsection, we present the optimization algorithm to find the optimal shape of the reflex tube. In the previous subsections we defined the shape derivative of the objective functional (5.4) and the level set function  $\Psi$  which has to represent the shape movement during the optimization process. But we still did not take into account the constraints (5.6)–(5.8), i.e. the conservation of the resonance frequency. As we mentioned above, we implement them in an iterative manner. We propose the following algorithm which helps to minimize the objective functional (5.4) and find the optimal shape of the reflex tube

1. Initialization of the geometry of the computational domain  $\Omega^6$ . In particular, we initialize the level set function  $\Psi(0, \mathbf{x}(0))$ .

---

<sup>6</sup>Here, the constraints (5.6)–(5.8) are satisfied and the volume of the reflex tube has to be fixed.

2. Iterations until convergence, for  $n \in \mathbb{N}$ 
  - a. Computation of the states  $p_1^n$  and  $p_2^n$  and adjoint states  $q_1^n$  and  $q_2^n$  defined in the domain  $\Omega_{t^n}$ .
  - b. Calculation of the velocity  $v^n$ , cf. (5.26).
  - c. Deformation of the shape by solving the Hamilton–Jacobi equation (5.36), i.e. new shape characterizes by the level set function  $\Psi(t^{n+1}, \mathbf{x}(t^{n+1}))$ . The initial condition is given by  $\Psi(t^n, \mathbf{x}(t^n))$ .
  - d. Stretching/gripe of the reflex tube in such a way that the conservation of the volume and the conservation of the resonance frequency are satisfied.
3. Save and plot the results.

The algorithm above has been implemented and the results of this optimization procedure are presented in Section 5.3.

### 5.3 Optimal Shape

In this section, we would like to present the results of the optimization procedure described above. We start from the definition of the initial shape. It has been chosen in such a way that the resonance frequency  $f_{\text{res}}$  is equal to 60 Hz. Next, we calculate the volume of the initial tube and fix it as the reference volume, cf. Fig. 5.2. In order to follow the shape changes we visualize them each 20<sup>th</sup> iteration, cf. Fig. 5.3–5.8. As we may conclude the shape of the reflex tube tends to the symmetrical one. We also present the values of the objective functional  $J$  for each "control" iteration, cf. Fig. 5.10. We are able to notice that the objective functional  $J$  indeed decreases.

### 5.4 The Main Results of the Chapter 5

Similarly to the previous chapters we summarize the main ideas of this chapter. In this chapter, we define the optimal shape design problem in the mathematical way, i.e. we define the objective functional  $J$ , which has to be minimized over the set  $\mathfrak{D}$  of admissible domains, i.e. the volume of such a domain has to be preserved and the resonance frequency  $f_{\text{res}}$  has to be equal to 60Hz. The objective functional represents the relation between the key note and the first order harmonic, which has been integrated over certain domain.

The optimization procedure is based on the shape sensitivity analysis (shape gradient method). Using two lemmas 5.2.2 and 5.2.3 and the theorem 5.2.4 one is able to find the shape derivative  $J'$ , which is defined as the Fréchet derivative in

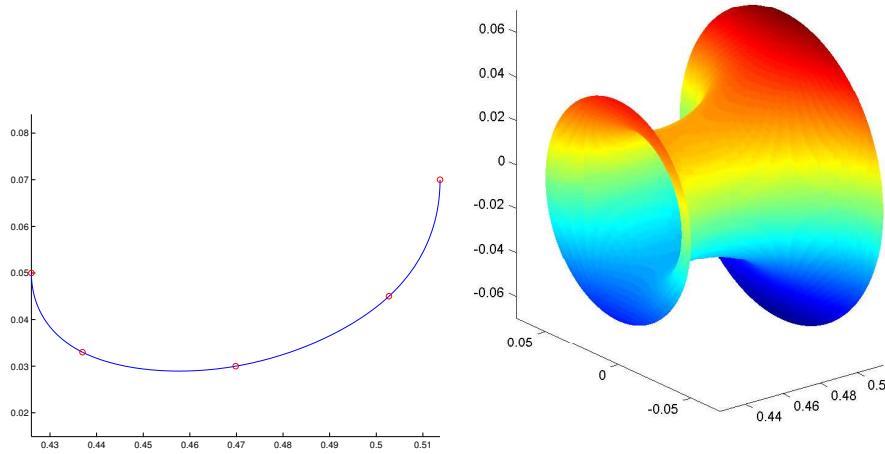


Figure 5.2: Initial shape of the reflective tube of the bass loudspeaker. 2D cut (left) and 3D tube (right).

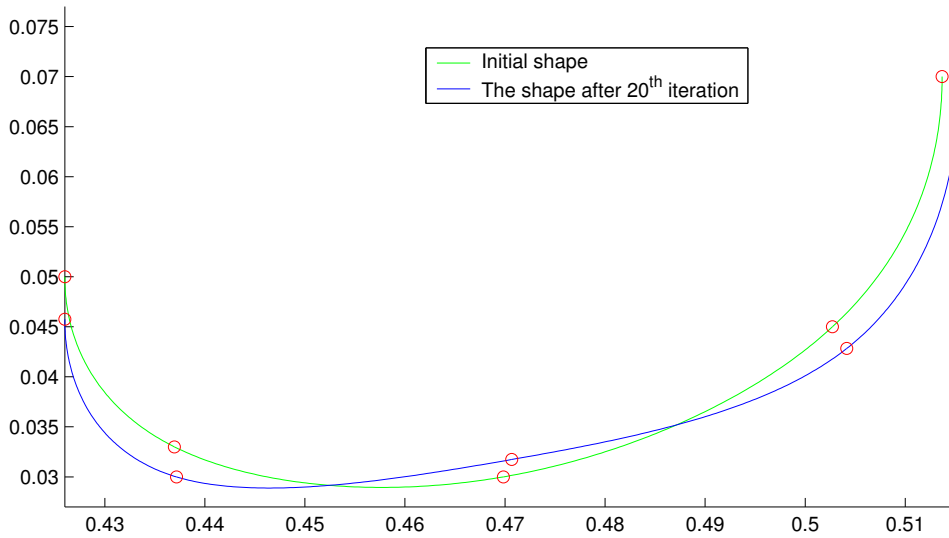


Figure 5.3: The shape of the reflective tube after 20<sup>th</sup> iteration.

$\mathcal{W}_\infty^1(\mathbb{R}^3, \mathbb{R}^3)$ . To find  $J'$ , two adjoint solutions  $q_1$  and  $q_2$  to  $p_1$  and  $p_2$ , respectively, have been found. The shape derivative  $J'$  has been further used to change the shape of the reflex tube. To find the optimal shape of the reflex tube, we applied the Level Set Method. This is the reason why the optimization procedure has an iterative nature, cf. Subsections 5.2.2 and 5.2.3. Moreover, we have to mention that the conservation of the resonance frequency  $f_{\text{res}}$  has been also taken into account iteratively.

The changes of the shape of the reflective tube have been visualized each 20<sup>th</sup> iteration.



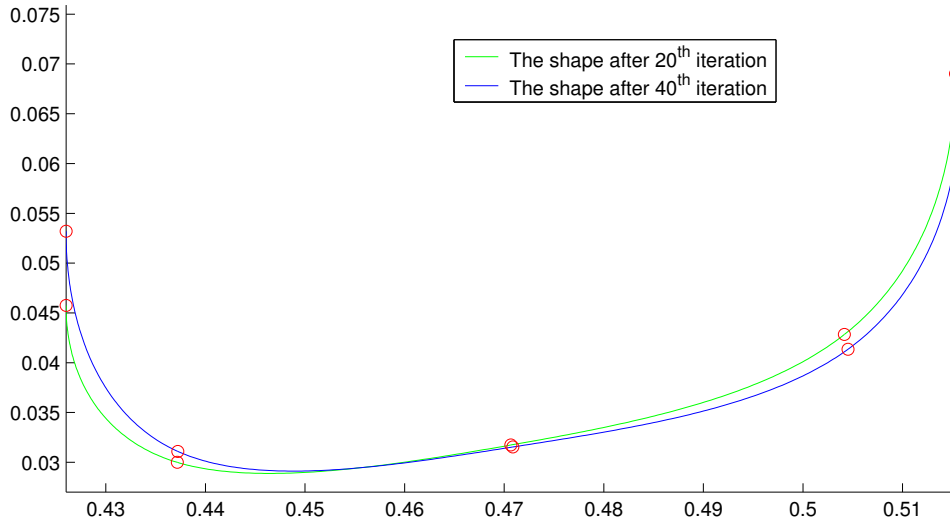


Figure 5.4: The shape of the reflective tube after 40<sup>th</sup> iteration.

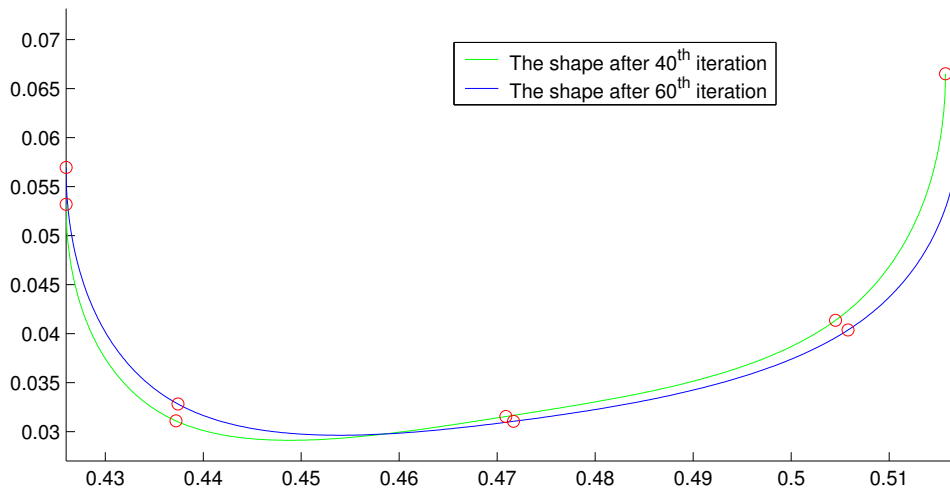
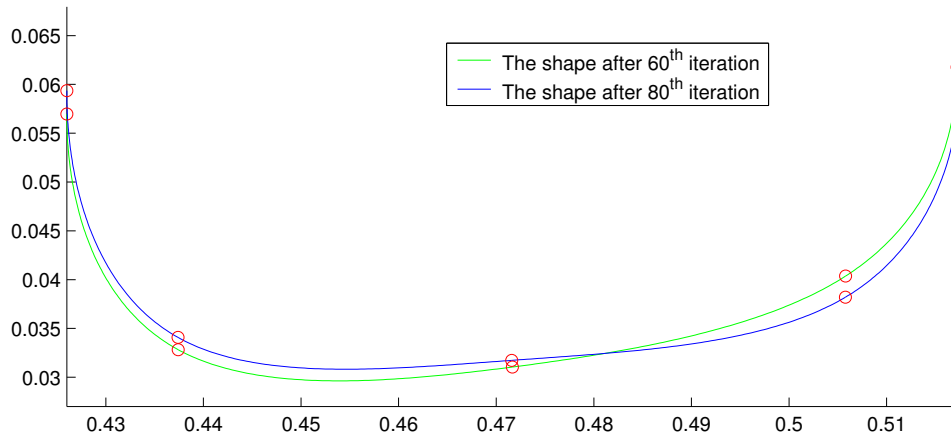
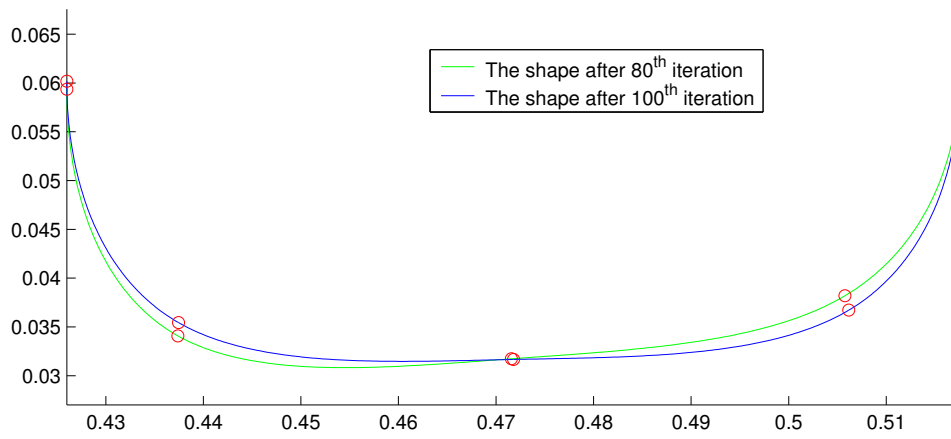
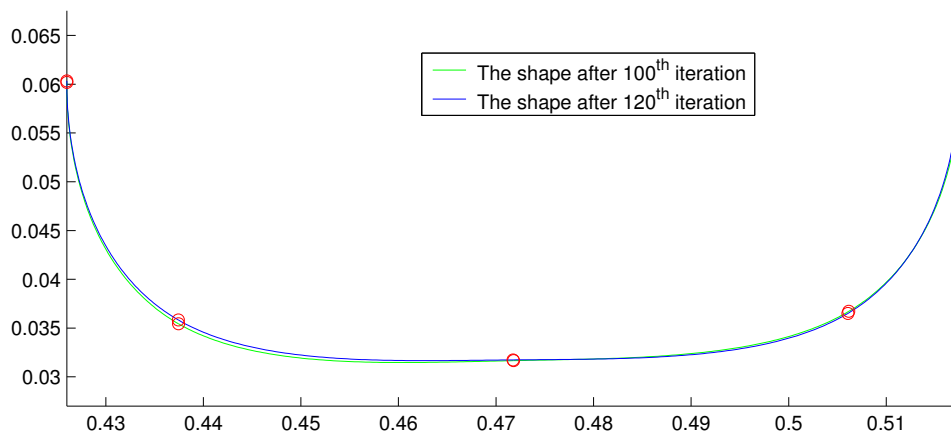


Figure 5.5: The shape of the reflective tube after 60<sup>th</sup> iteration.

Figure 5.6: The shape of the reflective tube after 80<sup>th</sup> iteration.Figure 5.7: The shape of the reflective tube after 100<sup>th</sup> iteration.Figure 5.8: The shape of the reflective tube after 120<sup>th</sup> iteration.

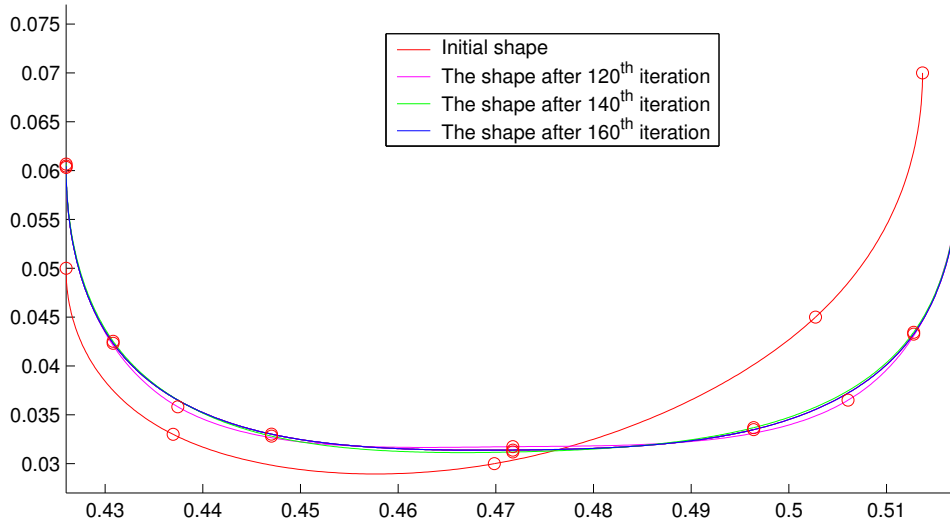


Figure 5.9: Initial shape and the shape of the reflective tube (approximated using 5 control points) after 120<sup>th</sup> iteration; The shapes of the reflective tube (approximated using 7 control points) after 140<sup>th</sup> and 160<sup>th</sup> iterations.

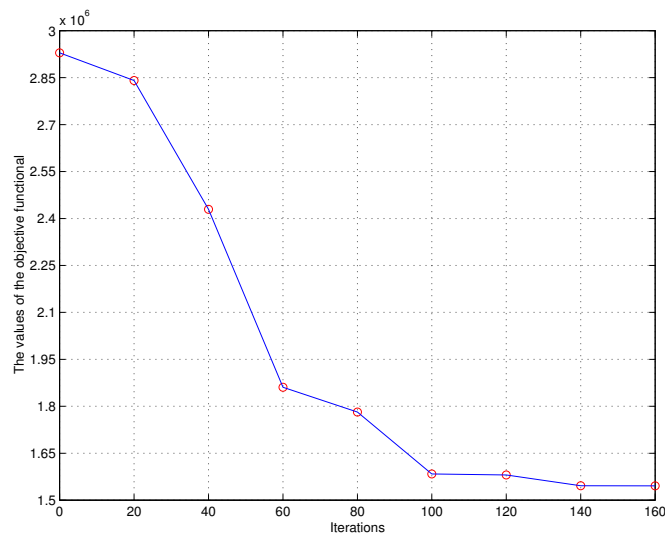


Figure 5.10: The values of the objective functional for each 20<sup>th</sup> iteration.

## Chapter 6

# Conclusion

In this thesis we presented a mathematical model which describes the behaviour of the acoustical pressure (sound), produced by a bass loudspeaker. The underlying physical propagation of sound is described by the non-linear isentropic Euler system in a Lagrangian description. This system has been expanded via asymptotical analysis up to third order in the displacement of the membrane of the loudspeaker. The differential equations which describe the behaviour of the key note and the first order harmonic were compared to classical results. The boundary conditions, which have been derived up to third order, are based on the principle that the small control volume sticks to the boundary and is allowed to move only along it. Further, the behaviour of the key note and the first harmonic has been considered. Also, two main computational domains have been defined, i.e. bounded and unbounded.

As a next step, using classical results of the theory of elliptic partial differential equations, we showed that under appropriate conditions on the input data the appropriate mathematical problems admit, by the Fredholm alternative, unique solutions. The input data is represented by the right hand sides of the governing equations (2.35) and (2.36), the right hand sides of the boundary conditions (2.76), (2.77), (2.101) and (2.102) and the boundary of the bounded domain. Moreover, certain regularity results have been shown. The case of the problems (2.35), (2.76), (2.104) and (2.36), (2.77), (2.105), defined in the unbounded domain, has been also investigated.

Further, the Wave Based Method has been applied to solve appropriate mathematical problems, cf. (2.35), (2.76), (2.104) and (2.36), (2.77), (2.105). However, the known theory of the Wave Based Method, which can be found in the literature, so far, allowed to apply WBM only in the cases of convex domains. We found the criterion which allows to apply the WBM in the cases of non-convex domains. In the case of 2D problems we represent this criterion as the Proposition 4.2.1. With the aid of this proposition one is able to subdivide arbi-

trary 2D domains such that the number of subdomains is minimal, WBM may be applied in each subdomain and the geometry is not altered, e.g. via polygonal approximation. Further, the same principles have been used in the case of 3D problem, cf. Section 4.6. However, the formulation of a similar proposition in cases of 3D problems has still to be done.

Next, we showed a simple procedure to solve an inhomogeneous Helmholtz equation using WBM. This procedure, however, is rather computationally expensive and can probably be improved. Several examples have been also presented.

We presented the possibility to apply the Wave Based Technique to solve steady-state acoustic problems in the case of an unbounded 3D domain. The main principle of the classical WBM, cf. [23], has been extended to the case of an external domain. Two numerical examples have been presented.

In order to apply the WBM to our problems, cf. Chapter 2, we had to subdivide the computational domain  $\Omega^+$  into three subdomains. Therefore, on the interfaces certain coupling conditions have been defined.

In order to be sure that WBM gives appropriate results we compared them to the numerical results calculated using FEM. However, the starting problems, cf. Chapter 4, did not coincide completely, the results were similar.

The description of the optimization procedure and the results of the optimization finalize the scientific part of the thesis. As it was stated above, the high order harmonics affects the sound due to the non-linear effects during the sound propagation. Therefore, one wanted to optimize the reflective tube of the bass loudspeaker to minimize the influence of high order harmonics (first order harmonic in our case). The objective functional represents the relation between the key note and the first harmonic integrated over certain area. The additional volume and resonance frequency conservation conditions have been also taken into account. The optimization procedure has an iterative nature and is based on the shape sensitivity analysis and on the level set method, where the level set function represents the shape of the reflective tube.

# Bibliography

- [1] M. Abramowitz and I. A. Stegun. *Handbook of Mathematical Functions with Formulas, Graphs, and Mathematical Table (Paperback)*. New York: Dover, 1972.
- [2] R.A. Adams. *Sobolev Spaces*. Pure and Applied Mathematics, Academic Press, New York, 1975.
- [3] G. Allaire, F. de Gournay, F. Jouve, and A-M. Toader. *Structural Optimization Using Topological and Shape Sensitivity via a Level-Set Method*. R.I. N<sup>o</sup> 555, October, 2004.
- [4] G. Allaire, F. Jouve, and A-M. Toader. *Structural Optimization Using Sensitivity Analysis and a Level-Set Method*. Journal of Computational Physics, pages 363–393, 194, 2004.
- [5] S. Amstutz and A. Heiko. *A New Algorithm for Topology Optimization Using a Level-Set Method*. Preprint submitted to Elsevier Science, 18th July, 2005.
- [6] G. Bal and K. Ren. *Reconstruction of Singular Surfaces by Shape Sensitivity Analysis and Level-Set Method*. Internet resource.
- [7] P.K. Banerjee. *The boundary element methods in engineering*. 2.Ed., 1994.
- [8] G. Beer and J.O. Watson. *Introduction to finite and boundary element methods for engineers*. Wiley-Verlag, 1992.
- [9] R.T. Beyer. *Nonlinear Acoustics*. Physical Acoustics, Vol.2, Part B, edited by W.P. Mason (Academic, New-York), pages 231–332, 1965.
- [10] M.S. Birman and M.Z. Solomjak. *Spectral Theory of Self-Adjoint Operators in Hilbert Space*. Mathematics and Its Applications (Soviet Series), D.Reidel Publishing Company, 1987.
- [11] L. Bjorno. *Nonlinear Acoustics*. in Acoustics and Vibration Progress, Vol.2, edited by R.W.B. Stephens and H.G. Leventhall (Chapman and Hall, London), pages 101–198, 1976.

- 
- [12] J.P. Boyd. *Chebyshev and Fourier Spectral Methods*. 2.Ed., Dover pub. inc., 2001.
- [13] D. Braess. *Finite Elemente*. Springer-Lehrbuch, 1991.
- [14] J.N. Bronstein, K.A. Semendjajew, G. Musiol, and H. Mühlig. *Taschenbuch der Mathematik*, 5. überarbeitete und erweiterte auflage. Verlag Harri Deutsch, 2001.
- [15] A. Browder. *Mathematical Analysis: An Introduction*. Springer-Verlag, New York, 1996.
- [16] C. Campos-Pozuelo, B. Dubus, and J.A. Gallego-Juárez. *Finite-Element Analysis of the Nonlinear Propagation of High-Intensity Acoustic Waves*. J. Acoust. Soc. Am. 106 (1), 1999.
- [17] C. Campos-Pozuelo and Ch. Vanhille. *Numerical Model for Nonlinear Standing Waves and Weak Shocks in Thermoviscous Fluids*. J. Acoust. Soc. Am. 109 (6), 2001.
- [18] G. Chen and J. Zhou. *Boundary Element Methods*. Academic press, 1992.
- [19] C. Coclici. Lecture Notes on PDE I. TU Kaiserslautern, SS 2002.
- [20] D. Colton and R. Kress. *Inverse Acoustic and Electromagnetic Scattering Theory*. Applied Mathematical Sciences 93. Second Edition, Springer Verlag, 1998.
- [21] D.G. Crighton, A.P. Dowling, J.E. Ffowcs Williams, M. Heckl, and F.G. Leppington. *Modern Methods in Analytical Acoustics*. Springer-Verlag, London, 1992.
- [22] R. Dautray and J.-L. Lions. *Mathematical Analysis and Numerical Methods for Science and Technology: Spectral Theory and Applications*. Springer-Verlag, 1990.
- [23] W. Desmet. *A wave based prediction technique for coupled vibro-acoustic analysis*. PhD Thesis, K.U. Leuven, division PMA, 1998.
- [24] W. Desmet, B. Pluymers, and E. Brechlin. *On the use of a novel wave based prediction technique for acoustic cavity analysis*. Proceedings of the 18th International Congress on Acoustics (ICA2004), Kyoto, Japan, 2004.
- [25] Zh. Ding. *A proof of the trace theorem of Sobolev spaces on Lipschitz domains*. Proceedings of the American Mathematical Society, Vol. 124, Nr. 2, 1996.

- 
- [26] R.R. Erickson and B.T. Zinn. *Modeling of Finite Amplitude Acoustic Waves in Closed Cavities Using the Galerkin Method*. J. Acoust. Soc. Am. 113 (4), 2003.
- [27] W. Freeden, T. Gervens, and M. Schreiner. *Constructive Approximation on the Sphere: with Applications to Geomathematics*. Clarendon Press, Oxford, 1998.
- [28] S. Garreau, P. Guillaume, and M. Masmoudi. *The Topological Asymptotic for PDE Systems: the Elasticity Case*. SIAM J. Control Optim., pages 1756–1778, 39(6), 2001.
- [29] K. Gerdes. *The Conjugated vs. the Unconjugated Infinite Element Method for the Helmholtz Equation in Exterior Domains*. Research Report No. 96–11, Seminar für Angewandte Mathematik Eidgenössische Technische Hochschule, Zürich, Switzerland, 1996.
- [30] D. Gilbarg and N.S. Trudinger. *Elliptic Partial Differential Equations of Second Order*. Springer-Verlag Berlin, 1977.
- [31] D. Gottlieb and S.A. Orszag. *Numerical Analysis of Spectral Methods: Theory and Applications*. 1977.
- [32] A. Gray. *Modern Differential Geometry of Curves and Surfaces with Mathematica*. 2nd ed. Boca Raton, pages 111–115, 1997.
- [33] P.G. Grinevich. *Introduction to the Theory of Solitons*. Lecture notes (Script), NMU (Independent Moscow University), in russian, 1999.
- [34] P. Grisvard. *Elliptic problems in non-smooth domains*. Monographs and Studies in Mathematics 24, 1985.
- [35] W. Hackbusch. *Theorie und Numerik Elliptischer Differentialgleichungen*. B.G. Teubner Stuttgart, 1996.
- [36] J. Haslinger and P. Neittaanmäki. *Finite Element Approximation for Optimal Shape Design*. Theory and Applications, John Wiley & Sons Ltd., 1988.
- [37] A. Hepberger, B. Pluymers, K. Jalics, H.-H. Pribsch, and Desmet W. *Validation of a Wave Based Technique for the Analysis of a Multi-domain 3D Acoustic Cavity with Interior Damping and Loudspeaker Excitation*. CD-ROM proceedings of the 33rd International Congress and Exposition on Noise Control Engineering (Internoise2004), Prague, Czech Republic, 2004.



- 
- [38] A. Hepberger, H.-H. Priebisch, W. Desmet, B. Van Hal, B. Pluymers, and P. Sas. *Application of the Wave Based Method for the Steady-state Acoustic Response Prediction of a Car Cavity in the Mid-frequency Range*. *Proceedings of the International Conference on Noise and Vibration Engineering ISMA2002*, Leuven, Belgium, 2002.
- [39] I. Herrera. *Boundary Methods: an Algebraic Theory*. Pitman Adv. Publ. Program, London, 1984.
- [40] J. Jegorovs. *Optimal Shape of the Reflex Tube of a Bass Loudspeaker*. Master Thesis, Fachbereich Mathematik, Universität Kaiserslautern, 2003.
- [41] J. Jegorovs. *On the Convergence of the WBM Solution in Certain Non-Convex Domains*. *Proceedings of the International Conference on Noise and Vibration Engineering ISMA 2006*, ID 183, Leuven, Belgium, 2006.
- [42] J. Jegorovs and J. Mohring. *On the Application of the Wave Based Method in the Case of an Exterior 3D Domain*. *Proceedings of the International Conference on Noise and Vibration Engineering ISMA 2006*, ID 184, Leuven, Belgium, 2006.
- [43] J. Jegorovs and J. Mohring. *A Third Order Correction to the Helmholtz Equation*. *Mathematical Modelling and Analysis*, pages 51–62, Vol. 10, Vilnius, 2005.
- [44] K. Kuttler. *Topics in Analysis*. Lecture notes. Department of Mathematics, Brigham Young University, 2005.
- [45] V.P. Kuznetsov. *Equations of Nonlinear Acoustics*. *Sovjet Physics – Acoustics*, pages 467–470, Vol. 16, No. 4, 1971.
- [46] O.A. Ladyzhenskaya. *The Boundary Value Problems of Mathematical Physics*. Springer-Verlag, New-York, 1985.
- [47] O.A. Ladyzhenskaya and N.N. Uraltseva. *Linear and Quasilinear Elliptic Equations*. *Mathematics in Science and Engineering* 46, Academic Press, New York and London, 1968.
- [48] R.J. LeVeque. *Numerical Methods for Conservation Laws*. Birkhäuser Verlag, 1998.
- [49] J. Mohring. *Simulating Bass Loudspeakers Requires Nonlinear Acoustics - a Second Order Correction to the Helmholtz Equation*. Springer-Verlag, pages 333–339, Heidelberg, 2002.

- 
- [50] J. Mohring and J. Jegorovs. *Optimal Shape of the Reflex Tube of a Bass Loudspeaker*. Proceedings of the International Conference on Noise and Vibration Engineering ISMA 2004, pages 3877–3890, Leuven, Belgium, 2004.
- [51] S. Osher and J.A. Sethian. *Front Propagating with Curvature Dependent Speed: Algorithms Based on Hamilton–Jacobi Formulations*. J. Comp. Phys., pages 12–49, 78, 1988.
- [52] O. Pironneau. *Optimal Shape Design for Elliptic Systems*. Springer Verlag, 1984.
- [53] B. Pluymers, C. Vanmaele, W. Desmet, D. Vandepitte, and P. Sas. *A high performance hybrid finite element-wave based method for steady-state acoustic analysis*. Proceedings of the Twelfth International Congress on Sound and Vibration (ICSV12), Lisbon, Portugal, 2005.
- [54] H. Prautzsch, W. Boehm, and M. Paluszny. *Bézier and B-Spline Techniques*. Springer-Verlag, 2002.
- [55] J.A. Sethian. *Level-Set Methods and Fast Marching Methods*. Cambridge University Press, 1999.
- [56] R.E Showalter. *Hilbert space methods for partial differential equations*. Monographs and Studies in Mathematics, Pitman, 1977.
- [57] J. Sokolowski and J.-P. Zolesio. *Introduction to Shape Optimization*. Springer Verlag, 1992.
- [58] E. Trefftz. *Ein Gegenstück zum Ritzschen Verfahren*. in Proc. of 2<sup>nd</sup> Int. Congress on Applied Mechanics, pages 131–137, Zuerich, 1926.
- [59] B. Van Hal, W. Desmet, D. Vandepitte, and P. Sas. *Hybrid finite element - wave based method for acoustic problems*. Computer Assisted Mechanics and Engineering Sciences (CAMES) 11, pages 375–390, 2003.
- [60] C. Vanmaele, W. Desmet, and D. Vandepitte. *A hybrid finite element-wave based method for the dynamic analysis of two-dimensional solids*. Proceedings of the 5th International Conference on Computation of Shell and Spatial Structures, Salzburg, Austria, 2005.
- [61] K. Willcox. *Numerical Optimization I*. Lecture Notes. Massachusetts Institute of Technology, Engineering Systems Division and Dept. of Aeronautics and Astronautics, 2004.
- [62] [www.all-science-fair-projects.com/science\\_fair\\_projects\\_encyclopedia](http://www.all-science-fair-projects.com/science_fair_projects_encyclopedia).

- [63] E. Zeidler. *Applied Functional Analysis*. Applied Mathematical Sciences 108, Springer-Verlag, 1995.
- [64] O. C. Zienkiewicz and R. L. Taylor. *The Finite Element Methods. Solid Mechanics*. 5.Ed., 2000.

# Curriculum Vitae

## **Jevgenijs Jegorovs**

11.12.1978	Geboren in Jelgava, Lettland
09.1986 – 06.1997	6. Mittelschule in Jelgava
09.1997 – 06.2001	Bachelor Studium an der Lettischen Universität, Fachbereich Physik und Mathematik, Abteilung Mathematik
10.2001 – 09.2003	Master Studium in Rahmen von Programm Mathematics International an der TU Kaiserslautern, Vertiefungsrichtung Industrial Mathematics
10.2003 – 09.2006	Promotionsstudium an der TU Kaiserslautern, Fachbereich Mathematik